

AD-A285 972

NAVAL POSTGRADUATE SCHOOL MONTEREY, CALIFORNIA

1

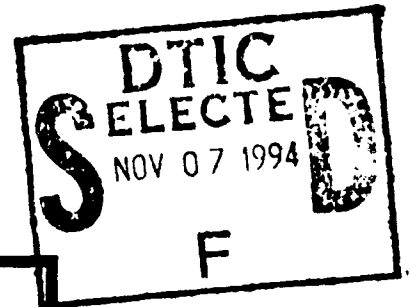


94-34406



587

THESIS



**EMITTER LOCATION VIA KALMAN FILTERING OF
SIGNAL TIME DIFFERENCE OF ARRIVAL**

by

Richard William Williamson

September 1994

Thesis Advisor:

Harold A. Titus

Approved for public release; distribution is unlimited.

07-11-4 060

REPORT DOCUMENTATION PAGE

Form Approved
OMB No. 0704-0188

Public reporting burden for this collection of information is estimated to average 1 hour per response, including the time for reviewing instructions, searching existing data sources, gathering and maintaining the data needed, and completing and reviewing the collection of information. Send comments regarding this burden estimate or any other aspect of this collection of information, including suggestions for reducing this burden, to Washington Headquarters Services, Directorate for Information Operations and Reports, 1215 Jefferson Davis Highway, Suite 1204, Arlington, VA 22202-4302, and to the Office of Management and Budget, Paperwork Reduction Project (0704-0188), Washington, DC 20503

1. AGENCY USE ONLY (Leave blank) Unclassified	2. REPORT DATE September 1994	3. REPORT TYPE AND DATES COVERED Electrical Engineer's Thesis
--	----------------------------------	--

4. TITLE AND SUBTITLE EMITTER LOCATION VIA KALMAN FILTERING OF SIGNAL TIME DIFFERENCE OF ARRIVAL	5. FUNDING NUMBERS
---	--------------------

6. AUTHOR(S) Richard William Williamson	
--	--

7. PERFORMING ORGANIZATION NAME(S) AND ADDRESS(ES) Naval Postgraduate School Monterey, CA 93943-5000	8. PERFORMING ORGANIZATION REPORT NUMBER
--	--

9. SPONSORING / MONITORING AGENCY NAME(S) AND ADDRESS(ES) Naval Research Laboratory Code 9120 4555 Overlook Ave. Washington, DC 20375-5320	10. SPONSORING / MONITORING AGENCY REPORT NUMBER None
--	--

11. SUPPLEMENTARY NOTES The views expressed in this thesis are those of the author and do not reflect the official policy or position of the Department of Defense or the U.S. Government.

12a. DISTRIBUTION / AVAILABILITY STATEMENT Approved for public release; distribution is unlimited.	12b. DISTRIBUTION CODE
---	------------------------

13. ABSTRACT (Maximum 200 words) A relatively simple time domain method is developed to calculate the time of arrival for radar signals. The error present in the estimate of the time of arrival for a single pulse and a burst of pulses are developed and the effects of SNR, PRF, pulsewidth, and sampling frequency are examined. Time of arrival is used with multiple sensors and the Kalman filter to estimate the location of the emitter. Algorithms estimate the location of an emitter given the Time Difference of Arrival (TDOA) of a single pulse as well as the TDOA of bursts of pulses received as the emitter scans past the receivers. The algorithms were tested on simulated data.

14. SUBJECT TERMS Kalman Filtering, Time Difference of Arrival, Optimal Estimation	15. NUMBER OF PAGES 158
	16. PRICE CODE

17. SECURITY CLASSIFICATION OF REPORT Unclassified	18. SECURITY CLASSIFICATION OF THIS PAGE Unclassified	19. SECURITY CLASSIFICATION OF ABSTRACT Unclassified	20. LIMITATION OF ABSTRACT U1
---	--	---	----------------------------------

Approved for public release; distribution is unlimited

**EMITTER LOCATION VIA KALMAN FILTERING OF
SIGNAL TIME DIFFERENCE OF ARRIVAL**

by

Richard W. Williamson
Captain, United States Marine Corps
B.S. Aeronautical Engineering, Embry-Riddle Aeronautical University, 1985

Submitted in partial fulfillment
of the requirements for the degree of

MASTER OF SCIENCE IN ELECTRICAL ENGINEERING

and

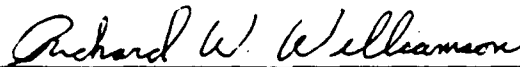
ELECTRICAL ENGINEER

from the

NAVAL POSTGRADUATE SCHOOL

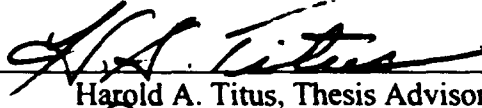
September, 1994

Author:



Richard W. Williamson

Approved by:



Harold A. Titus, Thesis Advisor



Phillip E. Pace, Second Reader



Michael A. Morgan, Chairman

Department of Electrical and Computer Engineering

ABSTRACT

A relatively simple time domain method is developed to calculate the time of arrival for radar signals. The error present in the estimate of the time of arrival for a single pulse and a burst of pulses are developed and the effects of SNR, PRF, pulsewidth, and sampling frequency are examined. Time of arrival is used with multiple sensors and the Kalman filter to estimate the location of the emitter. Algorithms estimate the location of an emitter given the Time Difference of Arrival (TDOA) of a single pulse as well as the TDOA of bursts of pulses received as the emitter scans past the receivers. The algorithms were tested on simulated data.

Accession For	
NTIS - DPA&I	<input checked="" type="checkbox"/>
DTIC - TAB	<input type="checkbox"/>
Unannounced	<input type="checkbox"/>
Justification	
By	
Distribution/	
Availability Codes	
Dist	Availability/ or Special
A-1	

TABLE OF CONTENTS

I. INTRODUCTION	1
A. BACKGROUND	1
B. RADAR EMITTER SIGNAL CHARACTERISTICS	2
C. EMITTER LOCATION PROBLEM DESCRIPTIONS	4
1. Burst TDOA Problem Description.	4
2. Single Pulse TDOA Problem Description	5
II. TDOA ESTIMATION	6
A. TIME OF ARRIVAL ESTIMATION AND ERROR MODELS	6
1. Time of Arrival Measurement	6
2. Pulse TOA Estimation	7
3. Burst TOA Estimation	12
B. BURST AND PULSE TDOA	16
III. EMITTER LOCATION	19
A. BURST TIME DIFFERENCE OF ARRIVAL (TDOA)	19
1. Problem Geometry	19
2. Loci of Constant TDOA	21
3. Orthogonality of TDOA Observations	23
4. Ambiguity in TDOA Observations.	25
B. SINGLE PULSE TIME DIFFERENCE OF ARRIVAL (TDOA)	25
1. Problem Geometry	25
2. Loci of Constant TDOA	27
3. Orthogonality of the Loci of Constant TDOA.	28
4. Ambiguity in Single Pulse TDOA Observations.	29
IV. KALMAN FILTERING	31
A. THE EXTENDED KALMAN FILTER	31
B. ERROR ELLIPSOIDS	34
V. SIMULATION RESULTS	38

A.	THE BURST TDOA KALMAN FILTER	38
1.	Extended Kalman Filter Equations	38
2.	Burst TDOA Simulations	42
a.	Scenario #1	46
b.	Scenario #2	49
c.	Scenario #3	52
3.	The Burst TDOA Filter Results	55
B.	SINGLE PULSE TDOA KALMAN FILTER	57
1.	Extended Kalman Filter Equations	57
2.	Pulse TDOA Kalman Filter Simulations	59
a.	Scenario #1	62
b.	Scenario #2	68
c.	Scenario #3	74
3.	Pulse TDOA Filter Results	77
VI.	CONCLUSIONS AND RECOMMENDATIONS	79
A.	CONCLUSIONS	79
B.	RECOMMENDATIONS	80
APPENDIX A.	TOA PROBABILITY DENSITY	81
A.	PULSE TOA PROBABILITY DENSITY	81
1.	Derivation of Probability Density	81
2.	Effect of Signal to Noise Ratio on Probability Density	86
3.	Calculated Mean and Standard Deviation of Sampled Pulses	87
B.	BURST TOA PROBABILITY DENSITY	88
1.	Derivation of Probability Density	88
2.	Effect of Signal to Noise Ratio on Burst TOA Probability Density	89
3.	Effect of PRF on the Burst TOA Probability Density	90
4.	Calculated Mean and Standard Deviation of Sampled Bursts	92
5.	Effect of the Pulwidth on the Probability Density	94
APPENDIX B.	LOCI OF CONSTANT TDOA	97
A.	BURST TDOA PROBLEM	97
B.	PULSE TDOA PROBLEM	98
APPENDIX C.	TDOA ORTHOGONALITY	101
A.	BURST TDOA ORTHOGONALITY	101

B. PULSE TDOA ORTHOGONALITY	103
APPENDIX D. BURST H_{xx} DERIVATION	107
APPENDIX E. MATLAB PROGRAMS	109
LIST OF REFERENCES	145
INITIAL DISTRIBUTION LIST	146

LIST OF FIGURES

Figure 1. Burst of pulses from a scanning emitter	4
Figure 2. Pulse envelope and sampled pulse	9
Figure 3. Pulse TOA probability densities vs. Gaussian approximations, pulsewidth 1.0 msec	11
Figure 4. A burst of pulses with a 6.0 kHz PRF and a 1.0 microsecond pulsewidth	14
Figure 5. Burst TOA probability density vs. Gaussian approximation, 2.0 millisecond burst, 6.0 kHz PRF and 1.0 microsecond pulsewidth	15
Figure 6. Burst TOA probability density vs. Gaussian approximation, 2.0 millisecond burst, 6.0 kHz PRF, and 1.0 microsecond pulsewidth	16
Figure 7. Burst TDOA geometry	20
Figure 8. Loci of constant TDOA for an emitter scanning at a constant rate, scan rate 360 degrees/sec, receiver separation 1.0 kilometers	22
Figure 9. Loci of constant TDOA for an emitter scanning at a constant rate, scan rate 360 degrees/second, receiver locations as shown	23
Figure 10. Single pulse TDOA geometry	26
Figure 11. Loci of constant pulse TDOA, sensor separation 500 meters	27
Figure 12. Loci of constant TDOA for two receiver platforms, sensor separation 500 meters	28
Figure 13. Flowchart for burst TDOA Kalman filter	41
Figure 14. Initial location and velocity of receivers	42
Figure 15. Emitter locations for burst TDOA filtering scenarios	43
Figure 16. Scenario #1 Estimates of the location of the emitter	47
Figure 17. Scenario #1 Estimates of emitter coordinates vs. observations	48
Figure 18. Scenario #1 Close-up of steady state estimate of emitter location	48
Figure 19. Scenario #2 Estimates of emitter location	50
Figure 20. Scenario #2 Estimates of emitter coordinates vs observations	51
Figure 21. Close-up of the steady state estimate of emitter location	51
Figure 22. Scenario #3 Estimates of emitter location	53

Figure 23. Scenario #3 Estimates of emitter coordinates vs observations	54
Figure 24. Close-up of the steady state estimate of emitter location	54
Figure 25. Receiver platform and sensor configuration	59
Figure 26. Emitter locations for the single pulse TDOA Kalman filter	60
Figure 27. Scenario #1 Estimates of emitter location	63
Figure 28. Scenario #1 Estimates of emitter coordinates vs. observations	64
Figure 29. Scenario #1 Close-up of steady state estimate of emitter location	64
Figure 30. Scenario #1 Estimates of emitter location for 300 km receiver separation	66
Figure 31. Scenario #1 Estimates of emitter coordinates vs. observations for 300 km receiver separation	67
Figure 32. Scenario #1 Close-up of steady state estimate of emitter location for 300 km receiver separation	67
Figure 33. Scenario #2 Estimates of emitter location	69
Figure 34. Scenario #2 Estimates of emitter coordinates vs. observations	70
Figure 35. Close-up of the steady state estimate of emitter location.	70
Figure 36. Scenario #2 Estimates of the location of the emitter with 150 km receiver separation.	72
Figure 37. Scenario #2 Estimates of emitter coordinates vs. observations with 150 km receiver separation	73
Figure 38. Close-up of the steady state estimate of emitter location with 150 km receiver separation	73
Figure 39. Scenario #3 Estimates of the emitter location.	75
Figure 40. Scenario #3 Estimates of emitter coordinates vs. observations	76
Figure 41. Close-up of the steady state estimate of the emitter location	76
Figure A-1. Pulse envelope and sampled pulse	81
Figure A-2. Pulse TOA probability density for peak signal to noise ratios of 15, 20, 25, and 30 dB	87
Figure A-3. A burst of sampled pulses from a scanning emitter	89
Figure A-4. Burst TOA probability densities for a 2 millisecond burst with a pulsewidth of 1.0 microseconds, and a PRF of 6 kHz.	90
Figure A-5. Bursts used to examine the effect of PRF on the TOA probability density	91
Figure A-6. Burst TOA probability densities for PRFs of 3, 6, 9, and 12 kHz.	92

Figure A-7. Burst TOA probability densities for pulse widths of 1.0, 2.0, 3.0,
and 4.0 microseconds 95

Figure B-1. Angular relationships, burst TDOA problem 96

Figure B-2. Pulse TDOA problem geometry 98

Figure C-1. Pulse TDOA geometry for emitter at a long distance 103

ACKNOWLEDGMENTS

I would like to express my gratitude to Professor Titus for his patient, professional, and timely guidance during the course of this research. I would also like to thank Professor Pace for his help and suggestions.

I would like to thank my wife Terri for her patience and encouragement throughout this period. She has been a pillar of support throughout. Lastly, I would like to thank my parents. Without them and their dedication and support, none of this would have been possible.

I. INTRODUCTION

A. BACKGROUND

During the Persian Gulf War UAVs (Unmanned Aerial Vehicles) proved useful by providing battlefield surveillance, targeting information, and naval gunfire spotting. They were able to provide the battlefield commander with up to the minute intelligence and offered the battlefield commander an over the horizon intelligence gathering asset that possessed the flexibility that he required to respond to the constantly changing circumstances and priorities of the battlefield. UAVs also provided a medium range aerial reconnaissance and intelligence gathering capability that was not hindered by the long lead time required for other reconnaissance assets. Current UAV capabilities are primarily limited to optical and infra-red surveillance, but the UAV would be very useful in electronic intelligence (ELINT) gathering. UAVs could remain on station listening to the enemy's electronic emissions for long periods of time, deep in enemy territory, without risking aircraft and pilots.

One application of electronic intelligence gathering is locating radar emitters from time difference of arrival (TDOA) observations. A time domain technique is presented here that uses the Kalman filter to estimate the location of a radar emitter from the time difference of arrival for a burst of pulses between two or more receivers, and time difference of arrival of individual pulses between two or more sensors. The background information and models used to develop the Kalman filter are presented, and the resulting

Kalman filter algorithms are tested for a variety of problem configurations. Conclusions are drawn about the usefulness of the algorithms and recommendations are made for further testing and evaluation.

B. RADAR EMITTER SIGNAL CHARACTERISTICS

The signal characteristics most important in the emitter location problem are the Pulse Repetition Interval (PRI), and the pattern and rate at which the emitter scans a target. These characteristics determine which estimation technique will be most effective, and they affect the ability of these algorithms to accurately estimate the location of the emitter.

The PRI is the period of time between successive pulses. This value can range from tens of milliseconds for long range search radars to microseconds for pulse Doppler radars. Range in many radar systems is determined by measuring the time required for a pulse to strike a target and return, and the unambiguous range of a radar system is determined by the length of the PRI. The longer the PRI the longer the unambiguous range of the radar. Similarly, the PRI affects the allowable separation of the sensors used to detect the pulse TDOA. The longer the PRI the greater the allowable separation of the sensors.

The vast majority of radar systems are designed to scan a volume of space to look for targets. All of these systems use a search mode that is used to scan the volume of space around the emitter in a regular pattern. Most radar emitters spend the majority of their operation in this mode and it is in this mode that most emitters can be passively detected.

The method that the emitter uses to scan and search for a target is important in the problem of estimating its location from its emitted signals. Radar systems typically scan their main beam mechanically or electronically.

Mechanically scanned radar systems designed for target location typically scan in azimuth in a circular pattern. Their antennas are rotated by motors and actuators in a circular manner, and are designed to provide 360 degree search coverage. Special radar systems designed for altitude finding, or tracking and fire control will not necessarily scan in azimuth alone. Most of these systems use electronically scanned antennas to steer the main beam of the radar, and can scan in elevation as well as azimuth. These systems can have very complex scan patterns that can be changed as required. This thesis will be primarily concerned with mechanically scanned radar emitters that scan circularly in azimuth. The majority of the emitters encountered will be of this type. The principles developed to locate these emitters can also be applied to emitters with more complex scan patterns.

As an emitter scans its main beam past a target, the amplitude of the pulses that strike the target will generally vary from zero to a maximum that occurs near the center of the main beam. Figure 1 shows the typical burst of pulses detected as the emitter scans past a receiver. The frequency of these bursts is a function of the scan rate of the emitter, and the width of the burst is a function of the scan rate of the emitter and the beamwidth.

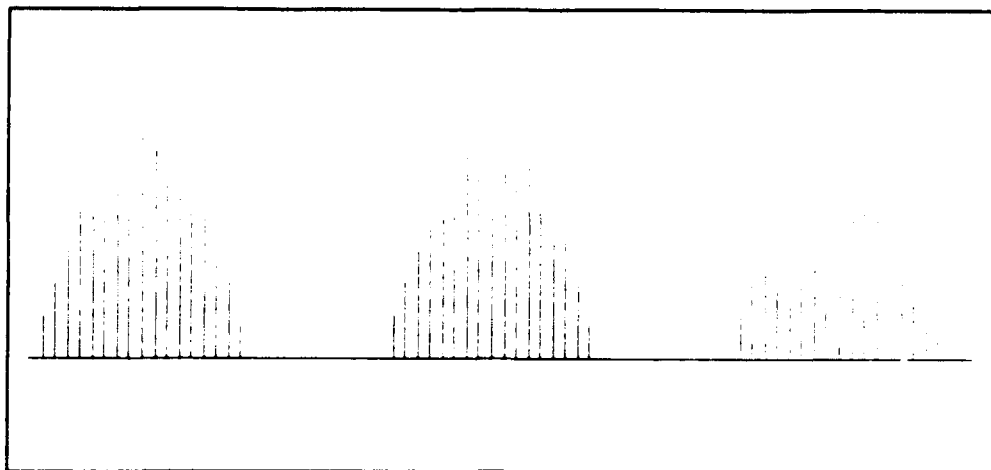


Figure 1. Burst of pulses from a scanning emitter

C. EMITTER LOCATION PROBLEM DESCRIPTIONS

Two basic approaches are used to estimate the location of the emitter from the TDOA of its signal. In the first approach the TDOA for the burst of pulses detected as the emitter scans past receivers is used to estimate the location of the emitter. The second approach uses the TDOA for individual pulses between two sensors on widely separated platforms to estimate the location of the emitter.

1. Burst TDOA Problem Description

The first TDOA filtering problem assumes that multiple receivers are used and that they are widely separated. The TDOA for the burst of pulses detected at each receiver are measured and used to estimate the location of the emitter. In this burst TDOA filtering problem, the following assumptions are made:

1. Enough information is obtained from the received signals to associate TDOA observations with the proper emitter, and thus the multi-emitter problem is reduced to a single emitter problem.

2. The receivers are referenced to a common time base. All time of arrival measurements are referenced to this common time base.
3. Global Positioning System (GPS) is used to determine the locations of the receivers. These estimates of the receiver locations are assumed to be exact and error introduced by the GPS is ignored.
4. The emitter scans in azimuth at a constant rate.
5. The PRI is constant for the entire length of the burst.

The receivers may be mounted on UAVs, aircraft, ground sites, or space platforms. For the UAV mounted receivers, the desired maximum detection range is assumed to be 500 kilometers. The algorithms developed are tested for ranges of 500 kilometers as well as shorter ranges of 150 kilometers and 30 kilometers.

2. Single Pulse TDOA Problem Description

The pulse TDOA problem estimates the location of the emitter by measuring the TDOA for an individual pulse between two sensors. The sensors are spaced close enough so that the TDOA can be measured for a single pulse without ambiguity. The following assumptions are made in the problem development:

1. Enough information can be obtained from the received signals to associate TDOA observations with the proper emitter, and thus the multi-emitter problem is reduced to a single emitter problem.
2. The receiver platforms are referenced to a common time base. All time of arrival measurements are referenced to this common time base.
3. Each receiver platform has two sensors and the TDOA for individual pulses between the two sensors can be measured accurately.
4. GPS is used to determine the locations of the receiver platforms. These estimates of the receiver locations are assumed to be exact and error introduced by the GPS is ignored.

The algorithms are tested for ranges of 500 kilometers as well as shorter ranges of 150 kilometers and 30 kilometers.

II. TDOA ESTIMATION

A. TIME OF ARRIVAL ESTIMATION AND ERROR MODELS

The Kalman filter can be used to estimate the location of the emitter from TDOA observations. Kalman filter theory, however, assumes that the noise corrupting observations is Gaussian distributed. Before applying the Kalman filter to the emitter location problem, an analysis of the error statistics of the TDOA observations is necessary. This determines if the noise present in TDOA observations can be approximated as Gaussian. One method of estimating the TDOA for emitter bursts and pulses is presented. The effect of noise on this estimation method's accuracy is explored, and the probability densities calculated are compared to Gaussian distributions.

1. Time of Arrival Measurement

TDOA measurements between widely separated receivers and sensors are used to estimate the location of the emitter. Since the receivers need to be widely separated to improve the accuracy of the location estimates and the orthogonality of the TDOA observations, physically linking the receivers together is not feasible. Therefore, it is important that the receivers are accurately referenced to some external time base. An onboard time base can be used to estimate the time of arrival (TOA) of signals, but drift would introduce error into the estimates of the TOA and subsequently the TDOA observations. To minimize drift, internal clocks aboard the receivers can be periodically

corrected with references to a more accurate external time base. If the receivers are mounted on UAVs equipped with GPS, the GPS system time could be used as the external time base. This approach is assumed for the balance of the development.

The TDOA observations in the burst TDOA filtering problem are on the order of milliseconds and tens of milliseconds. The error typically present in the GPS system time is much smaller than the typical TDOA observations and synchronizing all of the receivers to the GPS system time would not introduce appreciable error into the observations. For these observations, the receivers are assumed individually synchronized to the GPS system clock.

For the pulse TDOA observations, the length of the typical observations are a few microseconds or less. Using the GPS system time to estimate the time of arrival of a pulse at a sensor would introduce unacceptable error in the TDOA observations. This is because the error present in the GPS system clock would be on the same order as the observation it is being used to measure. To avoid ambiguity in the pulse TDOA observations, the sensors must be placed relatively close together. For the balance of the developments here the sensors will be assumed physically linked to the receiver platform, and the TOA observations for both sensors will be referenced to the same on board time base.

2. Pulse TOA Estimation

Envelope detection of the pulses received by the sensors is assumed. The envelopes of the received pulses are sampled and digitally encoded. An estimate of the

TOA for a pulse can be obtained from the time at which a sample is detected above a set threshold. This method of estimating the TOA is highly sensitive to the sampling rate and noise present in the sampled pulse. Spurious noise that is above threshold gives false TOA indications. Algorithms can be developed to test for false indications by examining multiple samples and announcing the arrival of a pulse only if a specified number of above threshold samples are detected. A more accurate estimate of the TOA can be obtained by integrating the samples of the pulse and calculating the TOA of the centroid of the pulse. The improvements gained from integration are similar to the improvements obtained in radar systems when pulse integration is used. All of the information present in the pulse is utilized and the effective signal to noise ratio is increased.

The time of arrival of the centroid of a sampled pulse can be found from equation (1):

$$TOA = \frac{\sum_{k=1}^N t(k)z(k)}{\sum_{k=1}^N z(k)} \quad (1)$$

Where TOA = the Time Of Arrival (TOA) of the pulse centroid,
 $z(k)$ = the magnitude of the k th sample,
 $t(k)$ = the time at which the k th sample was taken, and
 N = the number of samples in the pulse.

In the following development of the error present in the estimate of the pulse TOA, detected pulses are assumed to have the shape shown Figure 2. To these pulses, white, Gaussian distributed noise is added and its effect on the TOA is calculated.

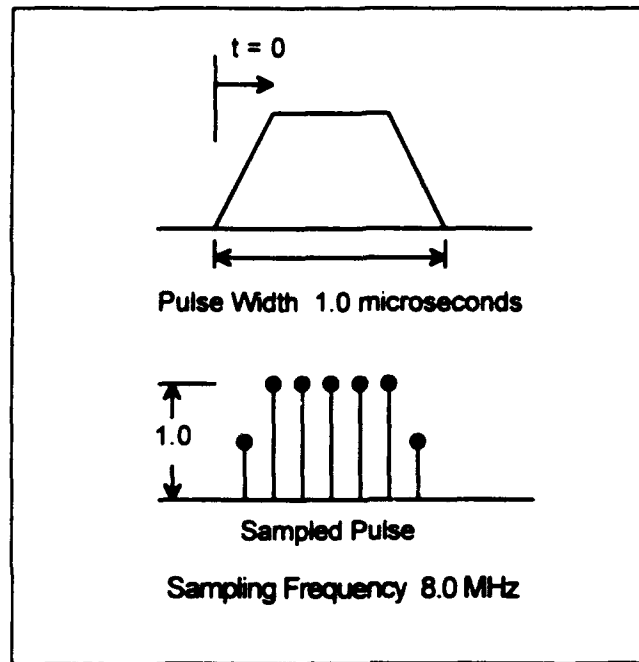


Figure 2. Pulse envelope and sampled pulse

The sampling interval is assumed to be much smaller than the pulse width so a sufficient number of samples of the pulse are taken and the sampled pulse is a reasonable representation of the original pulse. The sampling is assumed to be triggered by, and aligned with, the rising edge of the pulse. This assumption ignores the error introduced in the TOA when the first samples of the pulse are taken at some random point within the pulse.

Each sample of the pulse is considered a random variable as shown in equation (2).

$$z(k) = z_o(k) + v(k) \quad (2)$$

Where $z(k)$ = the random variable representing the amplitude of the kth sample,
 $z_o(k)$ = the deterministic variable that is the true amplitude of the kth sample, and
 $v(k)$ = the white Gaussian random variable that represents the noise present in the amplitude of the kth sample. The noise has zero mean and a variance of V , i.e.. $E[v(k)^2] = V$.

Since each sample of the pulse is modeled as a random variable, the time of arrival of the centroid of the pulse, calculated in equation (1), is also a random variable. A detailed derivation of the probability density of the pulse TOA is presented in Appendix A.

The peak signal to noise ratio is used as a means of representing the noise power present in the samples of the pulse. As shown in Figure 2, the peak amplitude of the pulse is assumed to be one. The peak signal to noise power ratio is calculated from the following equations:

$$\left(\frac{S_{\text{peak}}}{N} \right) = \frac{E[z_o(k)^2]}{E[v(k)^2]} \quad (3)$$

Where $z_o(k)$ = the true amplitude of the peak sample of the pulse, and
 $v(k)$ = the zero mean white noise sample with variance V , and
 $E[]$ = the expectation operator.

In decibels the peak signal to noise power ratio is given as:

$$\left(\frac{S_{\text{peak}}}{N} \right)_{\text{dB}} = 10 \log_{10} \left[\frac{E[z_o(k)^2]}{E[v(k)^2]} \right] \quad (4)$$

Since the peak amplitude of the pulse is one and the noise $v(k)$ is a random variable with zero mean and a variance V , the peak signal to noise power ratio reduces to:

$$\left(\frac{S_{\text{peak}}}{N}\right)_{\text{dB}} = -10 \log_{10}[V] \quad (5)$$

The MATLAB program Puldist.m, listed in Appendix E, calculates the probability density functions plotted in Figure 3. These curves depict the probability that the TOA of a pulse, calculated using equation (1), will fall within a specified range. The mean and standard deviation of the probability density functions are also calculated and Gaussian distributed density functions having the same mean and standard deviation are superimposed on the plots.

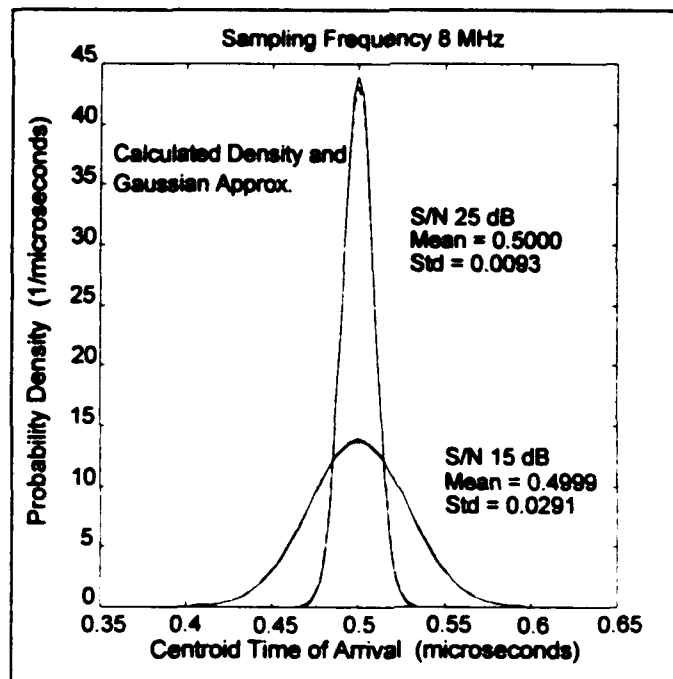


Figure 3. Pulse TOA probability densities vs. Gaussian approximations, pulsewidth 1.0 μsec

The Gaussian density functions are nearly indistinguishable from the actual probability density functions, so the pulse TOA can be considered Gaussian distributed in the Kalman filter developments. In Appendix A, a complete analysis is conducted of the effects of peak signal to noise ratio and sampling rate on the probability density function of the pulse TOA.

3. Burst TOA Estimation

As the main beam of an emitter sweeps past a receiver, the receiver detects a burst of pulses. The number of pulses received is a function of the beam width and scan rate of the emitter. The amplitude of the pulses change as the main beam of the emitter sweeps past the receiver. A burst typical for circularly scanning emitters is shown in Figure 1. The envelope of the burst can be approximated with the upper half of a sine wave.

$$x(t) = \sin \left[\frac{\pi(SR)}{BW} t \right] \quad (6)$$

Where $x(t)$ = the amplitude of the envelope of the burst,
 BW = the beamwidth of the main beam of the emitter in radians,
 SR = the scan rate of the emitter in radians/sec, and
 t = the time in seconds.

An estimate of the burst TOA can be obtained from the time of arrival for the first pulse of a burst, but this method of estimating the TOA assumes that for each receiver the same pulse in the burst will be detected first. Because of lower signal strength, more distant receivers may not detect some pulses as the start of the burst and the estimate of the TOA will be in error by some multiple of the PRI. Estimating the

centroid of the envelope of the burst and its time of arrival yields a better estimate of the TOA because the shape of the envelope detected by all of the receivers is the same, and only the amplitude of the envelope changes as a function of distance from the emitter.

An estimate of the TOA of the burst envelope is found by integrating the sampled pulses and their time of arrival over the length of the burst. If enough pulses are present in the burst, the centroid of the pulses lies sufficiently close to the centroid of the envelope. Integration of the pulses also reduces the effect of the noise by averaging its effect over a longer period of time, and effectively improving the signal to noise ratio by ignoring the interpulse periods where only noise is present.

Since the burst is considered a collection of sampled pulses, equation (1) is used to estimate the time of arrival of the centroid of the burst. The equations and algorithms used to calculate the probability density function, mean, and standard deviation of the pulse TOA are used to calculate these properties for the burst TOA.

The MATLAB program Burdist.m, listed in appendix E, generates the burst in Figure 4 and calculates its probability density for peak signal to noise ratios of 15 and 25 dB.

The burst has the following characteristics:

Burst Length:	2.0 milliseconds
Pulsewidth	1.00 microseconds,
Pulse Repetition Frequency	6000 Hz,
Maximum Amplitude	1.00

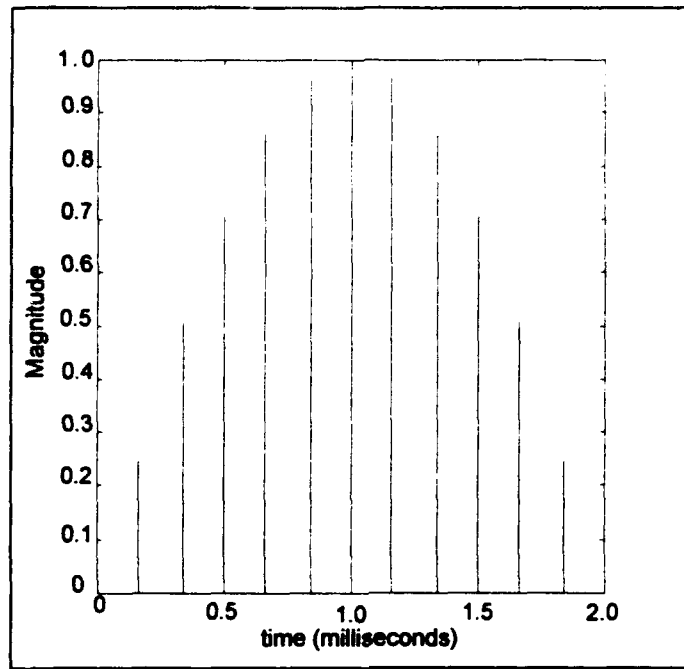


Figure 4. A burst of pulses with a 6.0 kHz PRF and a 1.0 microsecond pulsewidth

The envelope of the burst is calculated using equation (6), and the peak signal to noise ratios are calculated using equations (4) and (5). The burst in Figure 4 assumes that the pulses are spaced evenly throughout the envelope of the burst. If this is the case, the centroid of the pulses coincide with the true centroid of the envelope. For emitters with long PRIs where few pulses are present in the burst, this assumption may not be valid, and the error introduced could be significant. In all further developments emitter characteristics are chosen so that this error is insignificant.

For the probability density function of the burst shown in Figure 4, the mean and standard deviation are calculated, and Gaussian distributions having the same mean and standard deviation are simultaneously plotted. Figure 5 is a plot of the burst TOA

probability density function and the Gaussian approximation for a peak signal to noise ratio of 15 dB. Figure 6 is the plot of the burst TOA probability density function and Gaussian approximation for a peak signal to noise ratio of 25 dB.

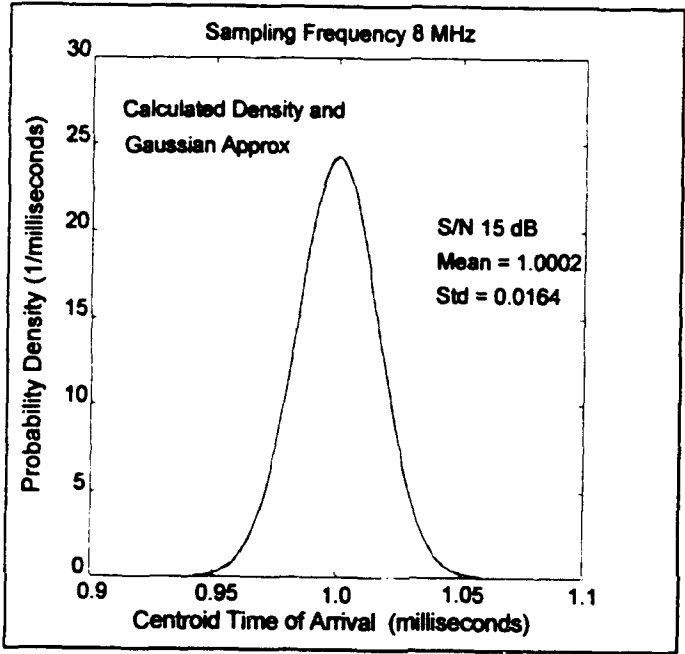


Figure 5. Burst TOA probability density vs. Gaussian approximation, 2.0 millisecond burst, 6.0 kHz PRF and 1.0 microsecond pulsewidth

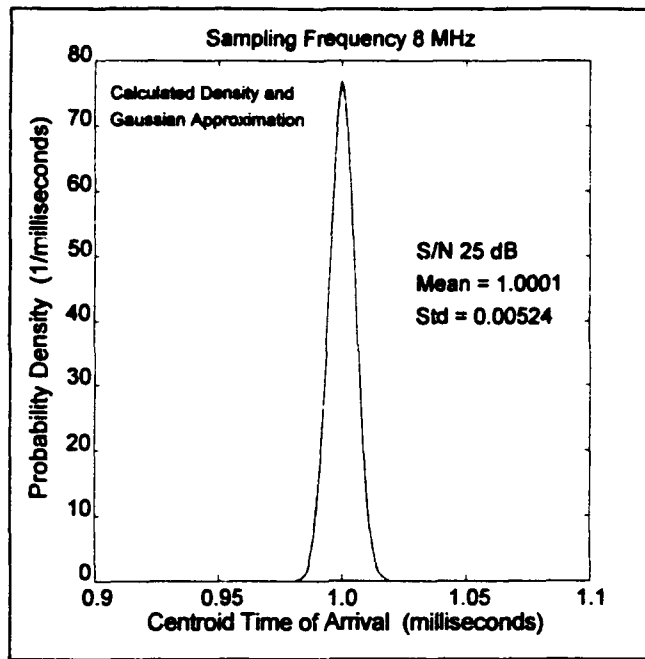


Figure 6. Burst TOA probability density vs. Gaussian approximation, 2.0 millisecond burst, 6.0 kHz PRF, and 1.0 microsecond pulsewidth

The burst TOA probability density functions are nearly indistinguishable from the Gaussian probability density function. The burst TOA can be considered Gaussian distributed in the Kalman filter development. In Appendix A a more complete analysis is conducted of the effects of peak signal to noise ratio, pulse width, and PRF on the probability density functions of the burst TOA.

B. BURST AND PULSE TDOA

As demonstrated in the previous sections, the TOA of pulse or burst can be approximated as a Gaussian random variable. If the TOA for each burst or pulse is considered independent, the TDOA can be calculated using the following equation:

$$\text{TDOA} = z_A - z_B \quad (7)$$

Where z_A = TOA of burst or pulse A, and
 z_B = TOA of burst or pulse B.

Time of arrival A and B can be bursts generated by an emitter scanning two different receivers, or the bursts generated by different scans of the emitter past the same receiver.

Time of arrival A and B can also be the time of arrival for two different pulses at the same sensor or the time of arrival of a single pulse at two different sensors.

If the TOA is expressed as the sum of a constant value which corresponds to the true TOA, and a zero mean Gaussian random variable, then the TOA is:

$$z_A = z_{0A} + v_A \quad (8)$$

Where z_A = the observed time of arrival,
 z_{0A} = the true time of arrival, and
 v_A = the noise present in the observed time of arrival.
 This noise has zero mean and variance V_A .

The noise term v_A is considered to be white noise, with zero mean and uncorrelated increments. Therefore, the expected value, $E[v_A v_B]$, is zero. The mean of the estimate of the TDOA are:

$$\mu_{\text{TDOA}} = E[z_A - z_B] = E[z_{0A} - z_{0B}] + E[v_A] - E[v_B] \quad (9)$$

$$\mu_{\text{TDOA}} = z_{0A} - z_{0B} \quad (10)$$

Therefore, the expected value of the TDOA is the difference between the true times of arrival for the two bursts, i.e. the true TDOA.

The variance of the estimate of the TDOA is:

$$\sigma_{TDOA}^2 = E[(TDOA - \mu_{TDOA})^2] \quad (11)$$

$$\sigma_{TDOA}^2 = E[(v_A - v_B)^2] \quad (12)$$

Since the increments of the noise are independent, and $E[v_A v_B] = 0$, the resulting variance of the TDOA estimate is:

$$\sigma_{TDOA}^2 = E[v_A^2 + v_B^2] = V_A + V_B \quad (13)$$

Therefore, the TDOA of a burst or a pulse is a Gaussian random variable with a mean value equal to the true TDOA, and a variance equal to the sum of the variances of the burst or pulse time of arrival estimates.

III. EMITTER LOCATION

The TDOA for a radar signal is the difference in the amount of time that a radar signal takes to reach two receivers. This research utilizes the time difference of arrival for bursts of pulses between two widely separated receivers and the TDOA for individual pulses between two closely spaced sensors to estimate the location of an emitter. Both of these TDOAs are functions of the emitter and receiver locations and the emitter characteristics. In the approaches pursued here only the two dimensional problem is considered, and the effect of altitude is ignored.

A. BURST TIME DIFFERENCE OF ARRIVAL (TDOA)

1. Problem Geometry

The TDOA of a radar signal burst for two widely separated receivers is primarily due to the amount of time required for the emitter to scan the two receivers. If the assumption is made that the emitter scans only in azimuth, then the TDOA is only a function of the scan rate of the emitter and the angle formed between the emitter and the two receivers. The scan rate is the angular rate of rotation of the emitter, and the angle formed by the emitter and the two receivers can be determined from the coordinates of the emitter and receivers. If the scan rate of the emitter is assumed constant and known a priori or from some other estimation method, then the TDOA becomes a function of

only the location of the emitter and the receivers. Figure 7 is the geometric relationship between the receivers, and the emitter.

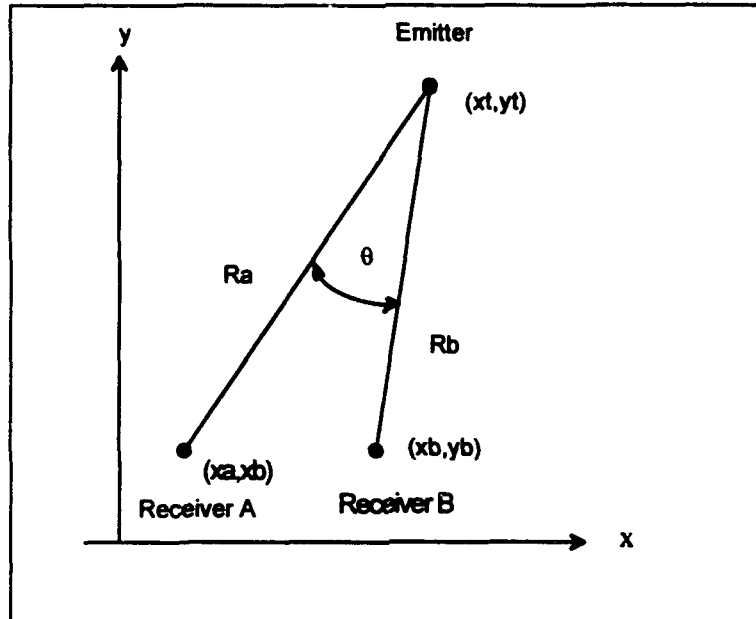


Figure 7. Burst TDOA geometry

Since the scan rate is known, the TDOA for an emitter scanning two receivers is only function of the angle θ formed by the emitters and the receivers. This angle can be found by applying vector geometry. If the positions of the receivers are known, the cross product of the position vectors from the two receivers to the target can be used to express the angle formed by the two receivers and the emitter in terms of the unknown quantities, the x and y coordinates of the emitter. The angle θ is calculated from the following equations:

$$\overline{Ra} \times \overline{Rb} = |\overline{Ra}| |\overline{Rb}| \sin(\theta) \quad (14)$$

$$\overline{Ra} = (xt - xa)\hat{i} + (yt - ya)\hat{j} \quad (15)$$

$$\overline{Rb} = (xt - xb)\hat{i} + (yt - yb)\hat{j} \quad (16)$$

$$\overline{Ra} \times \overline{Rb} = \begin{vmatrix} \hat{i} & \hat{j} & \hat{k} \\ (xt - xa) & (yt - ya) & 0 \\ (xt - xb) & (yt - yb) & 0 \end{vmatrix} \quad (17)$$

$$\sin(\theta) = \frac{(xt - xa)(yt - yb) - (yt - ya)(xt - xb)}{[(xt - xa)^2 + (yt - ya)^2]^{1/2} [(xt - xb)^2 + (yt - yb)^2]^{1/2}} \quad (18)$$

Where

- Ra = The position vector from receiver A to the emitter,
- Rb = the position vector from receiver B to the emitter,
- θ = the angle formed by the receivers and the emitter,
- xt, yt = the x and y coordinate of the emitter,
- xa, ya = the x and y coordinate of receiver A,
- xb, yb = the x and y coordinate of receiver B, and
- SR = the scan rate of the antenna in rad/sec.

If θ is small, the TDOA is found from the following equation.

$$TDOA = \frac{\theta}{SR} = \frac{1}{SR} \left[\frac{(xt - xa)(yt - yb) - (yt - ya)(xt - xb)}{[(xt - xa)^2 + (yt - ya)^2]^{1/2} [(xt - xb)^2 + (yt - yb)^2]^{1/2}} \right] \quad (19)$$

2. Loci of Constant TDOA

From equation (19) the burst TDOA for two widely separated receivers being scanned by a constantly rotating emitter is directly proportional to the angle formed by the two receivers and the emitter. In Appendix B an approximate relationship is developed to plot the loci of points where an emitter could lie and produce a specific TDOA observation. These loci of constant TDOA are shown in Figure 8.

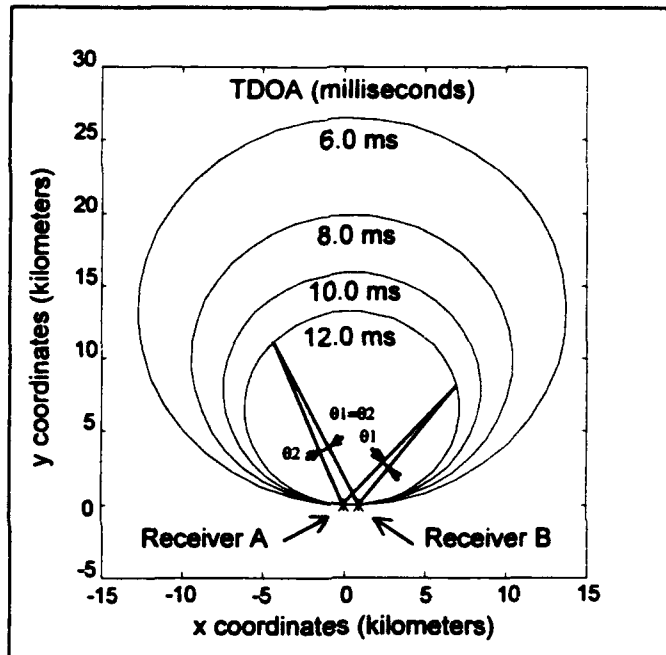


Figure 8. Loci of constant TDOA for an emitter scanning at a constant rate, scan rate 360 degrees/sec, receiver separation 1.0 kilometers

These loci demonstrate that for a single TDOA observation there exist an infinite number of possible location for the emitter. Another observation or measurement is required to uniquely estimate the location of the emitter.

If more than two receivers are used, a TDOA observation is available for each combination of receiver pairs. Plotting the loci of constant TDOA for each of the receiver pairs, multiple intersections occur, but all of the loci intersect at a common point, the location of the emitter. This is shown in Figure 9.

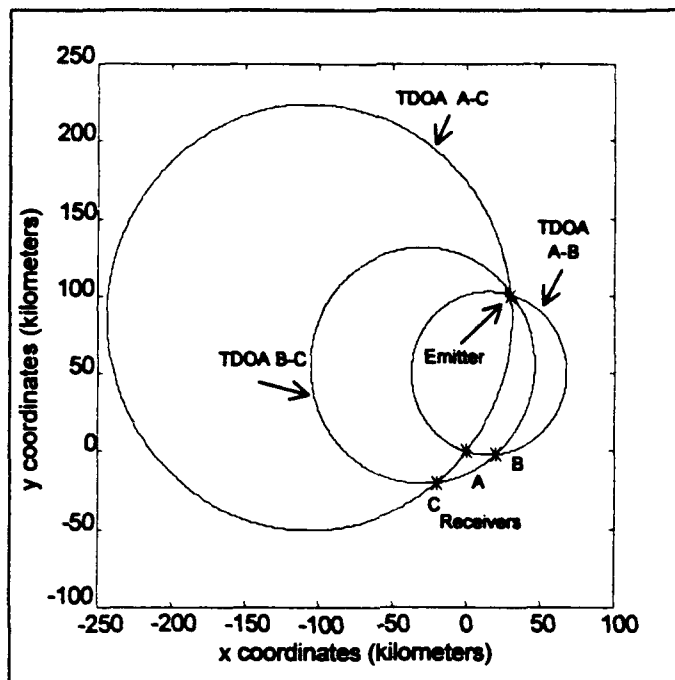


Figure 9. Loci of constant TDOA for an emitter scanning at a constant rate, scan rate 360 degrees/second, receiver locations as shown

3. Orthogonality of TDOA Observations

The performance of the Kalman filter varies based upon the quality of the observations available. Generally, the observations with the highest orthogonality perform the best. If data processing time or capability is limited, it is advantageous to use the observations with the highest orthogonality. The loci of constant TDOA are one way of visualizing and calculating the orthogonality of the observations.

A measure of the orthogonality of the TDOA observations is obtained from the dot product of the unit vectors tangent to the loci of constant TDOA. These vectors are calculated from the slope of the line tangent to the loci at the estimated location of the

emitter. Once the unit vectors tangent to the loci are found, their dot product yields the cosine of the angle formed by the two loci. The equation for the dot product is given below:

$$R_{t_1} \bullet R_{t_2} = \cos \theta \quad (20)$$

Where R_{t_1} = The unit vector tangent to the loci number 1,
 R_{t_2} = the unit vector tangent to loci number 2, and
 θ = the angle formed by the two loci.

The cosine of the angle formed by the loci is an indication of the orthogonality of the loci. If the cosine of θ is close to one then the loci are nearly parallel, and if the cosine of θ is zero the loci are orthogonal and lie at right angles to each other.

The unit vectors tangent to the loci are found using the following equation:

$$\bar{R}_t = \frac{1}{\sqrt{1+m^2}} \hat{x} + \frac{m}{\sqrt{1+m^2}} \hat{y} \quad (21)$$

Where R_t = the unit vector tangent to the loci, and
 m = the slope of the loci, dyt/dxt at the emitter.

The equations for the slope of the loci at an arbitrary point are developed in

Appendix C and presented here:

$$\frac{dyt}{dxt} = \frac{[(xt - xa)^2 \sin \psi - 2(xt - xa)(yt - ya) \cos \psi - (yt - ya)^2 \sin \psi]}{[(yt - ya)^2 \cos \psi - 2(xt - xa)(yt - ya) \sin \psi - (xt - xa)^2 \cos \psi]} \quad (22)$$

Where x_t, y_t = the x and y coordinates of the emitter,
 x_a, y_a = the x and y coordinates of receiver A,
 x_b, y_b = the x and y coordinates of receiver B, and
 ψ = the bearing from receiver A to receiver B.

The bearing from receiver A to receiver B is calculated from the following equation:

$$\psi = \arctan \left[\frac{y_b - y_a}{x_b - x_a} \right] \quad (23)$$

4. Ambiguity in TDOA Observations

Ambiguity in the burst TDOA observations is present if another burst is received by one of the receivers before all of the receivers detect the first burst. In the burst TDOA problem each of the receivers is scanned only once per rotation of the emitter. Ambiguity is possible if the distance separation between the receivers causes a burst from the next scan of the emitter to be received by a closer receiver before a distant receiver detects the burst from the first scan. This occurs if the time required for the signal to travel from one receiver to the next is greater than the time required for the emitter to complete one scan. This is unlikely. In even the fastest scanning emitters the scan rate is unlikely to be greater than 10 revolutions per second. For an emitter with a scan rate of 10 revolutions per second, the separation required to introduce ambiguity in the burst TDOA is 30,000 kilometers.

B. SINGLE PULSE TIME DIFFERENCE OF ARRIVAL (TDOA)

1. Problem Geometry

If two sensors are illuminated at the same time by the beam of an emitter sending out pulsed signals, the pulse TDOA is the difference in the amount of time required for a single pulse to reach the two sensors. Since electromagnetic waves travel at approximately the speed of light, the TDOA is a function of the difference in the distance that the pulse must travel. The difference in distance the pulse must travel is calculated from the geometry of the problem. Figure 10 is a diagram of the geometry of the problem.

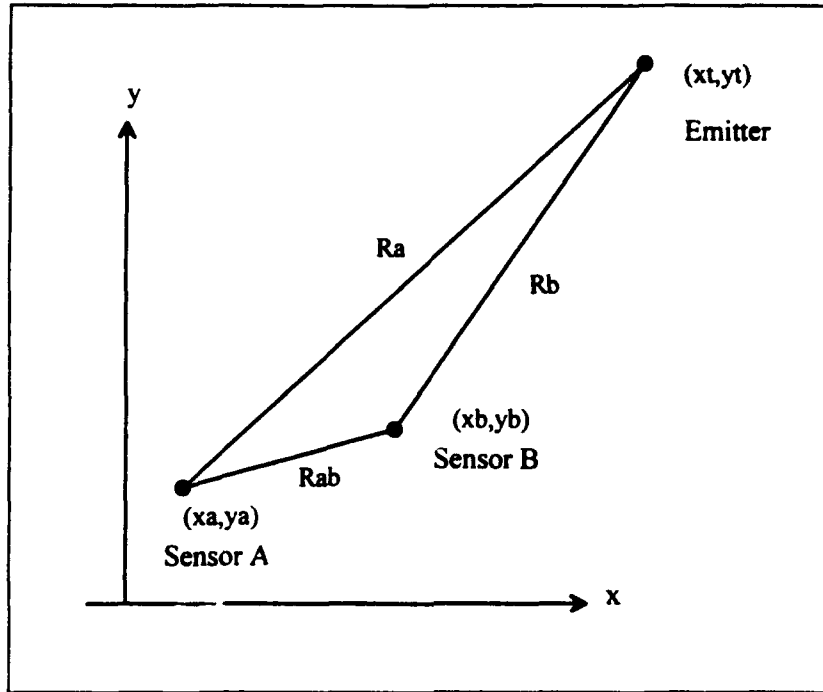


Figure 10. Single pulse TDOA geometry

The time difference of arrival for a pulse at sensors A and B is calculated from equation (24).

$$\text{TDOA} = \frac{\left[(x_t - x_a)^2 + (y_t - y_a)^2 \right]^{1/2} - \left[(x_t - x_b)^2 + (y_t - y_b)^2 \right]^{1/2}}{c} \quad (24)$$

Where

- TDOA = the time difference of arrival,
- x_t, y_t = the x and y coordinates of the emitter,
- x_a, y_a = the x and y coordinates of sensor A,
- x_b, y_b = the x and y coordinates of sensor B,
- c = the speed of light.

2. Loci of Constant TDOA

Given a pulse TDOA observation and sensor geometry, the possible location of the emitter is not unique and a locus of possible emitter locations exists. Figure 11 is a plot of equation (24) for constant values of TDOA and the sensor configuration shown. The sensors are separated by 500 meters. For the TDOA observations shown, the location of the emitter lies anywhere along these hyperbolic loci.

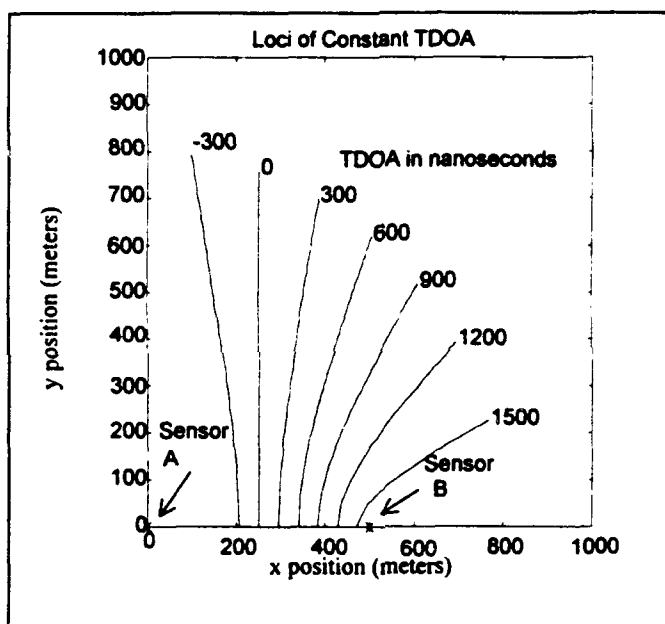


Figure 11. Loci of constant pulse TDOA, sensor separation 500 meters

If more than two sensors are used it is possible to determine a unique estimate of the emitter's location. The scenario shown in Figure 12 uses two widely separated receiver platforms with two sensors attached to each of the receiver platforms. With this

configuration, the loci of constant TDOA intersect at a single point and a unique estimate of the emitter's location can be obtained from the pulse TDOA observations.

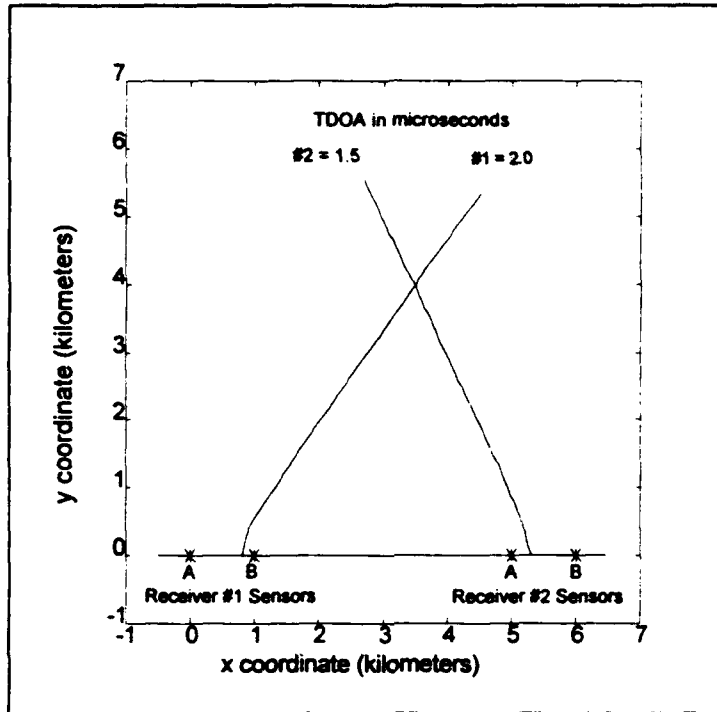


Figure 12. Loci of constant TDOA for two receiver platforms, sensor separation 500 meters

3. Orthogonality of the Loci of Constant TDOA

As previously developed in the burst TDOA problem the orthogonality of the TDOA observations can be related to the orthogonality of the loci of constant TDOA. The dot product of the unit vectors tangent to the loci give the cosine of the angle between the loci and a good indication of the orthogonality of the TDOA observations. The unit vectors tangent to the loci are calculated using equation (21). The equations for

the slope of the loci of constant TDOA are developed in Appendix C. The slope of the loci, dx/dy , is given by the following equation:

$$\frac{dy}{dx} = \frac{(y_t - y_a)^2 \cos \psi - (x_t - x_a)(y_t - y_a) \sin \psi}{(x_t - x_a)(y_t - y_a) \cos \psi - (x_t - x_a)^2 \sin \psi} \quad (25)$$

Where x_t, y_t = the x and y coordinates of the emitter,
 x_a, y_a = the x and y coordinates of sensor A,
 x_b, y_b = the x and y coordinates of sensor B, and
 ψ = the bearing from sensor A to sensor B.

The bearing from sensor A to sensor B is calculated from the following:

$$\psi = \arctan \left[\frac{(y_b - y_a)}{(x_b - x_a)} \right] \quad (26)$$

4. Ambiguity in Single Pulse TDOA Observations

Ambiguity in pulse TDOA observations develops if a second pulse is detected by one of the sensors before both of the sensors detect the first pulse. This can occur if the amount of time required for a pulse to travel from one sensor to the next is longer than the PRI. Therefore, the separation of sensors determines the highest PRF that signals can have and still be detected without ambiguity.

$$PRF_{\max} = \frac{1}{PRI} = \frac{c}{R_{ab}} \quad (27)$$

Where R_{ab} = the distance between sensor A and sensor B, and
 c = the speed of light.

For sensors separated by a distance of 500 meters the smallest PRI an emitter could have and be detectable without ambiguity is 1.66 microseconds. This corresponds to a PRF of approximately 600 kHz.

Estimates of the PRI of the emitter can be calculated from the time interval between pulses at each of the sensors. Therefore, the PRI can be estimated independently and used to test the TDOA observations for ambiguity.

IV. KALMAN FILTERING

A. THE EXTENDED KALMAN FILTER

There are several methods of linearizing a nonlinear problem to allow the Kalman filter to be used. The problem itself can be linearized by expanding the equations of state in a Taylor series around some norm. This approach is often used to derive equations of state in aircraft stability and control problems. The nonlinear equations of state are expanded and derived for perturbations around some equilibrium trim point. As long as the perturbations from the trim point are within acceptable limits this linear approximation will be acceptable and linear Kalman Filter theory can be applied. In the Extended Kalman Filter, the plant and full nonlinear equations of state are used, but the Kalman filter gain is calculated using a linear approximation of the model. The general equations of state are given by:

$$x(k+1) = f(x(k), w(k), k) \quad (28)$$

Where: $x(k)$ = state of the system,
 $w(k)$ = the plant driving noise.
The function $f(\bullet)$ can be a nonlinear function of the states, the noise, or k .

The general equations for the observations are given by:

$$z(k) = h(x(k), v(k), k) \quad (29)$$

Where: $z(k)$ = the measurements of the system, and
 $v(k)$ = the measurement noise of the system.

The function $h(\bullet)$ can be a nonlinear function of the states, the measurement noise, or k . The measurement noise and the plant driving noise are assumed to be zero mean white noise.

The extended Kalman filter is given by equations (30) through (32). These equations utilize the nonlinear relationships to predict the states and observations of the the system. The smoothed estimates of the states are calculated using the Kalman gain calculated with a linearized version of the Kalman gain equation.

$$\hat{x}(k+1|k) = f(\hat{x}(k|k), k) \quad (30)$$

$$\hat{z}(k+1|k) = h(\hat{x}(k+1|k), k) \quad (31)$$

$$\hat{x}(k+1|k+1) = \hat{x}(k+1|k) + G(k+1)(z(k+1) - \hat{z}(k+1|k)) \quad (32)$$

Where

- $\hat{x}(k|k)$ = the current estimate of the states,
- $\hat{x}(k+1|k)$ = the predicted estimate of the states,
- $z(k+1)$ = the observed measurements,
- $G(k+1)$ = the Kalman gain,
- $w(k)$, the plant driving noise, is assumed to be zero mean.
- $v(k)$, the measurement noise, is assumed to be zero mean.

Equation (30) is used to predict the next state of the system, given the current state of the system and the current input. Since the plant driving noise is assumed to have zero mean, it is assumed that the plant driving noise does not contribute the expected value of the next state. The next observation is predicted using equation (31). This equation uses the predicted state of the system. The measurement noise is assumed to have zero mean, and does not contribute to the the expected value of the observation. The smoothed estimates of the states of the system are found with equation (32). This equation uses the

Kalman gain which is calculated using equations (33) through (35). These equations use first order linear approximations of state prediction and observation equations. The covariance prediction equations and the Kalman gain equations are given as:

$$P(k+1|k) = \hat{\Phi}P(k|k)\hat{\Phi}^T + Q \quad (33)$$

$$P(k+1|k+1) = [I - G(k+1)\hat{H}]P(k+1|k) \quad (34)$$

$$G(k+1) = P(k+1|k)\hat{H}^T[\hat{H}P(k+1|k)\hat{H}^T + R]^{-1} \quad (35)$$

Where $P(k|k)$ = the current estimate of the covariance of the estimation error,
 $P(k+1|k)$ = the predicted covariance, given the current value,
 $P(k+1|k+1)$ = the predicted covariance given the current observation,
 Q = the covariance of the plant driving noise,
 R = the covariance of the measurement noise,

$$\hat{\Phi} = \left. \frac{\partial f(x(k), u(k), w(k), k)}{\partial x(k)} \right|_{x(k)=x(k|k), u(k)=u(k), w(k)=0}, \text{ and}$$

$$\hat{H} = \left. \frac{\partial h(x(k), v(k), k)}{\partial x(k)} \right|_{x(k)=x(k|k), v(k)=0}$$

To initialize the Kalman filter, initial estimates for the states and the covariance matrix must be provided. The values chosen are generally:

$$\hat{x}(0|0) = E[x(0)], \text{ and} \quad (36)$$

$$P(0|0) = E[\{x(0) - \hat{x}(0|0)\}\{x(0) - \hat{x}(0|0)\}^T] = \text{cov}[x(0)] \quad (37)$$

The Kalman filter provides optimal performance, and guarantees convergence and stability, but the extended Kalman filter does not. In many applications the extended

Kalman filter provides accurate estimates of the states, but may not guarantee convergence and stability. Generally the convergence and stability are highly dependent on the values chosen for the initial estimates of the states, and covariance. In any application of the extended Kalman filter, the convergence and stability of the solutions must be thoroughly explored for as wide a range of initial conditions as is possible.

B. ERROR ELLIPSOIDS

The error ellipsoid is a means of visualizing the error in the estimate of the states of the Kalman filter. The uncertainty in the estimate is expressed in the error covariance P. The error covariance matrix P is the expected value of the covariance of the error in the states.

$$P = E[(\hat{x} - \bar{x})(\hat{x} - \bar{x})^T] \quad (38)$$

Where \hat{x} = the state estimate of the Kalman filter,
 \bar{x} = the mean of the states of the Kalman filter

If the noise entering the Kalman filter is Gaussian then the estimates of the states of the Kalman filter also have a Gaussian distribution. This is because a linear transformation of a set of Gaussian random variables will result in another set of Gaussian random variables.

The equation for the probability density function for a joint Gaussian random variable is:

$$f_x(x) = \frac{1}{(2\pi)^{N/2} |\det P|^{1/2}} \exp[-1/2((x - \bar{x})^T P^{-1}(x - \bar{x}))] \quad (39)$$

Where x = the vector of N random variables,
 \bar{x} = the expected value of x , $E[x]$, and
 P = the error covariance matrix of x .

The error covariance matrix is given by the following:

$$P = \begin{bmatrix} p_{11} & p_{12} & \dots & p_{1N} \\ p_{21} & p_{22} & \dots & p_{2N} \\ \cdot & \cdot & \dots & \cdot \\ \cdot & \cdot & \dots & \cdot \\ p_{N1} & p_{N2} & \dots & p_{NN} \end{bmatrix} \quad (40)$$

Where $p_{ij} = E[(x_i - \bar{x}_i)(x_j - \bar{x}_j)]$

A surface in N space can be found where the probability of x will be a constant. This surface exists over the values of x for which the argument $(x - \bar{x})^T P^{-1}(x - \bar{x})$ is a constant. The total probability that the values of x are lie on the surface defined is found by integrating the probability density function over the entire surface. These surfaces of constant probability are called error ellipsoids of constant probability. If the argument $(x - \bar{x})^T P^{-1}(x - \bar{x})$ is set equal to the constant c^2 then the probabilities that the value of x will lie within the ellipsoid formed in N space is given in Table 1.

		c		
		1	2	3
N	1	0.683	0.955	0.997
	2	0.394	0.865	0.989
	3	0.200	0.739	0.971

Table 1. PROBABILITIES FOR ERROR ELLIPSOIDS

In the Kalman filter application pursued here the estimates of the location of the emitter are joint Gaussian random variables. The mean of the steady state estimate of the location of the emitter is considered the true location of the emitter, and the difference between the estimate of the location of the emitter and the mean of the steady state estimates is the error. This error term is used to form the error covariance in equation (38). Redefining the error in the estimate of the location of the emitter, the argument of the joint probability density function is:

$$c^2 = (\tilde{x}^T P^{-1} \tilde{x}) \quad (41)$$

Where $x = \begin{bmatrix} \tilde{x}_t \\ \tilde{y}_t \end{bmatrix} = \begin{bmatrix} \hat{x}_t - \bar{x}_t \\ \hat{y}_t - \bar{y}_t \end{bmatrix}$, the error in the estimate of the emitter location,
 $P =$ the error covariance matrix $\begin{bmatrix} P_{11} & P_{12} \\ P_{12} & P_{22} \end{bmatrix}$, and
 $c =$ a constant.

When the argument in equation (41) is expanded and the inverse of the P matrix is found, the following equation results:

$$c^2 = \frac{1}{P_{11}P_{22} - P_{12}^2} \begin{bmatrix} \tilde{x}_t & \tilde{y}_t \end{bmatrix} \begin{bmatrix} P_{22} & -P_{12} \\ -P_{12} & P_{11} \end{bmatrix} \begin{bmatrix} \tilde{x}_t \\ \tilde{y}_t \end{bmatrix} \quad (42)$$

This further reduces to:

$$c^2 = \frac{P_{22}\tilde{x}t^2 - 2P_{12}\tilde{x}t\tilde{y}t + P_{11}\tilde{y}t^2}{P_{11}P_{22} - P_{12}^2} \quad (43)$$

To facilitate plotting this equation, the y estimate of the location of the emitter is solved for in terms of the x coordinates of the emitter. Equation (43) is rewritten in the form of a quadratic equation $Ay^2 + By + C = 0$ where

$$A = \frac{P_{11}}{P_{11}P_{22} - P_{12}^2} \quad B = \frac{-2P_{12}\tilde{x}t}{P_{11}P_{22} - P_{12}^2} \quad C = \frac{P_{22}\tilde{x}t^2}{P_{11}P_{22} - P_{12}^2} - c^2$$

The quadratic formula is used to calculate the value of yt in terms of xt and the elements of the error covariance matrix. The following equation results:

$$yt = \frac{P_{12}\tilde{x}t}{P_{11}} \pm \sqrt{\frac{(P_{11}P_{22} - P_{12}^2)}{P_{11}^2}(P_{11}c^2 - \tilde{x}t^2)} \quad (44)$$

The maximum and minimum values of the error xt are found from the locations where $xt^2 = P_{11}c^2$. If $xt^2 > P_{11}c^2$ a real solution to equation (44) will not exist.

V. SIMULATION RESULTS

A. THE BURST TDOA KALMAN FILTER

1. Extended Kalman Filter Equations

An extended Kalman filter algorithm is developed to estimate of the emitter location from burst TDOA observations. Simulated data is used to test the accuracy and stability of the algorithm. The TDOA measurement noise is assumed to be white gaussian. The following assumptions are made to simplify the problem:

1. The emitter scans in azimuth at a constant rate.
2. An estimate of the scan rate of the emitter is known a priori.
3. Some method is used to calculate the TDOA of the radar signal between the two receivers, and the error on this TDOA observation is modeled as additive white Gaussian noise with variance R.
4. The emitter is stationary.
5. The x and y coordinates of the emitter and receivers are measured with respect to a fixed coordinate reference.
6. The exact locations of the receivers are known for all points in time.

These assumptions simplify the problem, but do not reduce its usefulness, because the algorithm can easily be modified to account for these assumptions.

The estimated state and observations are calculated from the following:

$$\hat{\mathbf{x}}(k+1) = \hat{\mathbf{x}}(k) = \begin{bmatrix} \hat{x}_t(k) \\ \hat{y}_t(k) \end{bmatrix} \quad (45)$$

$$\hat{z}_{ab}(k) = \frac{1}{SR} \left[\frac{(x_t - x_a)(y_t - y_b) - (y_t - y_a)(x_t - x_b)}{[[[(x_t - x_a)^2 + (y_t - y_a)^2][(x_t - x_b)^2 + (y_t - y_b)^2]]^{1/2}} \right] + v_{ab}(k) \quad (46)$$

$$\hat{z}_{ac}(k) = \frac{1}{SR} \left[\frac{(xt - xa)(yt - yc) - (yt - ya)(xt - xc)}{[[[(xt - xa)^2 + (yt - ya)^2][(xt - xc)^2 + (yt - yc)^2]]^{1/2}} \right] + v_{ac}(k) \quad (47)$$

$$\hat{z}_{bc}(k) = \frac{1}{SR} \left[\frac{(xt - xb)(yt - yc) - (yt - yb)(xt - xc)}{[[[(xt - xb)^2 + (yt - yb)^2][(xt - xc)^2 + (yt - yc)^2]]^{1/2}} \right] + v_{bc}(k) \quad (48)$$

Where

- xt, yt = the estimate of the emitter's x and y coordinates,
- SR = the scan rate of the emitter,
- v_{xx} = the measurement noise present in the TDOA observation between two receivers,
- xa, ya = the x and y coordinates of receiver A,
- xb, yb = the x and y coordinates of receiver B,
- xc, yc = the x and y coordinates of receiver C,
- $xt, yt, xa, ya, xb, yb, xc,$ and yc are all functions of k .

Since the emitter is stationary, the state transition matrix in equation (45) is the identity matrix. Therefore, the predicted estimate of the emitter's location is the same as the current estimate of the location. Since the coordinates of receivers A, B, and C are known at all points in time and the scan rate is known a priori, the predicted TDOA observations are only functions of the predicted states.

The Kalman filter is implemented as three separate Kalman filters linked together. Each receiver processes the received observations separately. They calculate Kalman gains and an error covariance matrix from its observations, and then use these to calculate an estimate of the location of the emitter. This estimate is then passed to the next receiver. This algorithm is used because it facilitates implementation in hardware.

The equations necessary for the Extended Kalman Filter implementation are:

$$P(k+1|k) = P(k|k) + Q \quad (49)$$

$$P(k+1|k+1) = [I - G_{xx}(k+1)\hat{H}_{xx}]P(k+1|k) \quad (50)$$

$$G_{xx}(k+1) = P(k+1|k)\hat{H}_{xx}^T [\hat{H}_{xx}P(k+1|k)\hat{H}_{xx}^T + V_{xx}]^{-1} \quad (51)$$

Where

- $P(k+1|k)$ = the predicted error covariance,
- $P(k|k)$ = the current error covariance,
- Q = the covariance of the state disturbances,
- $G_{xx}(k+1)$ = the Kalman Gain calculated for the TDOA observation between two of the receivers,
- V_{xx} = the covariance of the measurement noise for the TDOA observation between two of the receivers,
- $H_{xx} = \begin{bmatrix} \frac{\partial h_{xx}(k)}{\partial x_1} & \frac{\partial h_{xx}(k)}{\partial y_1} \end{bmatrix}$

The algebraic equations that make up the partial derivatives in H_{xx} are extensive and are omitted here for clarity. The derivation of H_{xx} is included in Appendix D.

The flow chart for the Kalman filtering algorithm is shown in Figure 13. This flowchart provides the basic logic flow of the Kalman filtering algorithm. In an actual implementation, TDOA observations are available, and only the portion contained within the dotted outline is required. The additional portion of the algorithm generates the observations used to test the algorithm.

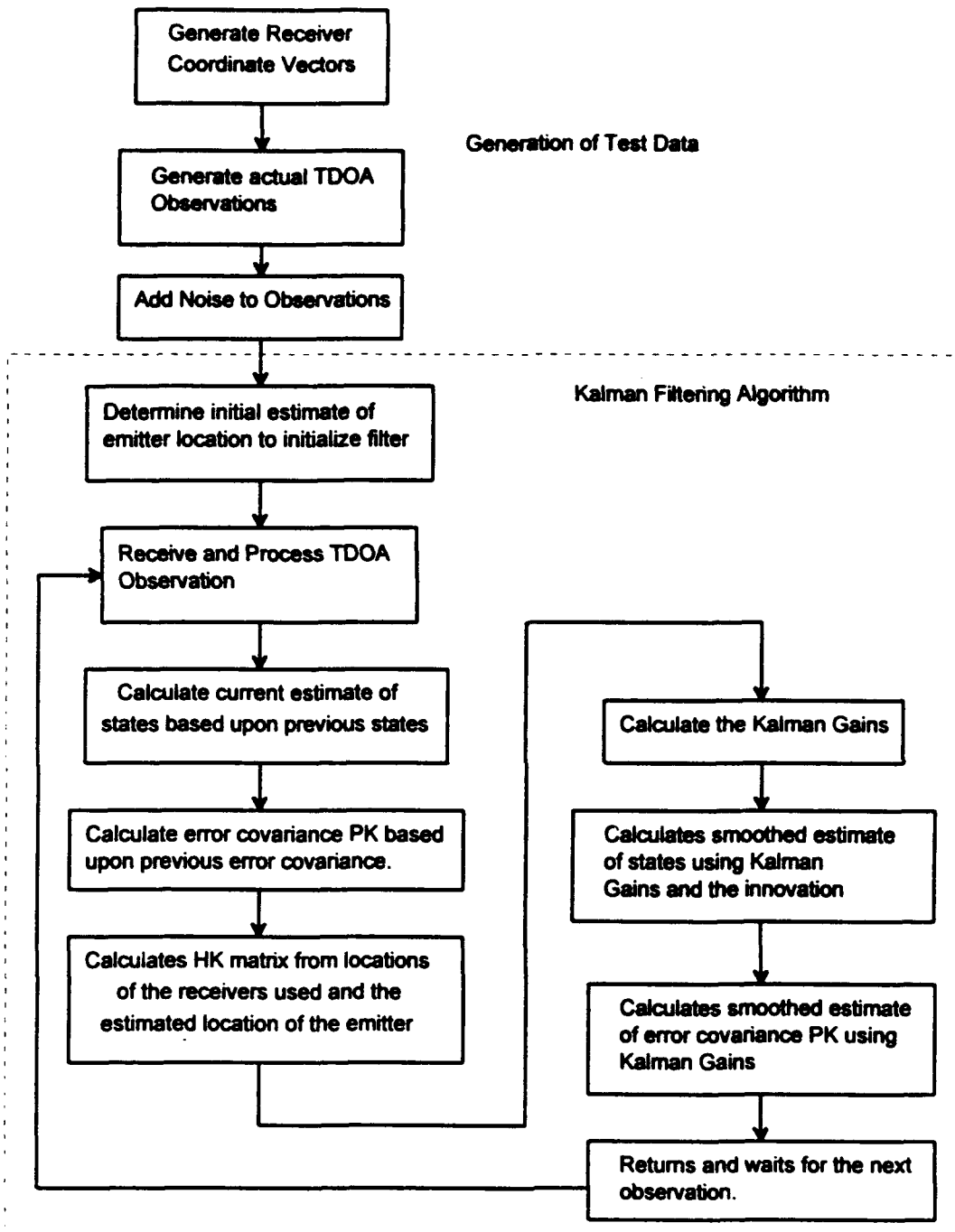


Figure 13. Flowchart for burst TDOA Kalman filter

2. Burst TDOA Simulations

The following scenario is used to test the burst TDOA Kalman filter algorithm. Three receivers are used and all three of the available TDOA observations are used to estimate the location of the emitter. The initial locations of the receivers and their velocities and bearings are shown in Figure 14.

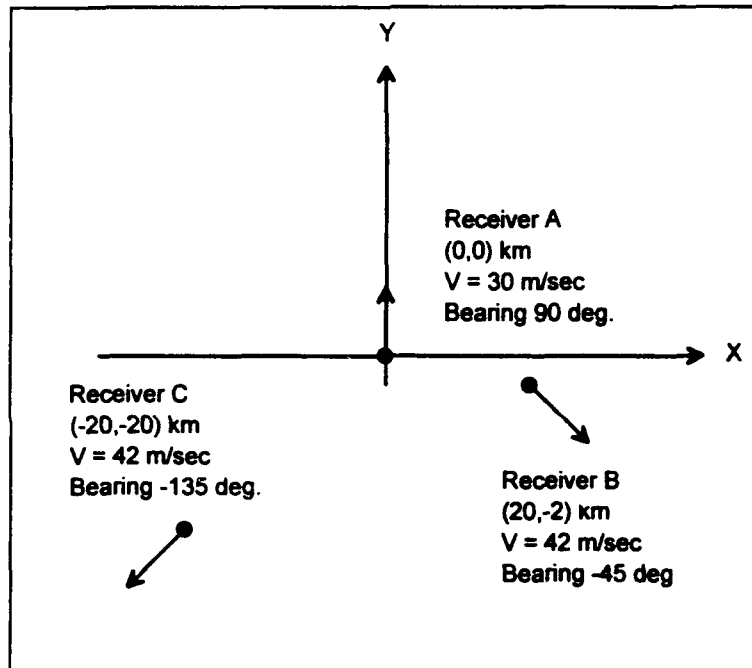


Figure 14. Initial location and velocity of receivers

The emitter locations are shown in Figure 15.

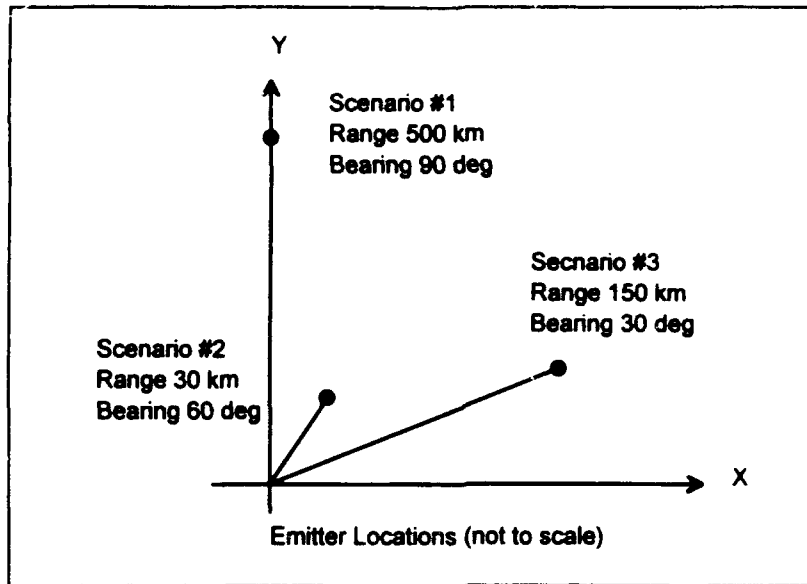


Figure 15. Emitter locations for burst TDOA filtering scenarios

The following characteristics are used for the emitter. These characteristics are typical for long range search radar.

Beamwidth	2.0 deg.
Scan Rate	360 deg/sec.
PRF	2000 Hz
Pulsewidth	1.0 microsecond
Peak Signal to Noise Ratio	15 dB

Although the algorithm has the capability to account for different signal strengths and resulting error variances, all of the receivers are considered identical with identical signal to noise ratios. An 8 MHz sampling rate is assumed. The algorithms developed in Appendix A are used to calculate the variance of the error present in the TDOA observations for the signal to noise ratio and the sampling rates chosen. In the tests of Kalman filtering algorithm, this error is modeled as zero mean white Gaussian noise, that

is added to the true TDOA observations. The variance of the TDOA observation noise is 5.660×10^{-9} for all of the scenarios.

For all of the scenarios the a priori estimate of the emitter location is chosen as (0,10) kilometers. The filter parameters Q , the covariance of the state excitation, and P_0 , the initial error covariance, are varied until the filter converges well. All of the scenarios are run for twenty five TDOA observations. Given the scan rate of the emitter, the real-time length of the simulation is twenty five seconds.

Three plots are presented for each scenario. The first plot is an X-Y plot of the estimates of the coordinates of the emitter. This plot demonstrates the track of the final estimate of the emitter location after all three TDOA observations are processed for each time step. In this plot the loci of constant TDOA that correspond to the final steady state TDOA observations are also plotted. Some of the loci do not intersect exactly at the emitter. The equations used to plot the loci assume that the distance to the emitter is much greater than the separation of the receivers, and in some of the scenarios this assumption is not valid. The loci visually illustrate the relationship between the TDOA observations and give a visual indication of the orthogonality of the observations. The 3σ error ellipsoids are also plotted for the 1st, 8th, 15th, and 22nd estimates of the emitter location. These ellipsoids provide a visual indication of the accuracy of the location estimate.

The second plot is the estimate of the x and y coordinates of the emitter vs. the number of TDOA observations. This plot gives a visual indication of how rapidly the estimates of the emitter location converge on the true coordinates of the emitter.

The third plot is an X-Y plot that shows the true emitter coordinates, the loci of constant TDOA, and the estimates of the emitter coordinates in the vicinity of the mean steady state estimate of the emitter coordinates. The 3σ error ellipsoid is plotted for the steady state estimate, and the length of the major and minor axis of the error ellipsoid give an indication of the maximum error in the estimate.

a. Scenario #1

In the first scenario the performance of the burst TDOA filter is tested for an emitter at a range of 500 kilometers from the origin and a bearing of 90 degrees from the x coordinate axis. The initial error covariance matrix, P_0 , and the variance of the state excitation, Q , are varied until the filter converges to a steady state value within ten observations. The plots presented in figures 16 through 18 are representative of the results obtained. The filter converges very well, and as shown in figures 16 and 18 the estimate of the location of the emitter converges to the true location of the emitter. The values that gave the best convergence were:

$$P_0 = \begin{bmatrix} 1.0 & 0 \\ 0 & 1.0 \end{bmatrix} \times 10^{20} \text{ m}^2, \text{ and} \quad Q = \begin{bmatrix} 4.0 & 0 \\ 0 & 4.0 \end{bmatrix} \times 10^6 \text{ m}^2.$$

As shown in Figure 16, the 3σ error ellipsoids grow larger as the estimate of the location of the emitter grows closer to the actual location. Because the distance to the emitter is large in relation to the separation of the receivers, the TDOA observations are very close to each other. The estimated location of the emitter does not approach the true location until the error covariance matrix and subsequently the Kalman gains grow large enough to amplify the very small differences in the TDOA and drive the states of the filter. A high value for Q is required to drive the error covariance matrix high enough. If a smaller value of Q is used, the filter reached a steady state value far from the true location of the emitter.

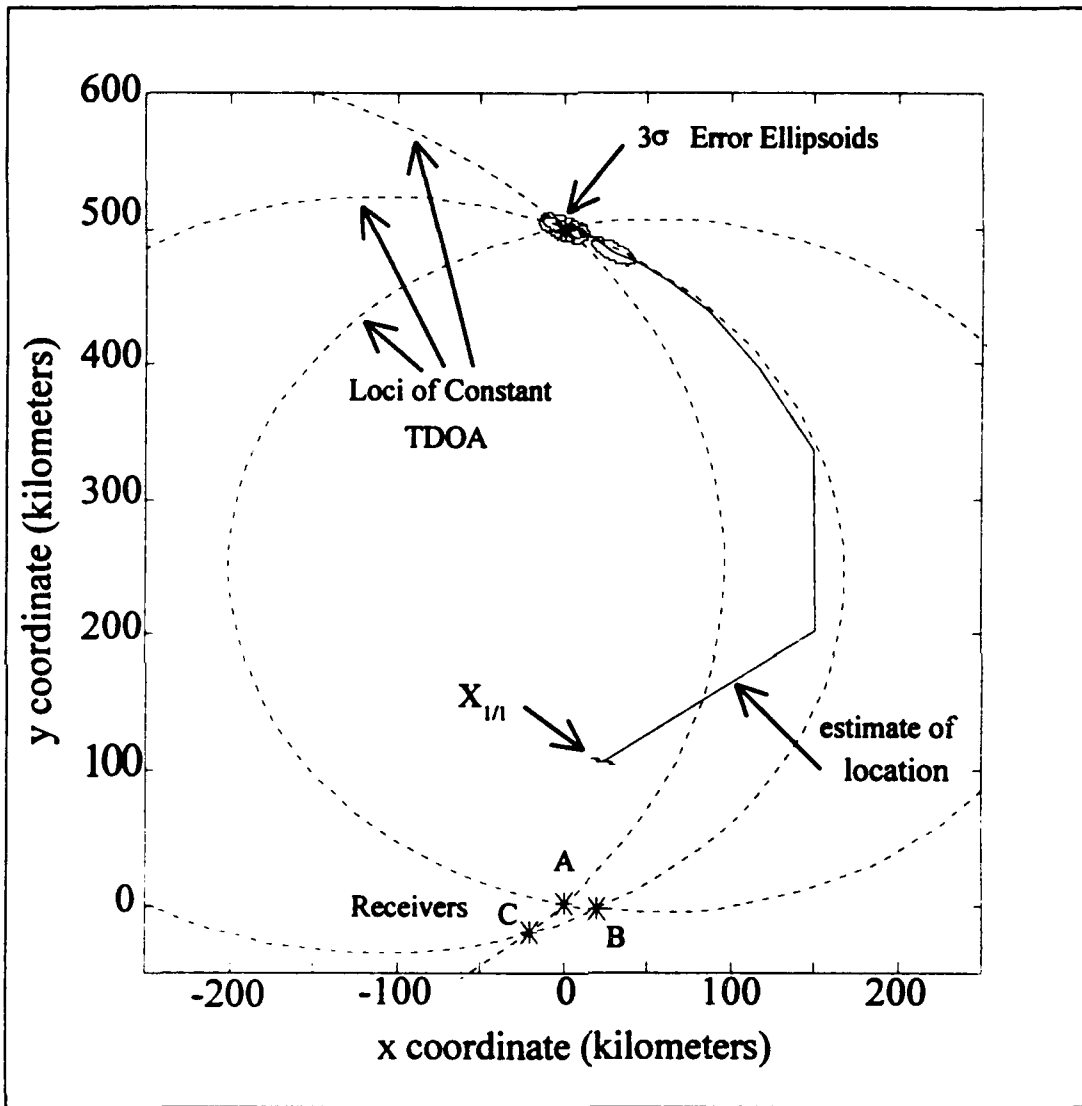


Figure 16. Scenario #1 Estimates of the location of the emitter

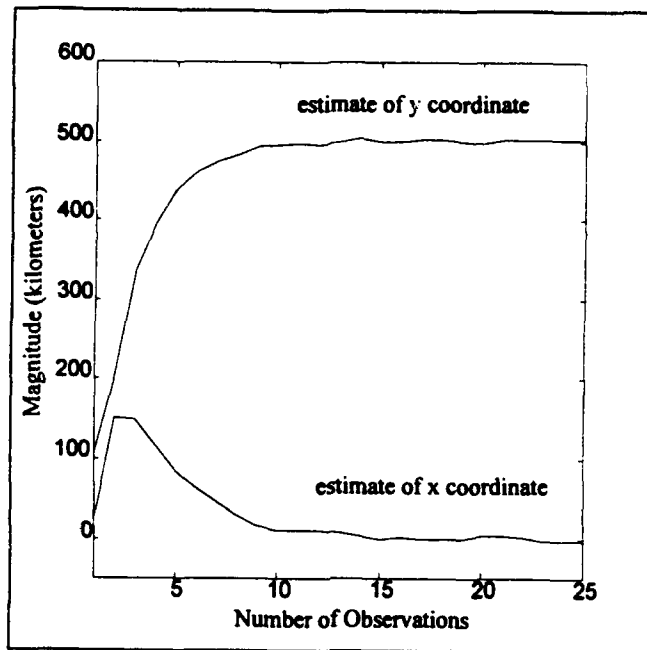


Figure 17. Scenario #1 Estimates of emitter coordinates vs. observations

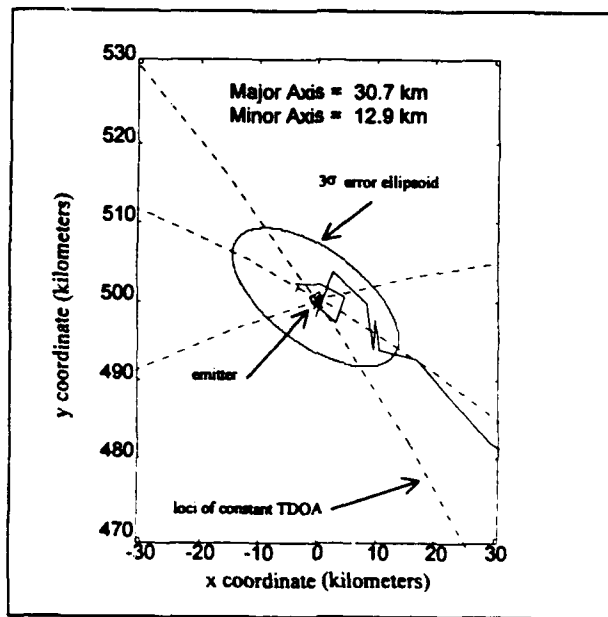


Figure 18. Scenario #1 Close-up of steady state estimate of emitter location

b. Scenario #2

In the second scenario, the performance of the burst TDOA filter is tested at an intermediate range. The emitter location is chosen at a range of 150 kilometers from the origin and at a bearing of 30 degrees from the x coordinate axis. The coordinates of the emitter are (130, 75) kilometers. The initial error covariance matrix, P_0 , and the variance of the state excitation term, Q , are varied until the filter converges to a the correct location within approximately ten observations. The plots presented in figures 19 through 21 are representative of the results obtained. The values that give the best results are:

$$P_0 = \begin{bmatrix} 1.0 & 0 \\ 0 & 1.0 \end{bmatrix} \times 10^{20} \text{ m}^2, \text{ and } Q = \begin{bmatrix} 5.0 & 0 \\ 0 & 5.0 \end{bmatrix} \times 10^4 \text{ m}^2.$$

The filter performed very well. The orthogonality of the TDOA observations in the vicinity of the emitter is high, and the estimate of the emitter location converged to the proper location quickly and smoothly. The final steady state estimate is stable and no numerical problems are present. The 3σ error ellipsoids are not visible in figure 19 because of the scale of the figure.

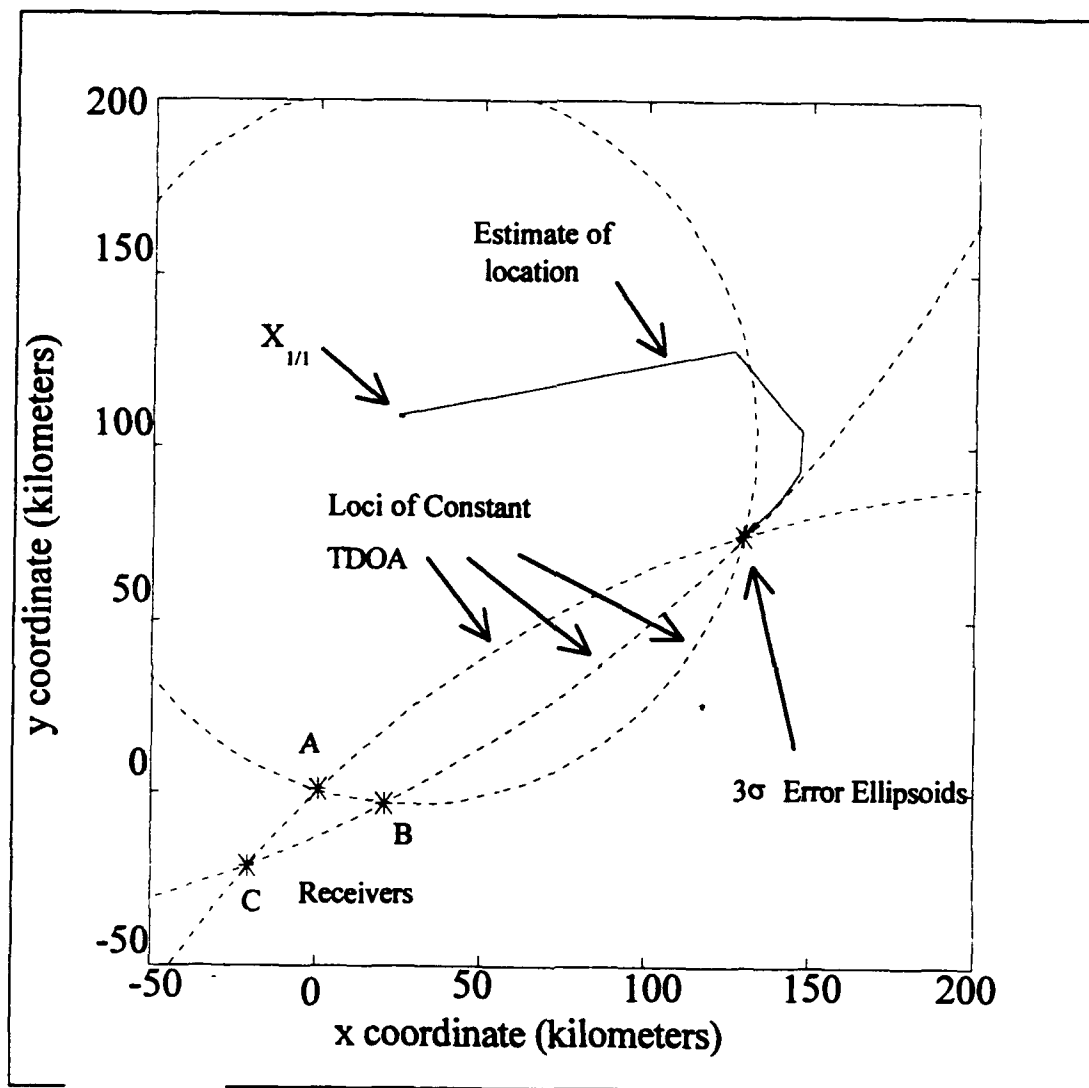


Figure 19. Scenario #2 Estimates of emitter location

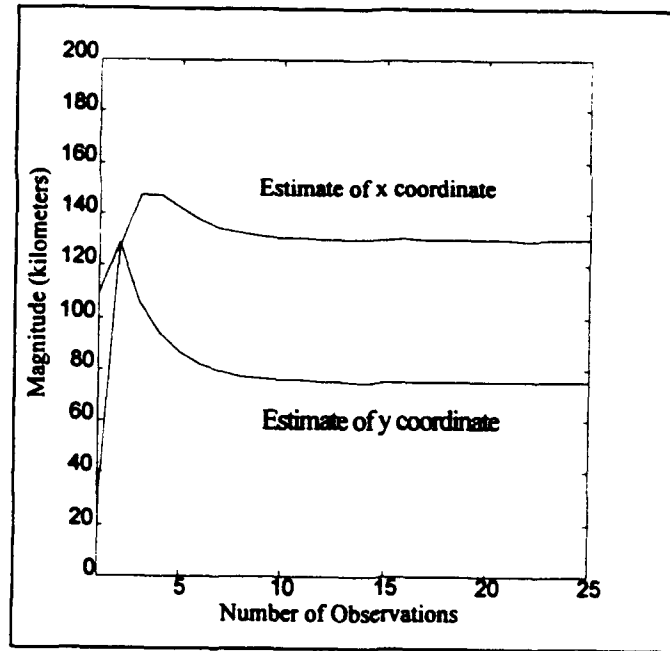


Figure 20. Scenario #2 Estimates of emitter coordinates vs observations

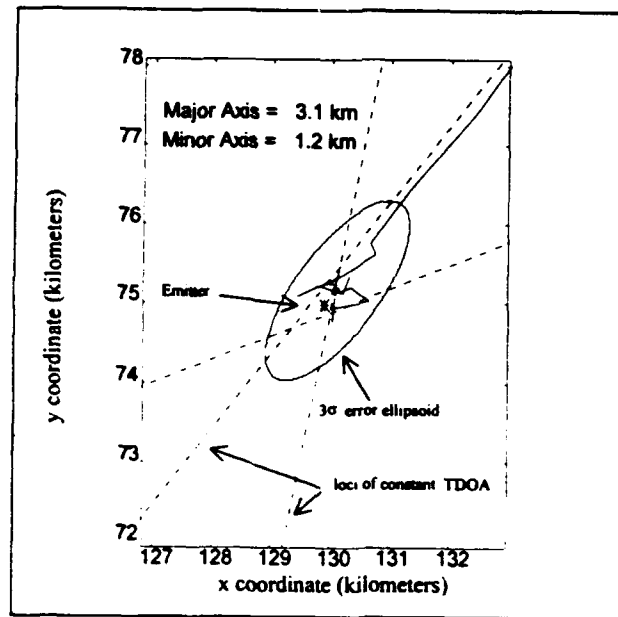


Figure 21. Close-up of the steady state estimate of emitter location

c. Scenario #3

In the third scenario the performance of the burst TDOA filter is tested for an emitter at close range. The emitter location is chosen at a range of 30 kilometers from the origin and at a bearing of 60 degrees from the x coordinate axis. The initial error covariance matrix, P_0 , and the variance of the state excitation term, Q , are varied until the filter converged to the correct location of the emitter within approximately ten observations. The plots presented in figures 22 through 24 are representative of the results obtained. The values that give the best results are:

$$P_0 = \begin{bmatrix} 1.0 & 0 \\ 0 & 1.0 \end{bmatrix} \times 10^{15} \text{ m}^2, \text{ and } Q = \begin{bmatrix} 40 & 0 \\ 0 & 40 \end{bmatrix} \text{ m}^2.$$

Although the loci of constant TDOA plotted in figure 22 do not intersect at the emitter, they indicate that the orthogonality of the TDOA observations is high and accurate results are expected. Figure 23 shows that the estimates of the emitter location converged to the correct location of the emitter rapidly and smoothly. Because of the large scale of the plot, the 3σ error ellipsoids are not visible in figure 22.

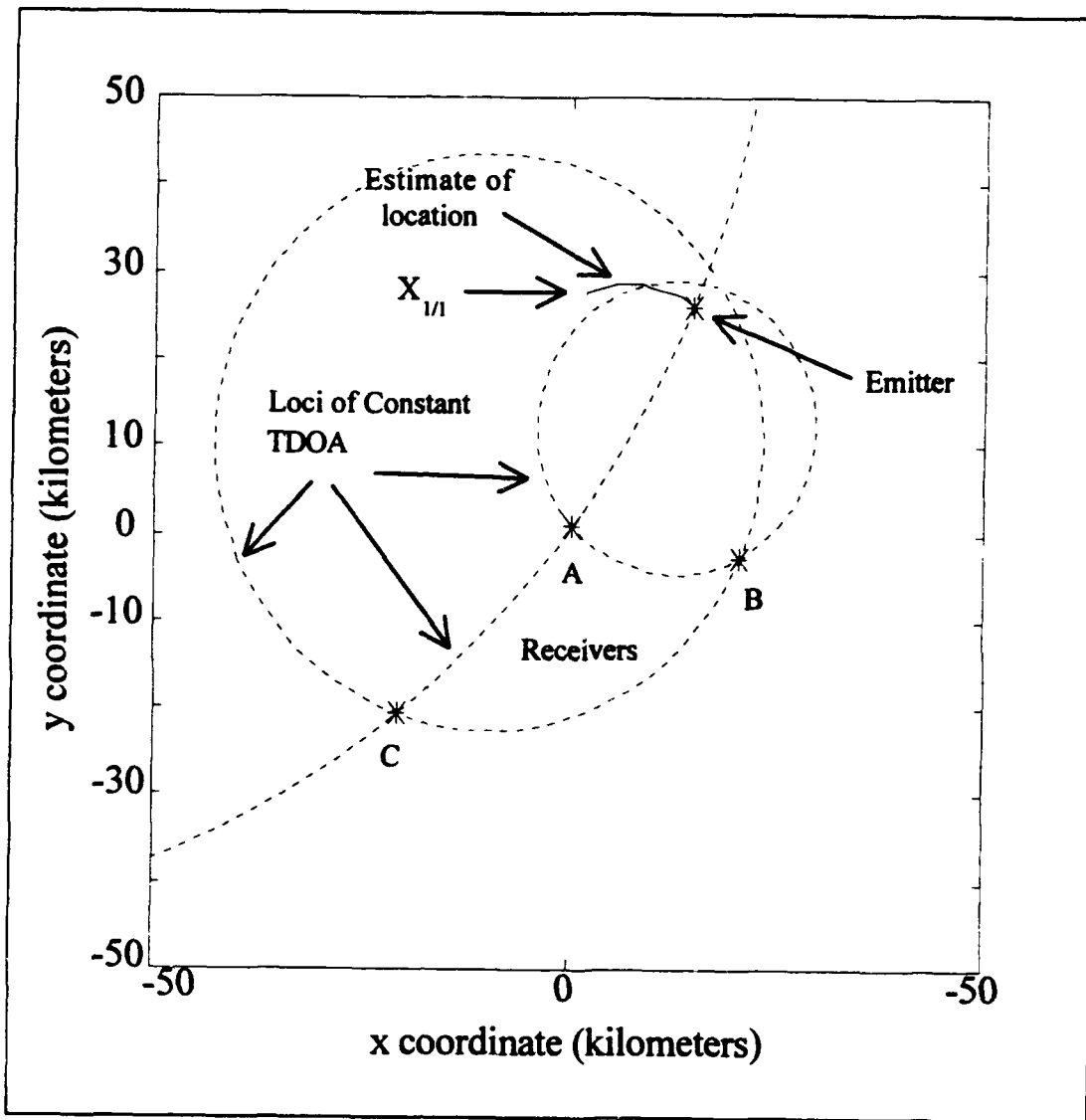


Figure 22. Scenario #3 Estimates of emitter location

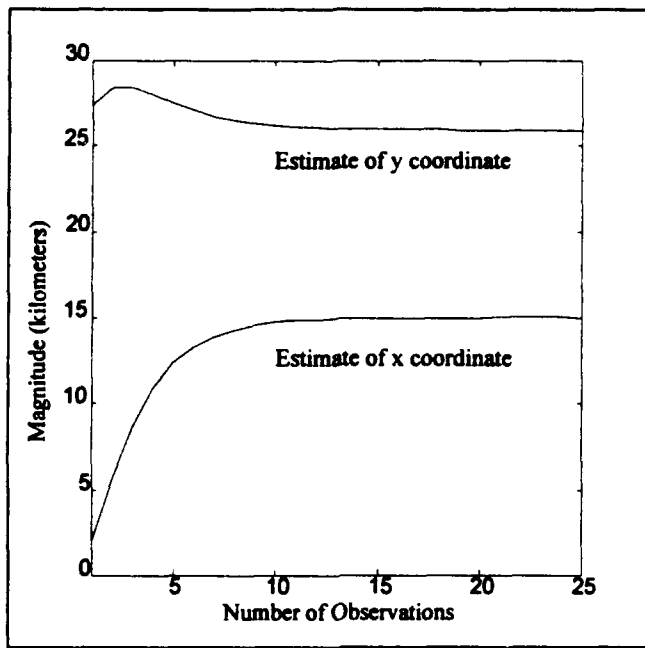


Figure 23. Scenario #3 Estimates of emitter coordinates vs observations

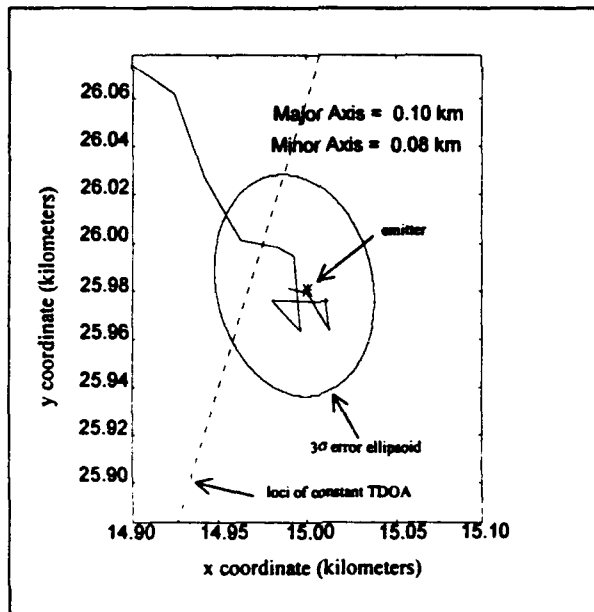


Figure 24. Close-up of the steady state estimate of emitter location

3. The Burst TDOA Filter Results

The simulations presented here in no way test all the possible implementations of this filtering algorithm. Further evaluation of the algorithm is necessary to fully evaluate its performance and capabilities given the wide variety of possible emitter locations, receiver configurations, and emitter characteristics. From the analysis conducted some general observations can be drawn.

For the burst TDOA Kalman filter the orthogonality among the TDOA observations is generally very good. For the three randomly chosen receiver locations, the orthogonality of the TDOA observations are not heavily dependent on the location of the emitter. As the locations of the receivers remained constant and the bearing to the emitter is varied throughout a 90 degree arc, and there does not appear to be any particular bearings where the orthogonality of all three observations would decrease to the point where the performance of the filter degrades. For all bearings and ranges examined at least two of the TDOA observations had good orthogonality.

The accuracy of the filter is heavily dependent on the values chosen for Q , the covariance of the state excitation. If this value is too low, the filter reaches a steady state value, but the steady state value is not the correct location of the emitter. As Q is increased, the steady state estimate of the location of the emitter reaches a stable point around the true emitter location. The magnitude of Q directly affects the magnitude of the error covariance P , and as Q is increased the error covariance and the 3σ error ellipsoids for the steady state estimate increase in size.

The filter performs well for the receiver configurations and emitter locations tested. Even at the maximum range, where the receivers are spaced closely in comparison to the distance from the emitter, the error present in the final estimate of the location of the emitter is reasonable. For scenario #1 the length of the 3σ error ellipsoid, which represents effectively the maximum error in the estimate given the noise present in the observations, is roughly 30 kilometers in bearing direction and 10 kilometers in range. These represent errors of about 3 degrees in bearing and 2 percent in range. In scenarios #2 and #3, the distance to the emitter decreases relative to the separation of the receivers and the maximum error decreases to about 0.5 and 0.20 degrees in bearing, and 2 percent, and 0.3 percent in range respectively.

These results are accomplished filtering the TDOA observations one at a time. This filtering technique tends to skew the error ellipsoids to align them with the loci of constant TDOA that corresponded to the last TDOA observation. This places the major axis of the error ellipsoid along this loci and tends to increase the error along that loci. If all three of the TDOA observations are processed simultaneously as the filter reaches a steady state solution, the error covariance and thus the error ellipsoids and maximum error present in the estimate can be decreased further.

B. SINGLE PULSE TDOA KALMAN FILTER

1. Extended Kalman Filter Equations

An extended Kalman filter algorithm is developed to estimate of the emitter location from pulse TDOA observations. Simulated data is used to test the accuracy and stability of the algorithm. The following assumptions are made to simplify the problem:

1. Two receiver platforms are used, and each receiver platform is equipped with two sensors to detect the pulse TOA.
2. The error present in the pulse TDOA observation is modeled as zero mean additive white Gaussian noise with variance R.
3. The emitter is stationary.
4. The x and y coordinates of the emitter and receivers are measured with respect to a fixed coordinate system, and the coordinates of the sensors are known exactly.
5. The PRI is long enough that ambiguity is not present in the pulse TDOA observations.

These assumptions simplify the problem, but do not reduce its usefulness, because the algorithm developed can easily be modified to account for these assumptions.

The estimated state and predicted observation are calculated from the following:

$$\hat{\mathbf{x}}(k+1) = \hat{\mathbf{x}}(k) = \begin{bmatrix} \hat{x}_t(k) \\ \hat{y}_t(k) \end{bmatrix} \quad (52)$$

$$\hat{z}(k+1|k) = \frac{[(\hat{x}_t(k) - x_a(k))^2 + (\hat{y}_t(k) - y_a(k))^2]^{1/2} - [(\hat{x}_t(k) - x_b(k))^2 + (\hat{y}_t(k) - y_b(k))^2]^{1/2}}{c} \quad (53)$$

The Kalman filter equations are:

$$\hat{\mathbf{x}}(k+1|k+1) = \hat{\mathbf{x}}(k+1|k) + G(k+1)[z(k+1) - \hat{z}(k+1|k)] \quad (54)$$

$$P(k+1|k) = P(k|k) + Q \quad (55)$$

$$P(k+1|k+1) = [I - G(k+1)\hat{H}(k)]P(k+1|k) \quad (56)$$

$$G(k+1) = P(k+1|k)\hat{H}(k)^T [\hat{H}(k)P(k+1|k)\hat{H}(k)^T + R]^{-1} \quad (57)$$

Where $\hat{x}_t(k)$ $\hat{y}_t(k)$ = the estimate of the x and y coordinates of the emitter,
 $z(k+1)$ = the TDOA observations for receiver platforms 1 and 2,
 $\hat{z}(k+1|k)$ = the predicted TDOA based upon the estimates of emitter location.
 x_a, y_a = the x and y coordinates of the sensor A of the receiver platform,
 x_b, y_b = the x and y coordinates of the sensor B of the receiver platform,
 $G(k+1)$ = the Kalman gains,
 $P(k|k)$ = the error covariance,
 $H(k)$ = the gradient of the observation equation,
 Q = the covariance of the plant noise,
 R = the covariance of the measurement noise,
 c = the speed of light,
 x_a, x_b, y_a, y_b are all functions of k.

The gradient of the observation equation $H(k)$ is calculated from the following equations.

$$H(k) = \left[\frac{1}{c} \left(\frac{\hat{x}_t(k) - x_a}{R_a(k)} - \frac{\hat{x}_t(k) - x_b}{R_b(k)} \right) \quad \frac{1}{c} \left(\frac{\hat{y}_t(k) - y_a}{R_a(k)} - \frac{\hat{y}_t(k) - y_b}{R_b(k)} \right) \right] \quad (58)$$

Where, $R_a(k) = [(\hat{x}_t(k) - x_a)^2 + (\hat{y}_t(k) - y_a)^2]^{1/2}$, and (59)

$$R_b(k) = [(\hat{x}_t(k) - x_b)^2 + (\hat{y}_t(k) - y_b)^2]^{1/2} \quad (60)$$

The flowchart for the pulse TDOA Kalman filter algorithm is identical to the flowchart used for the burst TDOA Kalman filter shown in Figure 13. The simulation calculates the pulse TDOA observation using the known locations of the emitter and sensors. Zero mean white Gaussian noise is added to the calculated observations and the filter estimates the location of the emitter from these noisy observations. The variance of the measurement noise is calculated from the emitter parameters and an assumed signal to

noise ratio. The filtering algorithm is tested for a number of emitter locations. In each scenario the initial error covariance matrix and the variance of the plant excitation noise are varied until the filter converges to the emitter's true coordinates

2. Pulse TDOA Kalman Filter Simulations

Three scenarios are used to test the performance of the pulse TDOA Kalman filter. The receiver locations remain the same for all of the scenarios and are shown in Figure 25. The sensors are stationary for all of the scenarios. The sensors are separated by 500 meters, and the receiver platform separation is 20 kilometers.

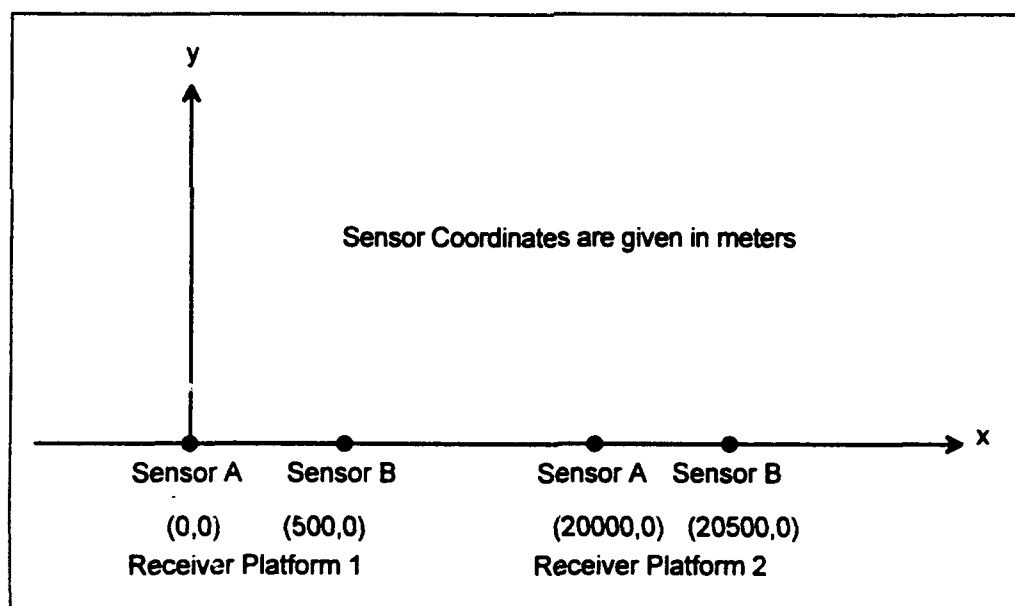


Figure 25. Receiver platform and sensor configuration

The emitter locations chosen to test the pulse TDOA algorithm are shown in Figure 26.

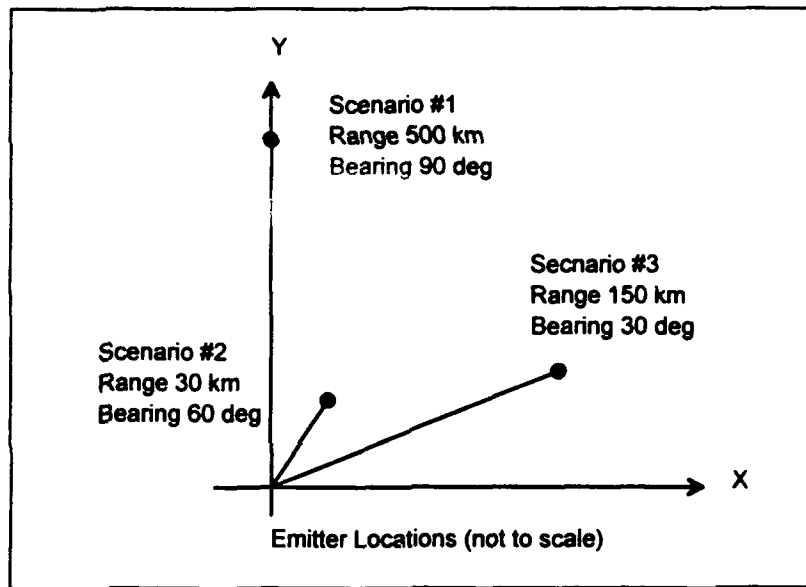


Figure 26. Emitter locations for the single pulse TDOA Kalman filter

The emitter has the following characteristics. These characteristics are typical for long range search radar.

Beamwidth	2.0 deg.
Scan Rate	360 deg/sec.
PRF	2000 Hz
Pulsewidth	1.0 microsecond
Peak Signal to Noise Ratio	15 dB

All of the sensors are considered identical with identical peak signal to noise ratios. An 8 MHz sampling rate is assumed. The algorithms developed in Appendix A are used to calculate the variance of the error present in the TDOA observations for the sampling rate and signal to noise ratio chosen. In the tests of the Kalman filtering

algorithm, this error is modeled as zero mean white Gaussian noise, and is added to the true TDOA observations. The variance of the TDOA observation noise is 1.694×10^{-15} for all of the scenarios.

For all of the scenarios the a priori estimate of the emitter's location is (10,5) kilometers. This a priori estimate provided good convergence for a wide range of emitter locations. The variance of the plant excitation noise Q , and the initial error covariance are varied until the filter converges to the actual coordinates of the emitter. All three of the scenarios are run for sixty TDOA observations. For the emitter characteristics chosen, this represents a real run time of 30 milliseconds.

Three plots are presented for each of the scenarios examined. The first plot is an X-Y plot of the estimates of the coordinates of the emitter. This plot demonstrates the track of the final estimate of the emitter location after both TDOA observations are processed at each time step. The loci of constant TDOA that correspond to the final steady state TDOA observations are also plotted. These loci illustrate the relationship between the TDOA observations and give a visual indication of the orthogonality of the observations. Also, the 3σ error ellipsoids are plotted for the 1st, 20th, 39th, and 58th estimates of the emitter location. These ellipsoids provide a visual indication of the accuracy of the location estimate.

The second plot is the estimate of the x and y coordinates of the emitter vs. the number of TDOA observations. This plot gives a visual indication of how rapidly the states of the filter converge to the true coordinates of the emitter.

The third plot is an X-Y plot of true emitter coordinates, the loci of constant TDOA, and the estimates of the emitter coordinates in the vicinity of the mean steady state estimate of the emitter coordinates. The 3σ error ellipsoid is plotted for the steady state estimate. The length of the major and minor axis of the error ellipsoid give an indication of the maximum error in the estimate.

a. Scenario #1

In the first scenario the performance of the pulse TDOA filter is tested for an emitter located at a range of 500 kilometers from the origin at a bearing of 90 degrees from the x coordinate axis. The initial error covariance matrix, P_0 , and the variance of the state excitation, Q , are varied until the filter converges to a steady state value. The plots presented in Figures 27 through 29 are representative of the results. In each simulation, a total of sixty observations are filtered. The values that give the best results are:

$$P_0 = \begin{bmatrix} 5.0 & 0 \\ 0 & 5.0 \end{bmatrix} \times 10^{20} \text{ m}^2, \text{ and } Q = \begin{bmatrix} 1.0 & 0 \\ 0 & 1.0 \end{bmatrix} \times 10^8 \text{ m}^2.$$

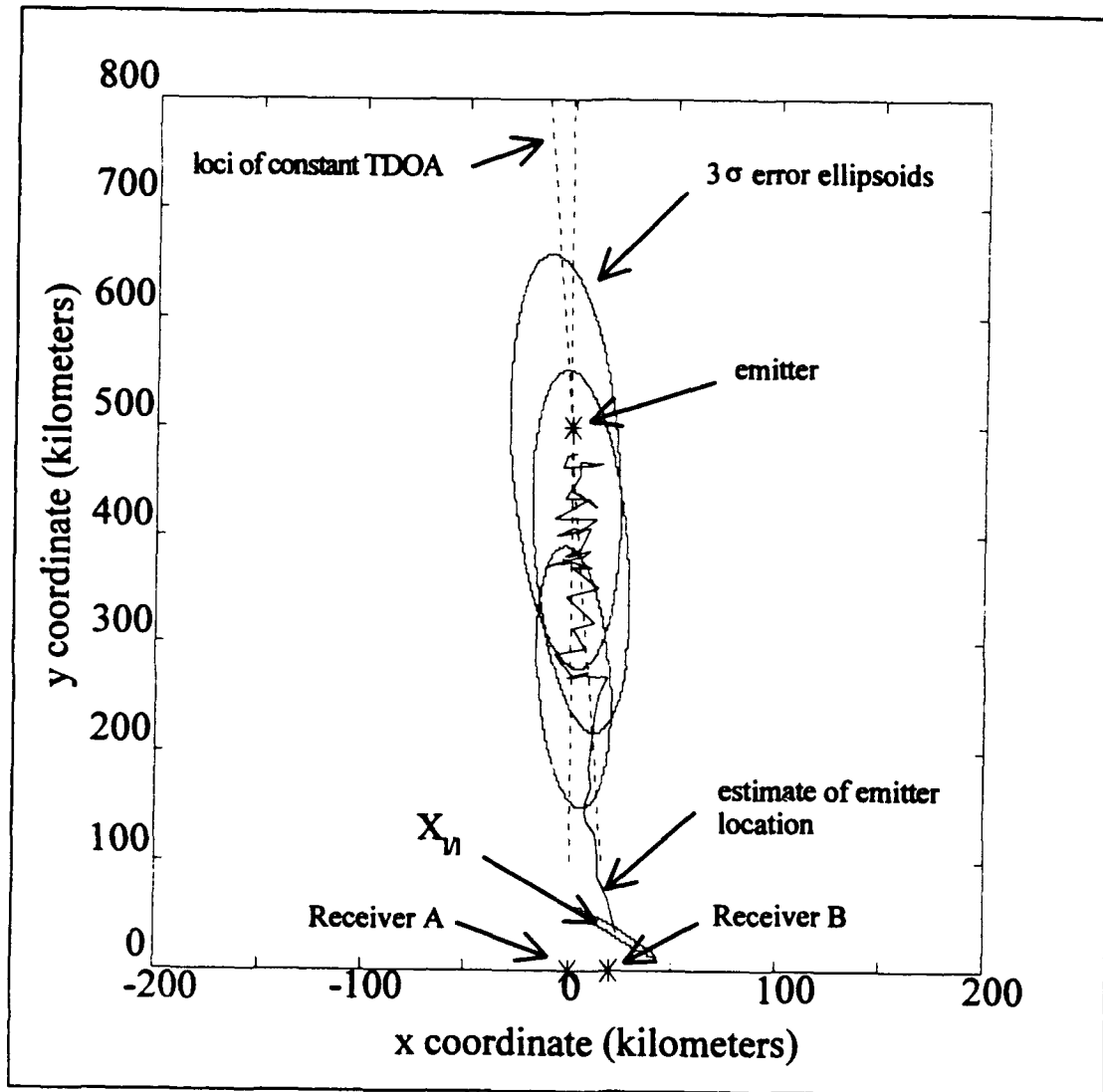


Figure 27. Scenario #1 Estimates of emitter location

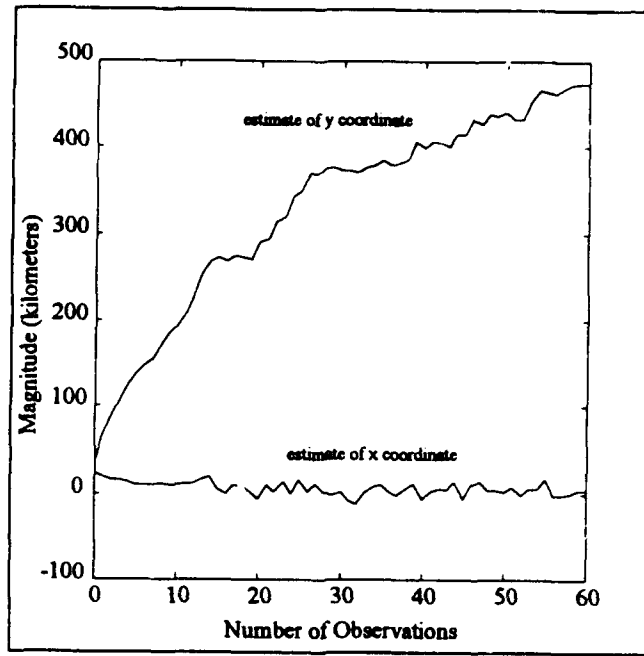


Figure 28. Scenario #1 Estimates of emitter coordinates vs. observations

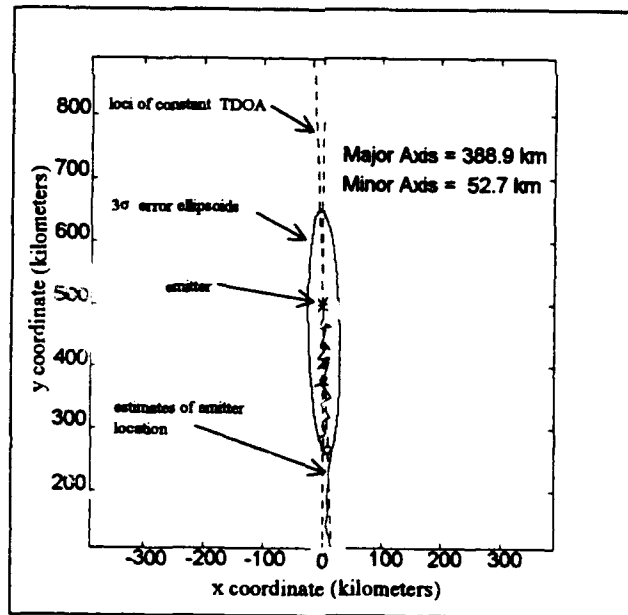


Figure 29. Scenario #1 Close-up of steady state estimate of emitter location

The filter performs well, but the error in the steady state estimate is high, and the estimate of the y coordinate of the emitter, shown in Figure 28, converges very slowly. Because the distance to the emitter is large in relation to the separation of the receivers, the TDOA observations are very close to each other. The estimated location of the emitter does not approach the true location of the emitter until the error covariance matrix and subsequently the Kalman gains grow large enough to amplify the very small differences in the TDOA to drive the states of the filter near the true location. A large value for Q is required to drive the error covariance matrix high enough. If a smaller value of Q is used, the filter reaches a steady state far from the true location of the emitter. Because of the magnitude of the error covariance matrix, the 3σ error ellipsoids grow large. The major axis of the steady state error ellipsoid is nearly 400 kilometers. Considering that the distance to the emitter is only 500 kilometers, a location estimate with that much possible error has limited usefulness.

In a second attempt, the separation of the receiver platforms is increased to 300 kilometers to determine if greater separation of the receiver platforms can increase the orthogonality of the TDOA observations and improve the performance of the filter. The separation of the sensors is maintained at 500 meters. The results of the simulation are shown in Figures 30 through 32. The value chosen for Q in this simulation is

$\begin{bmatrix} 2.0 & 0 \\ 0 & 2.0 \end{bmatrix} \times 10^6$. The value chosen for P_0 is the same as the previous simulation.

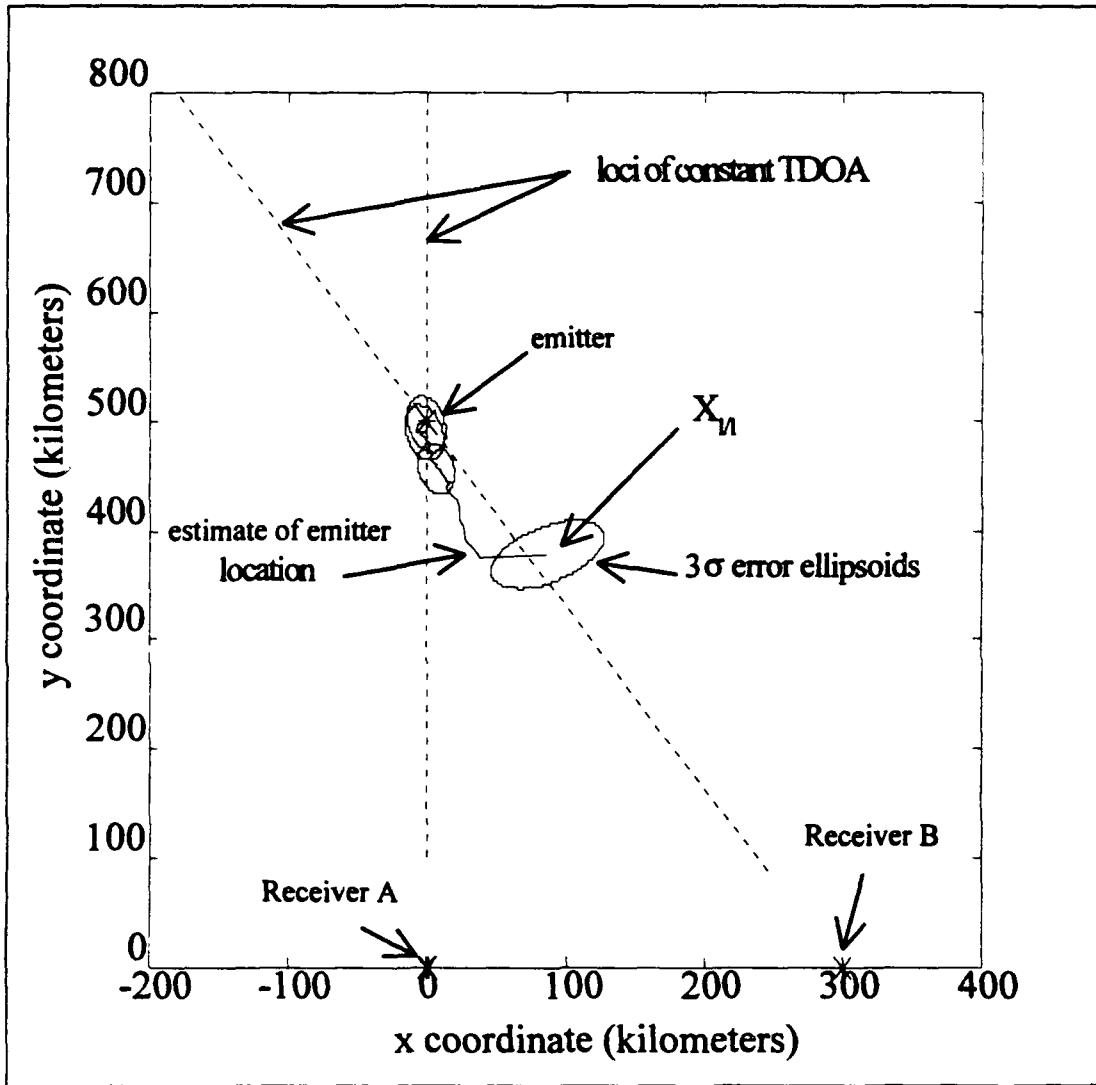


Figure 30. Scenario #1 Estimates of emitter location for 300 km receiver separation

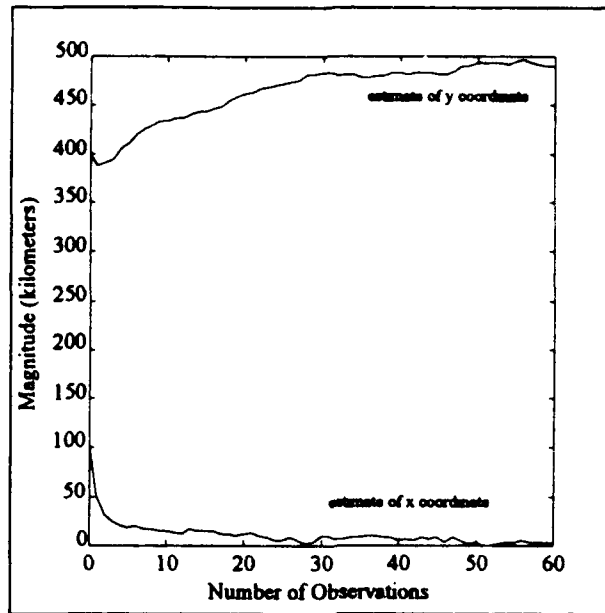


Figure 31. Scenario #1 Estimates of emitter coordinates vs. observations for 300 km receiver separation

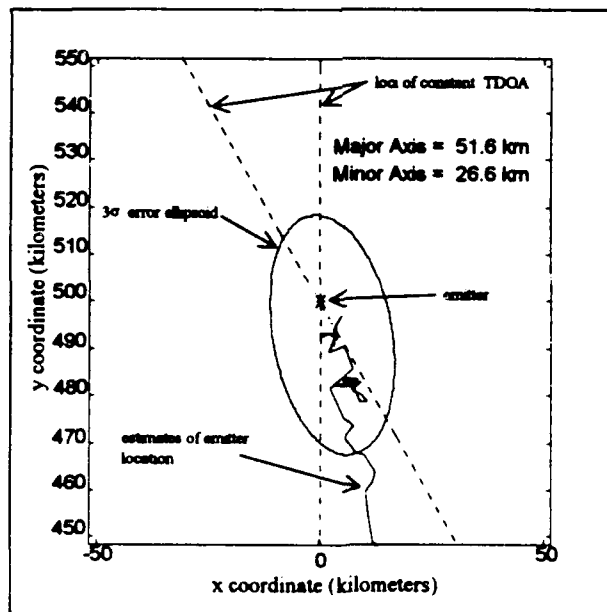


Figure 32. Scenario #1 Close-up of steady state estimate of emitter location for 300 km receiver separation

As shown in Figure 31 the estimates of the emitter coordinates approached the true coordinates of the emitter more quickly and directly than the previous simulation. This is largely due to the greater orthogonality of the TDOA observations. The steady state 3σ error ellipsoid plotted in Figure 32 is considerably smaller than in the previous simulation and the major axis of the error ellipsoid is only 51 kilometers.

b. Scenario #2

In the second scenario the performance of the burst TDOA filter is examined with the emitter located at an intermediate range. An emitter is located at a range of 150 kilometers from the origin and a bearing of 30 degrees from the x coordinate axis. The x and y coordinates of the emitter are (130, 75) kilometers. As in the first simulation, the initial error covariance matrix, P_0 , and the variance of the state excitation term, Q , are varied until the filter converges to the true coordinates of the emitter. The values that give the best convergence are:

$$P_0 = \begin{bmatrix} 1.0 & 0 \\ 0 & 1.0 \end{bmatrix} \times 10^{20} \text{ m}^2, \text{ and } Q = \begin{bmatrix} 1.0 & 0 \\ 0 & 1.0 \end{bmatrix} \times 10^7 \text{ m}^2.$$

The plots presented in Figures 33 through 35 are representative of the results obtained.

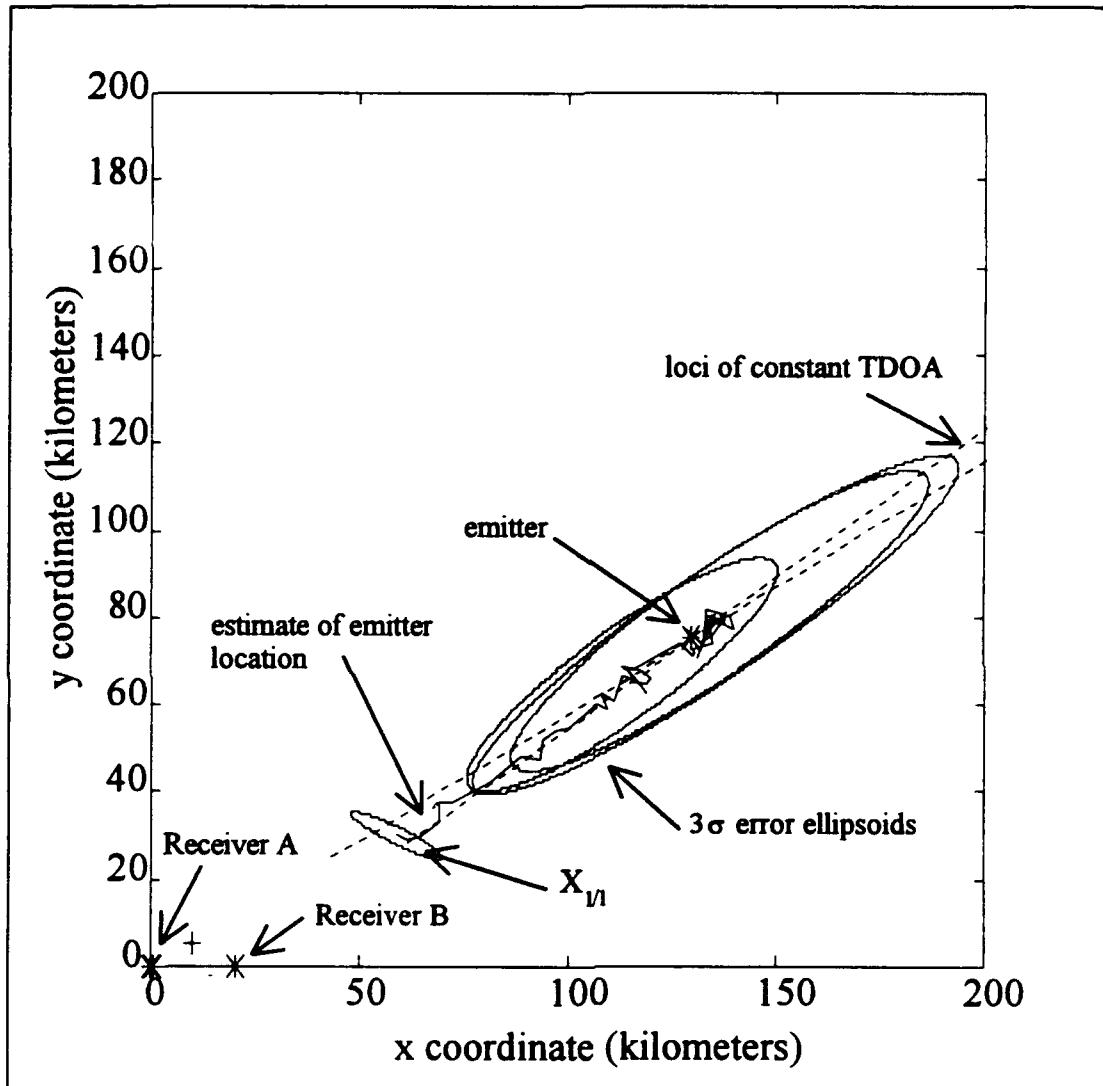


Figure 33. Scenario #2 Estimates of emitter location

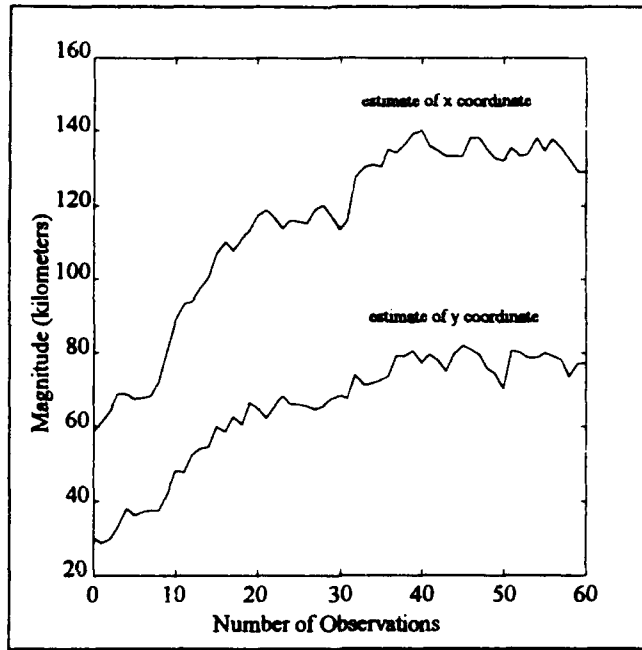


Figure 34. Scenario #2 Estimates of emitter coordinates vs. observations

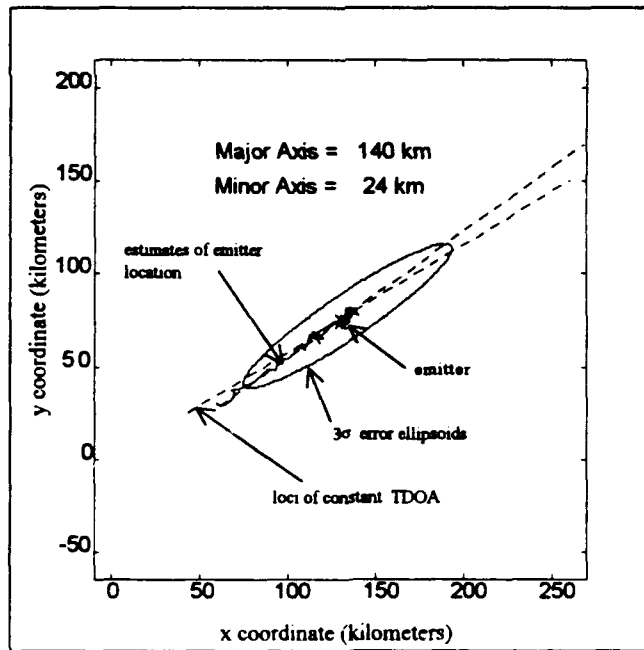


Figure 35. Close-up of the steady state estimate of emitter location.

The filter performs well, but the error in the steady state estimate is high, and the estimates of the x and y coordinates of the emitter, shown in Figure 34, converge very slowly. The distance from the receiver platforms to the emitter is much less than in scenario #1, but the orthogonality of the TDOA observations is low because of the location of the emitter in relation to the receivers. As shown in figures 33 and 35, the loci of constant TDOA are nearly parallel in the vicinity of the emitter. Although the filter converges to a steady state value close to the actual emitter location, the error covariance is very high. The major axis of the 3σ error ellipsoid for the steady state estimate is approximately 140 kilometers. Considering that the distance to the emitter is only 150 kilometers, a location estimate with an error ellipsoid this large has limited usefulness.

As shown in the first scenario, greater separation of the receiver platforms can increase the orthogonality of the TDOA observations and improve the performance of the filter. When the separation of the receiver platforms is increased to 150 kilometers and the separation of the sensors maintained at 500 meters, the performance improves dramatically. The results of the simulation are shown in figures 36 through 38. The final value chosen for Q is $\begin{bmatrix} 5.0 & 0 \\ 0 & 5.0 \end{bmatrix} \times 10^5$. The value chosen for P_0 is the same as the previous simulation.

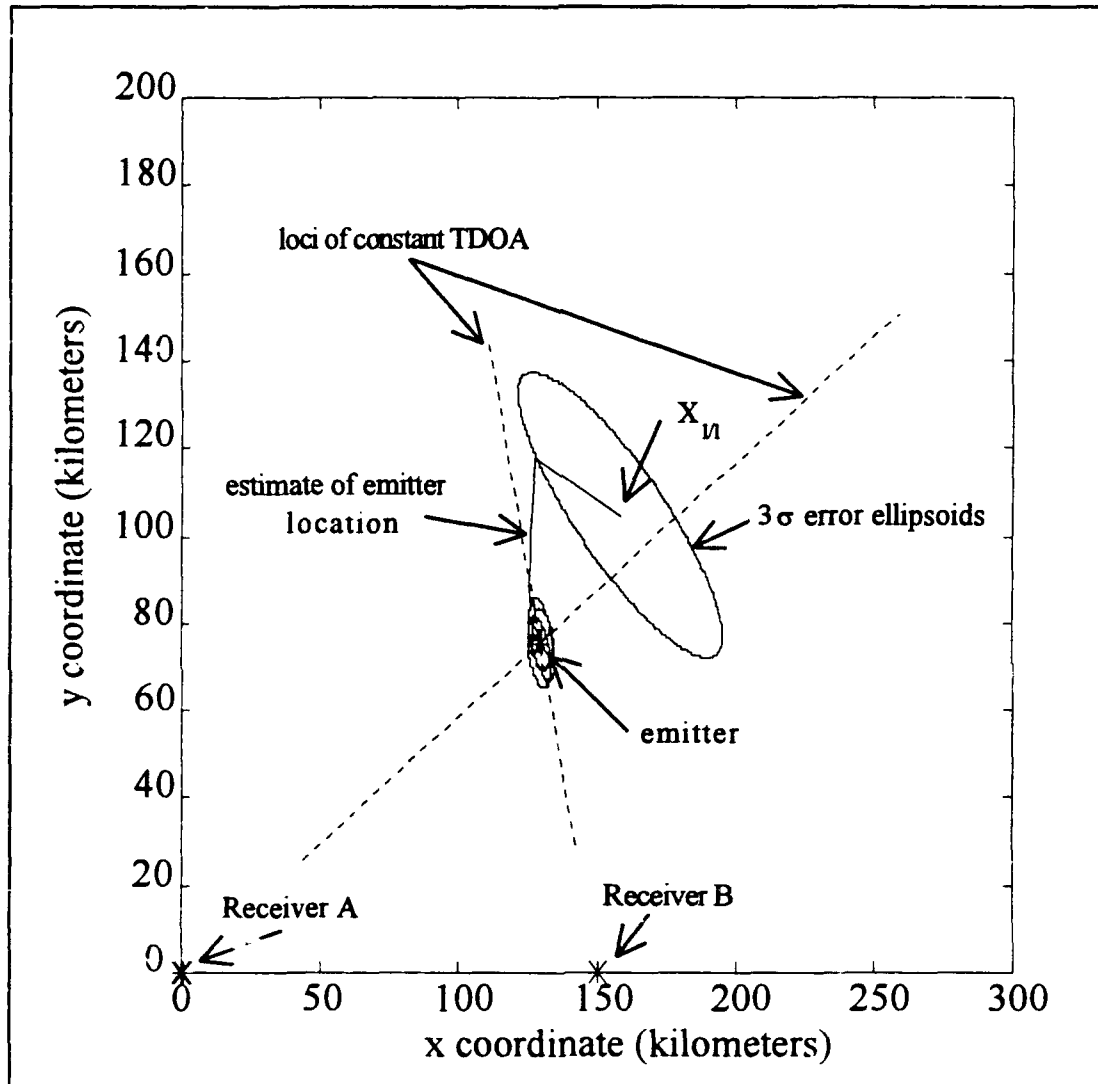


Figure 36. Scenario #2 Estimates of the location of the emitter with 150 km receiver separation.

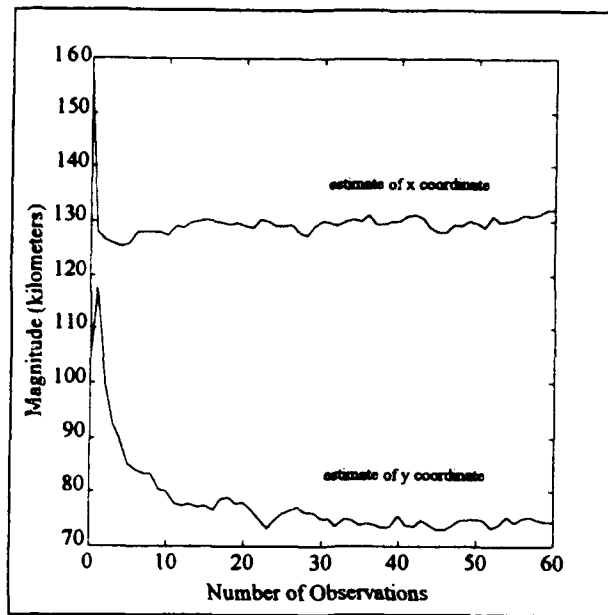


Figure 37. Scenario #2 Estimates of emitter coordinates vs. observations with 150 km receiver separation

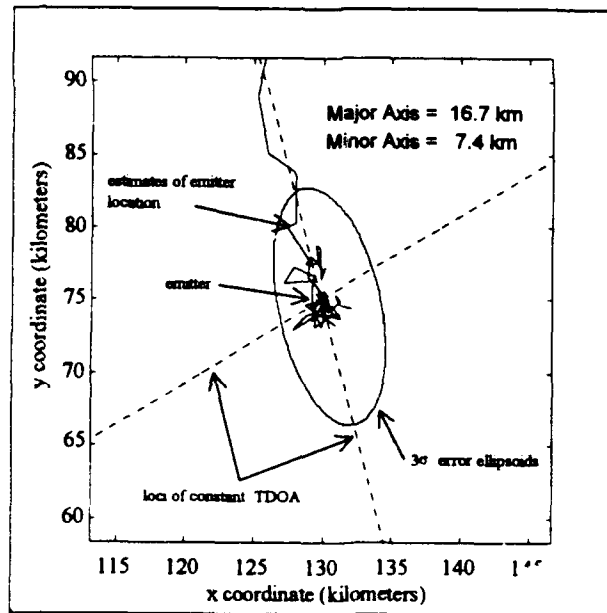


Figure 38. Close-up of the steady state estimate of emitter location with 150 km receiver separation

As shown in Figure 37, the estimates of the emitter coordinates approach the true values more quickly and directly than the previous simulation. This is largely due to the greater orthogonality of the TDOA observations. The 3σ error ellipsoid plotted in Figure 38 is considerably smaller than in the previous simulation. The major axis of the error ellipsoid is only 16.7 kilometers.

c. Scenario #3

In the third scenario the performance of the pulse TDOA filter is tested for an emitter located at close range in comparison to the separation of the receivers. The emitter location is located at a range of 30 kilometers from the origin and at a bearing of 60 degrees from the x coordinate axis. The x and y coordinates of the emitter are (15, 26) kilometers. As in the previous simulations, the initial error covariance matrix and the variance of the state excitation term, are varied until the filter converges to the true coordinates of the emitter. The values that give the best convergence are:

$$P_0 = \begin{bmatrix} 1.0 & 0 \\ 0 & 1.0 \end{bmatrix} \times 10^{15} \text{ m}^2, \text{ and } Q = \begin{bmatrix} 40 & 0 \\ 0 & 40 \end{bmatrix} \text{ m}^2.$$

The plots presented in Figures 39 through 41 are representative of the results obtained.

As shown in Figure 40 the estimate of the emitter location converges to the true coordinates of the emitter quickly. Increasing the value of Q improves the convergence of the filter, but also increases the error present in the final estimate and increases the size of the error ellipsoid. For the values of Q chosen the major axis of the 3σ error ellipsoid is only 1.4 kilometers.

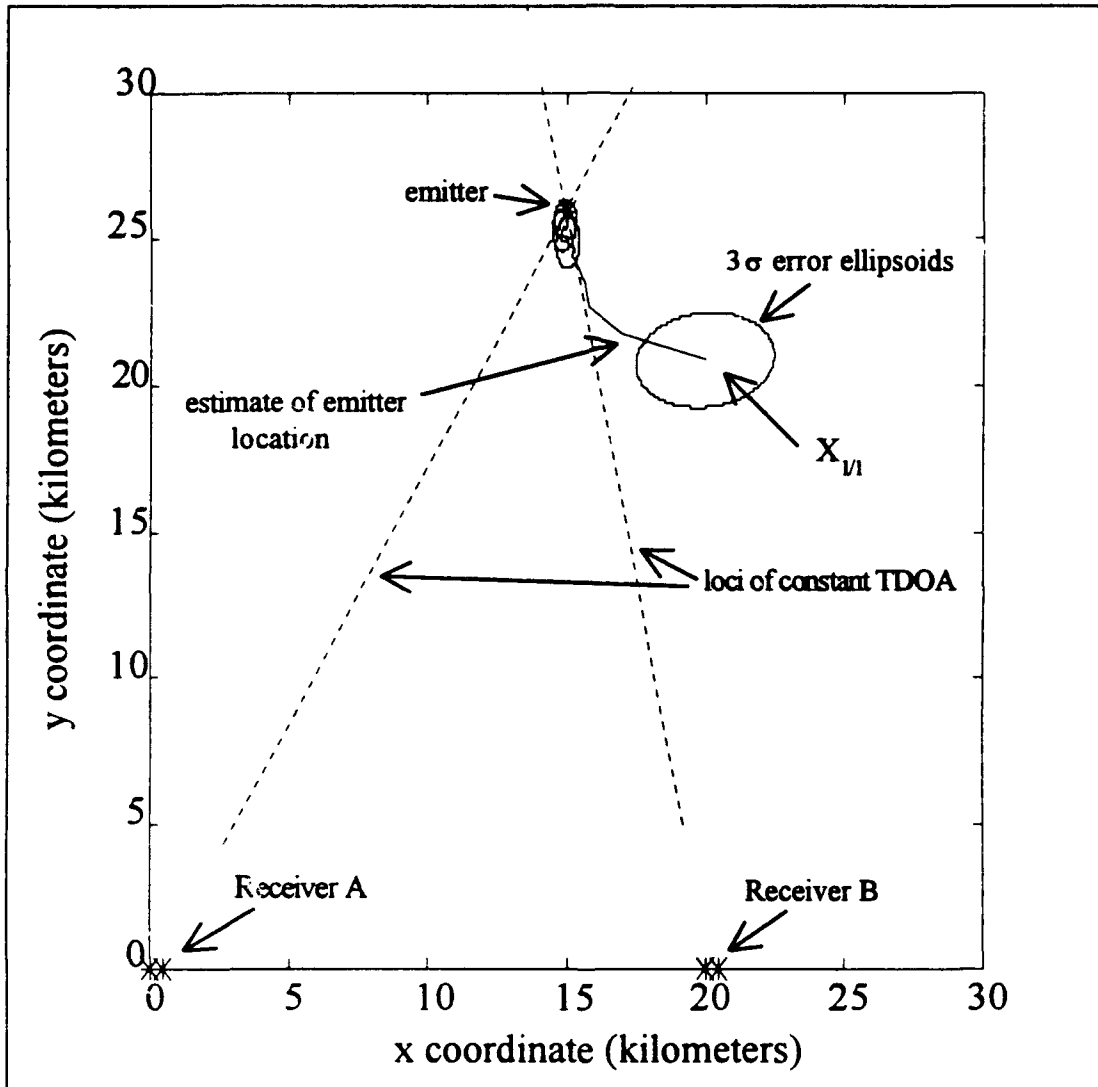


Figure 39. Scenario #3 Estimates of the emitter location.

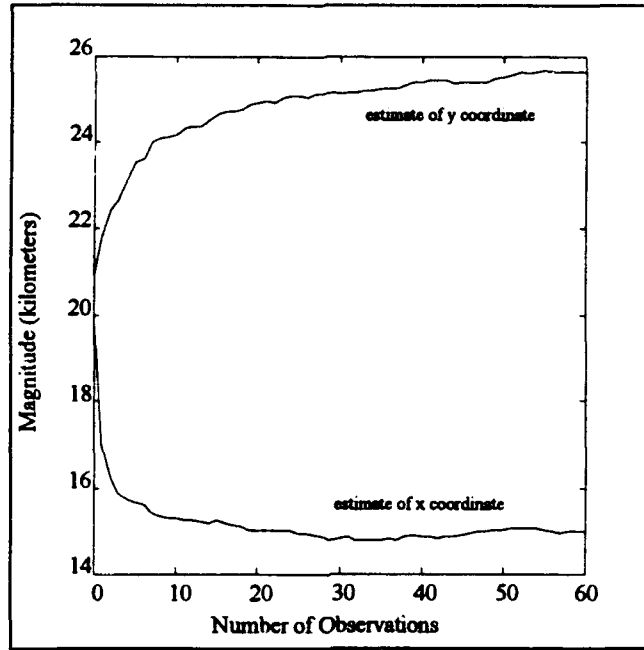


Figure 40. Scenario #3 Estimates of emitter coordinates vs. observations

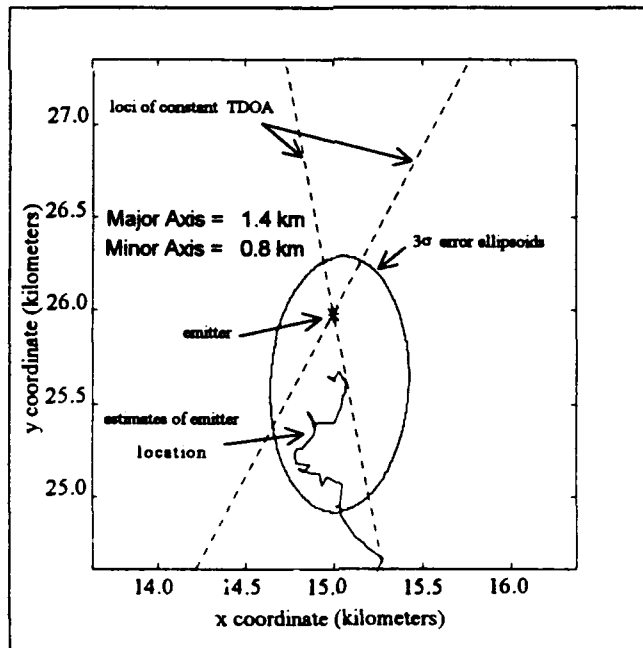


Figure 41. Close-up of the steady state estimate of the emitter location

3. Pulse TDOA Filter Results

The simulations presented here do not test all the possible implementations of this filtering algorithm. Further evaluation of the algorithm is necessary to fully evaluate its performance and capabilities given the infinite variety of possible emitter locations, receiver configurations, and emitter characteristics. From the analysis conducted some general observations can be drawn.

The pulse TDOA filter accuracy and effectiveness is heavily dependent on the orthogonality of the TDOA observations. As the orthogonality of the TDOA observations decreased, the error present in the estimate increased. When the receiver platforms are closely spaced relative to the distance to the emitter, the loci are nearly parallel to each other and the TDOA observations have low orthogonality. To obtain good filtering results the spacing between the receiver platforms has to be increased.

The receiver locations chosen for the single pulse TDOA filtering problem yielded areas where the orthogonality of the TDOA observations is low. In these areas, the ability of the algorithm to estimate accurately the location of the emitter is limited. These blind areas can be avoided with different sensor configurations or more receivers.

The accuracy of the algorithm filter is also heavily dependent on choosing the correct values for the covariance of the state excitation, Q . If this value is too low, the filter reaches steady state, but the steady state estimate of the location is far from the true location of the emitter. As Q is increased, the algorithm reaches a steady state around the emitter's true location, but the error covariance and the error present in the final estimate

risers much higher. Consequently the size of the 3σ error ellipsoids and the maximum error present in the final estimates are much larger.

The final approaches used in each of the scenarios yield good results. In the second approach used in scenario #1, the accuracy obtained from the filtering is approximately 3 degrees in bearing and about 10 percent range. For scenario #2 the error is approximately 5 degrees in bearing and 5 percent in range, and in the third scenario, the error is approximately 2 degrees in bearing and 3 percent in range.

The pulse TDOA algorithm filters the TDOA observations one at a time. This filtering technique tends to skew the error ellipsoids and align them with the loci of constant TDOA that corresponded to the last TDOA observation. This places the major axis of the error ellipsoid along this loci and tends to increase the error in that direction. If both of the TDOA observations are processed simultaneously as the filter reaches steady state, the error covariance and the error ellipsoids can be decreased.

VI. CONCLUSIONS AND RECOMMENDATIONS

A. CONCLUSIONS

Both of the Kalman filtering algorithms considered here perform well. Given the proper parameters, both algorithms accurately estimate the location of the emitter to a reasonable degree of accuracy. The orthogonality of the TDOA observations is the largest factor that affects the accuracy of the final estimates.

Overall, the geometry of the burst TDOA filtering problem yields TDOA observations with better orthogonality. Even when the distance to the emitter is much larger than the distance between the receivers, the orthogonality of the TDOA observations are good. In the burst TDOA filtering problem, the orthogonality of the observations is not as sensitive to the location of the emitter in relation to the receivers. The receiver configuration provides good orthogonality for a wide range of emitter locations. To obtain good orthogonality in the pulse TDOA filtering problem, the receivers require wide separation.

The major disadvantage of the burst TDOA filter is the slow rate at which observations are obtained. Observations are obtained at the scan rate of the emitter, and for the scenarios examined, this means that only one observation is made per second. For the simulations pursued, the total run time is 25 seconds, but reasonably accurate estimates of the location are available within about 10 observations. The number of

observations required to reach steady state could be reduced further with better *a priori* estimates.

The most attractive feature of the pulse TDOA filter is the rate at which observations are obtained. Observations are available at the rate of the PRF of the emitter, and for the scenarios pursued here, the pulse TDOA filter could obtain 2000 observations for every observation obtained by the burst filter.

It may be possible to combine the two filtering algorithms and utilize the best features of both. As stated previously, with only two receivers the location of the emitter can not be determined uniquely from the burst TDOA observations. However, if the receivers are equipped with multiple sensors, as in the pulse TDOA filtering problem, bearing estimates could be obtained and the location of the emitter along the burst TDOA locus could be uniquely determined.

B. RECOMMENDATIONS

The analysis and development conducted here is limited in its scope. Further testing and evaluation are required to more accurately evaluate the algorithms and models presented. Specifically, the following are recommended

1. Further evaluation and testing of the burst and pulse TDOA algorithms be done to assess their performance for a wider variety of receiver and emitter configurations and scenarios.
2. Perform a detailed analysis of the effect of *a priori* estimates on the convergence and accuracy of both filters.
3. Explore the possibility of using the orthogonality of the TDOA observations to pick the best observations to filter and its effect on the performance of the filter.
4. Obtain more detailed models of the error present in the burst and pulse TDOA observations, and determine their effect on the performance of the filter.
5. Explore the possibility of combining the two filtering approaches to take advantage of the best features of both.

APPENDIX A. TOA PROBABILITY DENSITY

A. PULSE TOA PROBABILITY DENSITY

1. Derivation of Probability Density

The pulses received and detected by the sensors are assumed to have the envelope shown in Figure A-1.

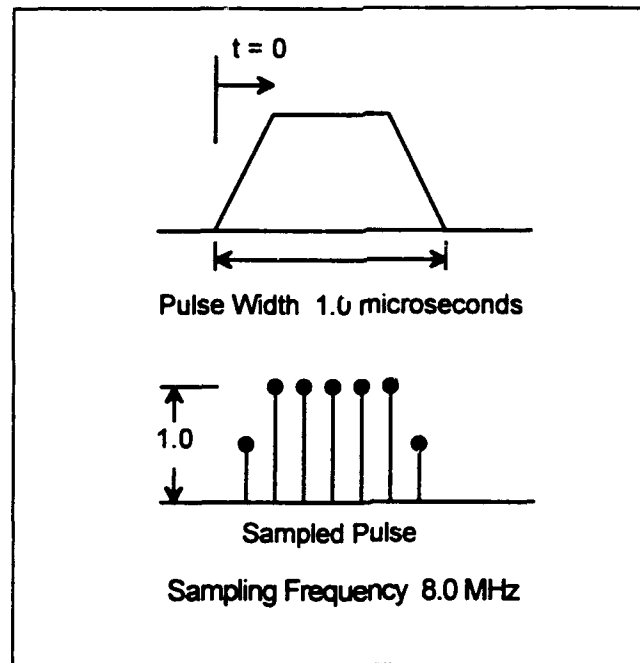


Figure A-1. Pulse envelope and sampled pulse

The sampling interval is assumed much smaller than the pulse width so the sampled pulse is a reasonable representation of the original pulse. The higher the sampling

probability density function of the pulse TOA, each sample of the pulse is considered a random variables as shown in equation (A-1).

$$z(k) = z_o(k) + v(k) \quad (A-1)$$

Where $z(k)$ = the random variable representing the amplitude of the kth sample,
 $z_o(k)$ = the deterministic variable that is the true amplitude of the kth sample, and
 $v(k)$ = the white Gaussian random variable that represents the noise present in the amplitude of the kth sample. The noise has zero mean and a variance of V , i.e.. $E[v(k)^2] = V$.

The mean and variance of $z(k)$ are:

$$\mu_{z(k)} = E[z_o(k) + v(k)] = E[z_o(k)] + E[v(k)] = z_o(k) \quad (A-2)$$

$$\sigma_{z(k)} = E[(z(k) - \mu_{z(k)})(z(k) - \mu_{z(k)})] \quad (A-3)$$

$$\sigma_{z(k)} = E[(z_o(k) + v(k) - z_o(k))(z_o(k) + v(k) - z_o(k))] = E[v(k)^2] = V \quad (A-4)$$

Each sample is uncorrelated.

$$E[z(k)z(k + \tau)] = E[z_o(k)z_o(k + \tau)] = 0 \quad (A-5)$$

Since they are Gaussian random variables, they are independent.

Equation (A-6) is used to calculate the time of arrival for the centroid of the pulse.

$$\text{TOA} = \frac{X}{Y} = \frac{\sum_{k=1}^N t(k)z(k)}{\sum_{k=1}^N z(k)} \quad (\text{A-6})$$

Where
 TOA = the time of arrival for the pulse centroid,
 X = numerator of the pulse centroid TOA equation,
 Y = denominator of the pulse centroid TOA equation,
 t(k) = the time at which the kth sample of the pulse is taken,
 z(k) = the amplitude of the kth sample of the pulse, and
 N = the number of samples in the pulse.

The time base from which the time of the samples are measured is arbitrary, but is common for all TOA measurements. This value is assumed deterministic and is therefore known exactly for each sample.

The numerator and denominator of equation (A-6) are themselves Gaussian random variables. As shown in reference [1], if W is a linear combination of independent Gaussian distributed random variables,

$$W = a_1 X(1) + a_2 X(2) + a_3 X(3) + \dots a_n X(n) \quad (\text{A-7})$$

then W is a Gaussian distributed random variable with a mean and variance given by:

$$\mu_w = a_1 \mu_{X(1)} + a_2 \mu_{X(2)} + a_3 \mu_{X(3)} + \dots a_n \mu_{X(n)} \quad (\text{A-8})$$

$$\sigma_w^2 = a_1^2 \sigma_{X(1)}^2 + a_2^2 \sigma_{X(2)}^2 + a_3^2 \sigma_{X(3)}^2 + \dots a_n^2 \sigma_{X(n)}^2 \quad (\text{A-9})$$

Based upon these relations the mean and variance of the numerator and denominator of equation (A-6) are given by:

$$\mu_X = \sum_{k=1}^N t(k)z_o(k) \quad (\text{A-10})$$

$$\sigma_X^2 = \sum_{k=1}^N t(k)^2 V \quad (\text{A-11})$$

$$\mu_Y = \sum_{k=1}^N z_o(k) \quad (\text{A-12})$$

$$\sigma_Y^2 = \sum_{k=1}^N V = NV \quad (\text{A-13})$$

Equation (A-6), the estimate of the TOA of the pulse centroid, is the ratio of two Gaussian distributed random variables. The joint probability density function for two Gaussian distributed random variables x and y is:

$$f(x, y) = \frac{\exp \left\{ -\frac{1}{2(1-\rho^2)} \left[\left(\frac{x-\mu_x}{\sigma_x} \right)^2 - 2\rho \left(\frac{x-\mu_x}{\sigma_x} \right) \left(\frac{y-\mu_y}{\sigma_y} \right) + \left(\frac{y-\mu_y}{\sigma_y} \right)^2 \right] \right\}}{2\pi\sigma_x\sigma_y(1-\rho^2)^{1/2}} \quad (\text{A-14})$$

Where μ_x, μ_y = the mean of x and y ,
 σ_x, σ_y = the standard deviation of x and y ,
 ρ = the correlation coefficient which is given by:

$$\rho = \frac{\text{cov}[xy]}{\sigma_x\sigma_y} = \frac{E[(x-\mu_x)(y-\mu_y)]}{\sigma_x\sigma_y} \quad (\text{A-15})$$

For equation (A-6), the covariance and correlation coefficient are calculated from the following:

$$\text{cov}[X, Y] = E \left[\left(\sum_{k=1}^N t(k)z(k) - \sum_{k=1}^N t(k)z_o(k) \right) \left(\sum_{k=1}^N z(k) - \sum_{k=1}^N z_o(k) \right) \right] \quad (\text{A-16})$$

$$\text{cov}[X, Y] = E \left[\left(\sum_{k=1}^N t(k)v(k) \right) \left(\sum_{k=1}^N v(k) \right) \right] \quad (\text{A-17})$$

Since the noise term $v(k)$ is considered white noise with zero mean and variance V , the cross terms in the multiplication in equation (A-17) will be zero and the resulting covariance is:

$$\text{cov}[X, Y] = \sum_{k=1}^N t(k)v(k)^2 = \sum_{k=1}^N t(k)V \quad (\text{A-18})$$

Thus the correlation coefficient is:

$$\rho = \frac{V \sum_{k=1}^N t(k)}{\sqrt{V^2 N \sum_{k=1}^N t(k)^2}} = \frac{\sum_{k=1}^N t(k)}{\sqrt{N \sum_{k=1}^N t(k)^2}} \quad (\text{A-19})$$

The correlation coefficient does not depend upon the variance of the noise V only on the number of samples and the sampling interval.

From reference [2], the probability density function, $f_z(z)$, for the ratio of two random variables, $Z = \frac{X}{Y}$, is found from the following equation:

$$f_z(z) = \int_{-\infty}^{\infty} |y| f(zy, y) dy \quad (\text{A-20})$$

Where $f(zy, y)$ is the joint probability density function $f(x, y)$ with the variables zy substituted for x .

The probability density function for the pulse centroid TOA is:

$$f_z(z) = \int_{-\infty}^{\infty} |y| \left[\frac{\exp \left\{ -\frac{1}{2(1-\rho^2)} \left[\left(\frac{yz-\mu_x}{\sigma_x} \right)^2 - 2\rho \left(\frac{yz-\mu_x}{\sigma_x} \right) \left(\frac{-\mu_y}{y\sigma_y} \right) + \left(\frac{-\mu_y}{y\sigma_y} \right)^2 \right] \right\}}{2\pi\sigma_x\sigma_y(1-\rho^2)^{1/2}} \right] dy \quad (\text{A-21})$$

Where z = the pulse centroid TOA,
 y = the denominator of the pulse centroid TOA equation ,
 $\mu_x \mu_y$ = the mean of the numerator and denominator of the centroid TOA equation, calculated from equations (A-10) and (A-12),
 $\sigma_x^2 \sigma_y^2$ = the variance of the numerator and denominator of the centroid TOA equation, calculated from equations (A-11) and (A-13), and
 ρ = the correlation coefficient calculated from equation (A-15),

A closed form solution for this integral is not available, so a MATLAB program is used to numerically calculate the probability density function. The MATLAB program Puldist.m, in Appendix E, calculates the probability density function for the pulse centroid TOA .

2. Effect of Signal to Noise Ratio on Probability Density

The plots in Figure A-2 demonstrate the effect of the peak signal to noise ratio on the probability density function of the pulse TOA. Samples of white Gaussian noise are added to the 1.0 microsecond pulse shown in Figure A-1. The variances of the noise are chosen to give peak signal to noise ratios of 15, 20, 25, and 30 dB. The variance of the noise is calculated from the peak signal to noise ratio with equation (A-22).

$$\left(\frac{S_{\text{peak}}}{N} \right)_{\text{dB}} = 10 \log_{10} \left[\frac{1}{V} \right] \quad (\text{A-22})$$

Where V = the variance of the noise required to give the specified peak signal to noise ratio for the unit pulse.

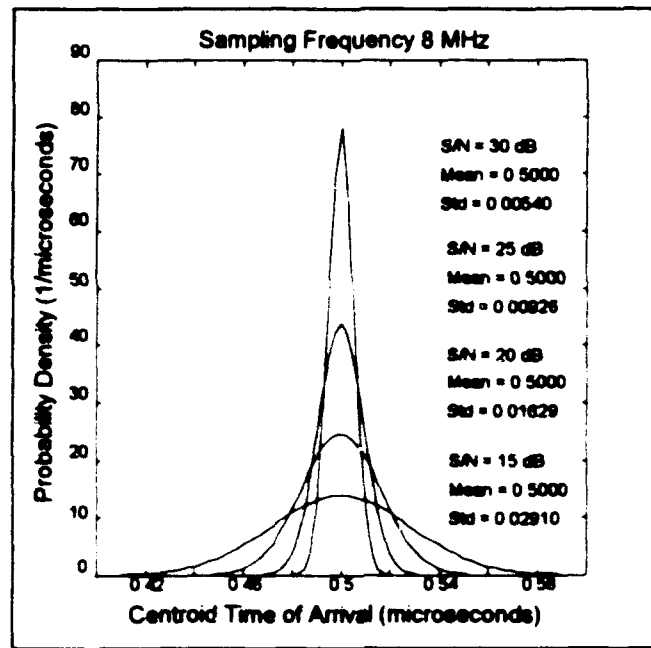


Figure A-2. Pulse TOA probability density for peak signal to noise ratios of 15, 20, 25, and 30 dB

As expected, as the signal to noise ratio increases, the variance of the error present in the estimate of the TOA decreases and the estimate of the pulse TOA becomes more accurate.

3. Calculated Mean and Standard Deviation of Sampled Pulses

The mean and standard deviation are calculated for the one microsecond pulse shown in Figure A-1. A variety of peak signal to noise ratios and sampling rates are used. For all of the sampled pulses the mean time of arrival for the centroid is 0.5 microseconds. The calculated standard deviations are shown in Table A-1.

S/N	Sampling Rate			
	4 MHz	8 MHz	12 MHz	16 MHz
15 dB	0.05873	0.02910	0.02241	0.01883
20 dB	0.03221	0.01629	0.01258	0.01058
25 dB	0.01819	0.00925	0.00713	0.00598
30 dB	0.01062	0.00542	0.00412	0.00344

TABLE A-1. STANDARD DEVIATION FOR 1.0 MICROSECOND SAMPLED UNIT PULSE (microseconds)

The pulse TOA standard deviations listed in Table A-1 indicate that there is a tradeoff between sampling rate and peak signal to noise ratio. If a lower sampling rate is used, a larger peak signal to noise ratio is required to obtain the same TOA error level. There exists an inversely proportional relationship between the variance of the pulse TOA error and the peak signal to noise ratio. From Table A-1, the relationship between the variance of the TOA error and the peak signal to noise ratio for a sampling rate of 8 MHz.

$$\frac{\text{Var}_{15\text{dB}}}{\text{Var}_{25\text{dB}}} = \frac{(0.02910)^2}{(0.00925)^2} = 9.897 \approx (25\text{dB} - 15\text{dB})$$

B. BURST TOA PROBABILITY DENSITY

1. Derivation of Probability Density

The algorithm that calculates the probability density function for the sampled pulse is used to calculate the probability density function for a burst of pulses. The MATLAB program `Burdist.m`, listed in Appendix E, generates the burst shown in

Figure A-3 and calculates the probability density function for a variety of peak signal to noise ratios, PRFs and pulse widths.

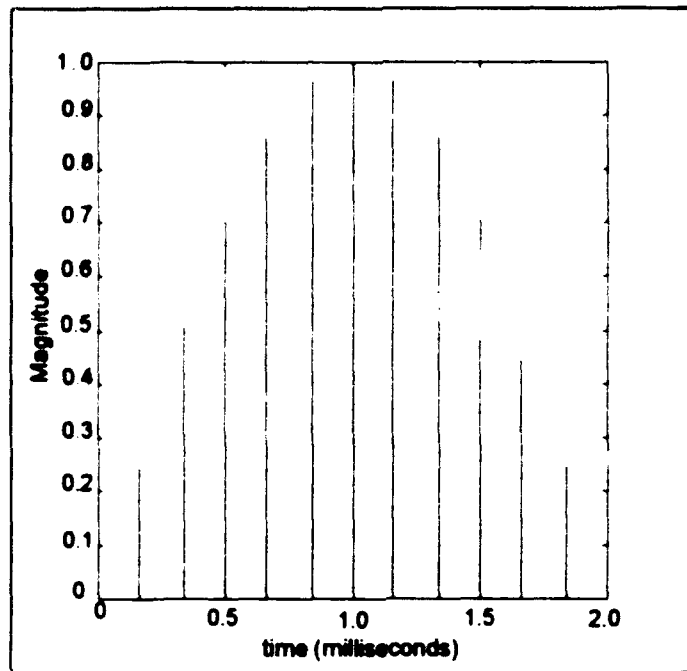


Figure A-3. A burst of sampled pulses from a scanning emitter

The envelope of the burst is approximated as the upper half of a sinewave, and the peak signal to noise ratios are calculated using equation (A-22).

2. Effect of Signal to Noise Ratio on Burst TOA Probability Density

Figure A-4 demonstrates the effect of signal to noise ratio on probability density of the burst TOA. The probability densities for the burst in Figure A-3 are calculated for peak signal to noise ratios of 15, 20, 25, and 30 dB. The noise variances required are calculated using equation (A-22).

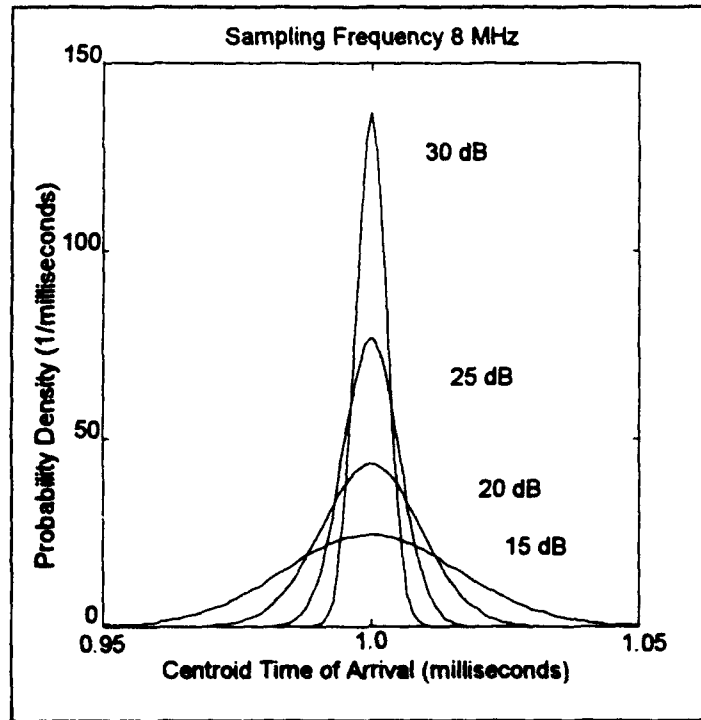
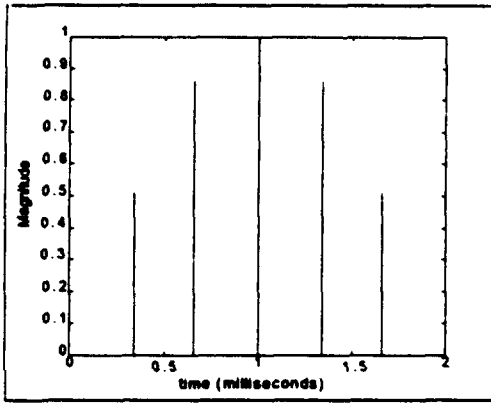


Figure A-4. Burst TOA probability densities for a 2 millisecond burst with a pulsewidth of 1.0 microseconds, and a PRF of 6 kHz.

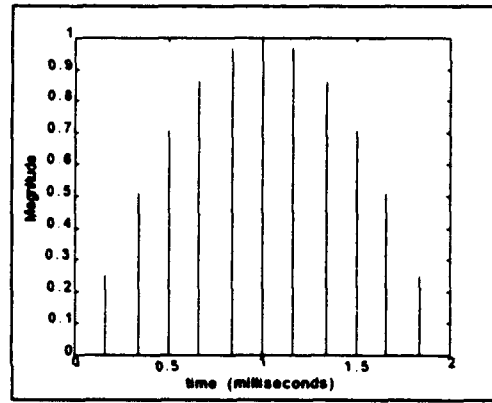
As expected, as the signal to noise ratio is increased, the variance of the error present in the estimate of the TOA decreases and the estimate of the burst TOA becomes more accurate.

3. Effect of PRF on the Burst TOA Probability Density

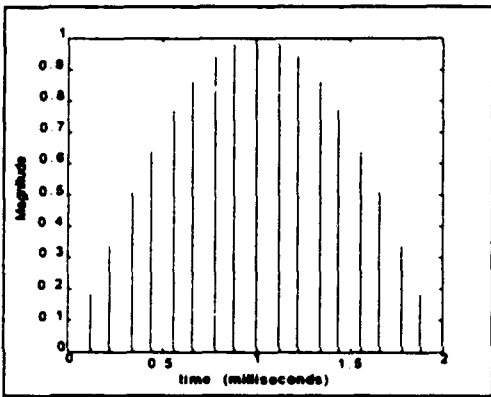
The probability density is calculated for a burst with a variety of pulse repetition frequencies (PRF). The PRFs chosen are 3, 6, 9, and 12 kHz. Plots showing the bursts used are presented in Figure A-5.



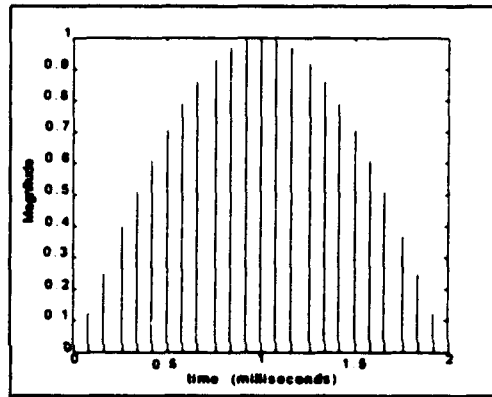
PRF = 3 kHz



PRF = 6 kHz



PRF = 9 kHz



PRF = 12 kHz

Figure A-5. Bursts used to examine the effect of PRF on the TOA probability density

The other burst characteristics are:

Burst Length:	2.0 milliseconds
Pulsewidth	1.00 microseconds,
Peak Signal to Noise Ratio	25 dB,
Sampling Rate	8 MHz

The calculated probability density functions for the bursts in Figure A-5 are plotted in Figure A-6.

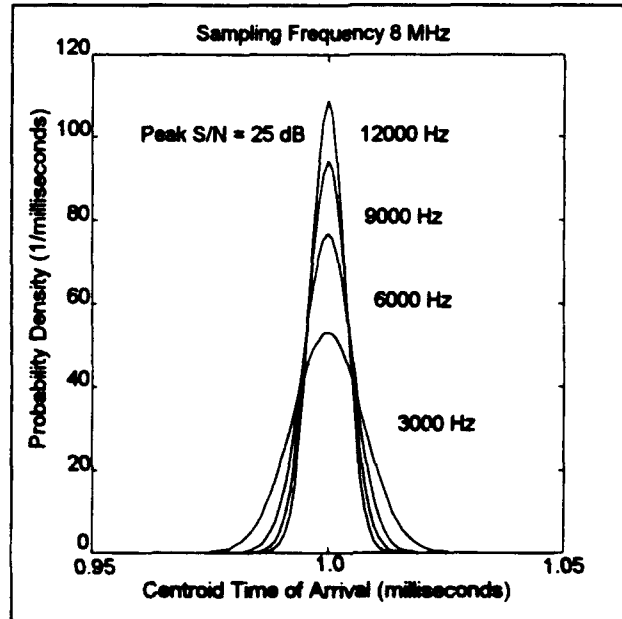


Figure A-6. Burst TOA probability densities for PRFs of 3, 6, 9, and 12 kHz.

As the PRF increases the standard deviation of the burst TOA error decreases. With an increase in the PRF more energy is contained in the burst and the effect of the noise present diminishes.

4. Calculated Mean and Standard Deviation of Sampled Bursts

The means and standard deviations are calculated for the bursts in Figure A-5 for a variety of peak signal to noise ratios. The mean time of arrival for the centroid of the

burst is 1.0 milliseconds for all of the bursts. The standard deviations are listed in

Table A-2.

S/N	Sampling Rate			
	3000 Hz	6000 Hz	9000 Hz	12000 Hz
15 dB	0.02392	0.01665	0.01353	0.01185
20 dB	0.01337	0.00925	0.00755	0.00655
25 dB	0.00754	0.00524	0.00428	0.00373
30 dB	0.00428	0.00300	0.00248	0.00218

TABLE A-2. STANDARD DEVIATION FOR 2.0 MILLISECOND SAMPLED UNIT BURST (milliseconds)

The data in Table A-2 show that the PRFs and the variances of the burst TOA are inversely proportional. The relationship between the PRF and the variance of the burst TOA is shown below for a signal to noise ratio of 20 dB:

$$\frac{\text{Var}_{12000}}{\text{Var}_{3000}} = \frac{(0.00655)^2}{(0.01337)^2} = 0.240 \approx \frac{3000 \text{ Hz}}{12000 \text{ Hz}}$$

Similar to the relationship between the PRF and the variance of the burst TOA, the peak signal to noise ratio and the variance of the burst TOA are inversely proportional. For a PRF of 6000 Hz:

$$\frac{\text{Var}_{15\text{dB}}}{\text{Var}_{25\text{dB}}} = \frac{(0.01665)^2}{(0.00524)^2} = 10.0 \approx (25\text{dB} - 15\text{dB})$$

5. Effect of the Pulsewidth on the Probability Density

The probability density function of the burst TOA is calculated to examine the effect of the pulsewidth on the probability density. A burst is generated with the following characteristics:

Burst Length:	2.0 milliseconds
Peak Signal to Noise Ratio	20 dB,
Pulse Repetition Frequency	6000 Hz,
Sampling Rate	8 MHz

For this burst the pulse width is varied from 1.0 microseconds to 4.0 microseconds and the probability density function is calculated and the mean and standard deviations are examined. The probability densities for each of the bursts are plotted in Figure A-7.

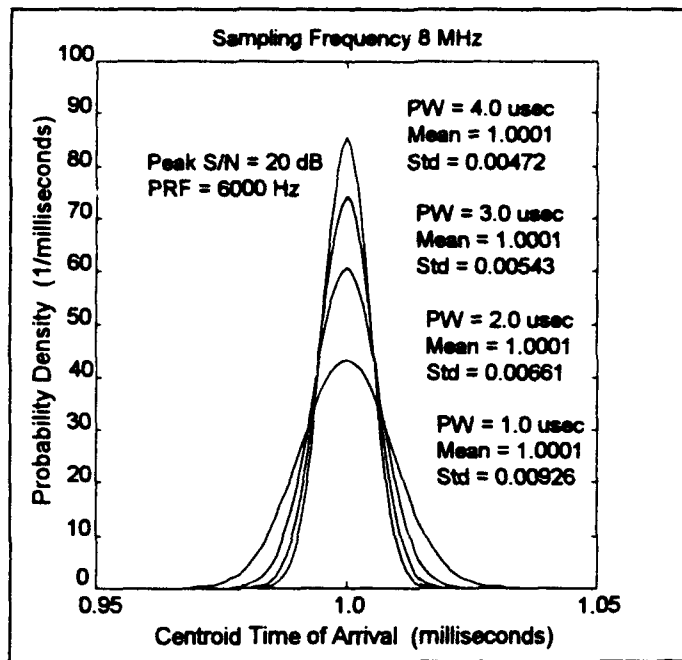


Figure A-7. Burst TOA probability densities for pulse widths of 1.0, 2.0, 3.0, and 4.0 microseconds

As shown in Figure A-7, the effect of the pulsewidth on the probability density function is similar to the effect of the PRF and the peak signal to noise ratio on the probability density function. As the pulsewidth increases, the standard deviation of the probability density decreases. As the pulse width, and effectively the power present in the burst increases, the estimate of the TOA of the centroid of the burst becomes more accurate. The pulsewidth and the variance of the TOA of the burst centroid are inversely proportional. The relationship between the pulse width and the variance of the probability density function is shown below for a signal to noise ratio of 20 dB and a PRF of 6000 Hz:

$$\frac{\text{Var}_{4.0}}{\text{Var}_{1.0}} = \frac{(0.00472)^2}{(0.00926)^2} = 0.240 \approx \frac{1.0 \mu \text{sec}}{4.0 \mu \text{sec}}$$

APPENDIX B. LOCI OF CONSTANT TDOA

A. BURST TDOA PROBLEM

The burst TDOA for two widely separated receivers being scanned by a constantly rotating emitter is directly proportional to the angle formed by the two receivers and the emitter.

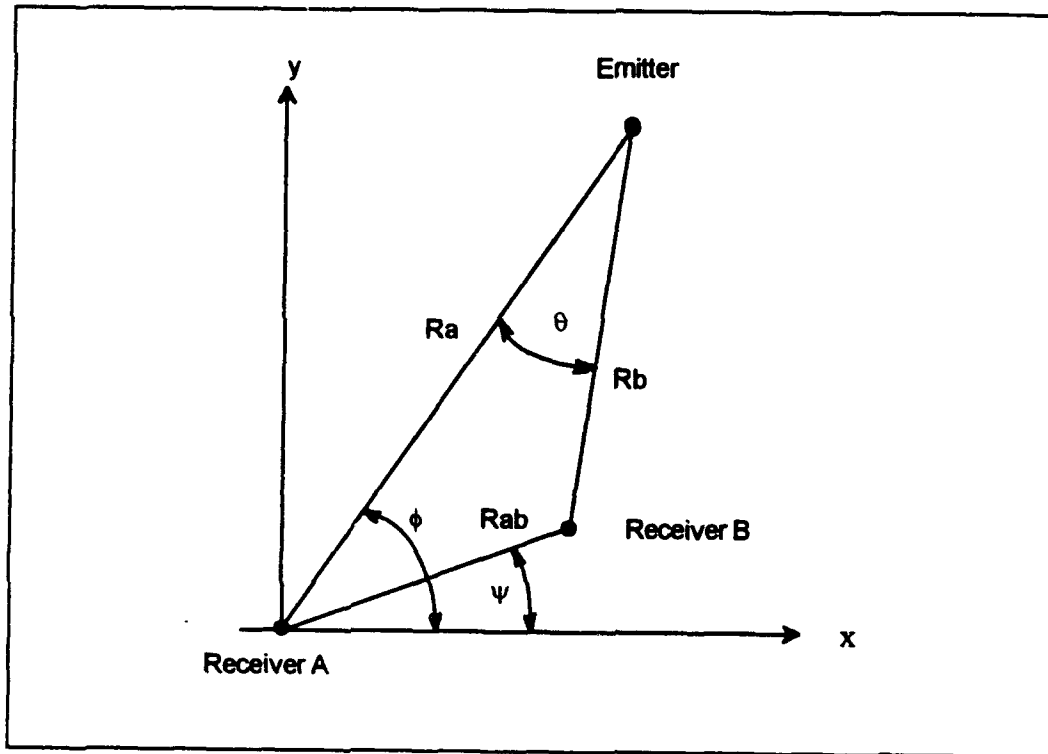


Figure B-1. Angular relationships, burst TDOA problem

Using the geometry in Figure B-1, a relationship exists between the bearing and range from receiver A to receiver B, the bearing and range to the emitter, and the angle θ .

$$\frac{R_a}{\sin(\pi - (\theta + \phi - \psi))} = \frac{R_{ab}}{\sin(\theta)} \quad (B-1)$$

Where
 SR = the scan rate of the emitter in radians/second,
 Ra = the range to the emitter,
 ϕ = the bearing to the emitter,
 Rb = the range to receiver B,
 ψ = the bearing to receiver B, and
 θ = the angle formed by the receivers and the emitter.

When this equation is rearranged:

$$\tan(\theta) = \frac{\sin(\phi - \psi)}{SR \left[\frac{R_a}{R_{ab}} - \cos(\phi - \psi) \right]} \quad (B-2)$$

If the assumption is made that the angle θ is small, then the tangent of θ is approximately equal to the angle θ and the TDOA can be found from the following equation:

$$TDOA = \frac{\theta}{SR} = \frac{\sin(\phi - \psi)}{SR \left[\frac{R_a}{R_{ab}} - \cos(\phi - \psi) \right]} \quad (B-3)$$

Equation (B-3) is used to plot all of the possible locations that an emitter could be located given a TDOA observation.

B. PULSE TDOA PROBLEM

A simple relationship exists that can be used to plot the loci of constant TDOA for the pulse TDOA problem. The pulse TDOA problem geometry is shown in Figure B-2.

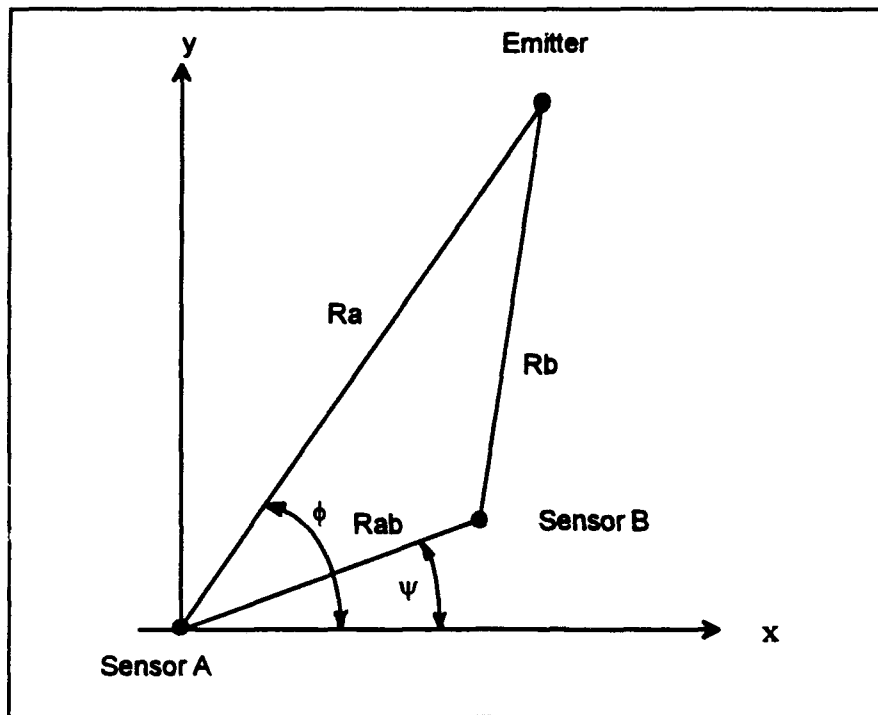


Figure B-2. Pulse TDOA problem geometry

From the law of cosines:

$$R_b^2 = R_a^2 + R_{ab}^2 - 2R_aR_{ab} \cos(\phi - \psi) \quad (\text{B-4})$$

The difference between R_a and R_b is the distance that a pulse must travel to reach the more distant receiver A. The amount of time required to travel this distance is the pulse TDOA. This distance D can be found from the following equation:

$$D = (\text{TDOA})c \quad (\text{B-5})$$

Where TDOA = the pulse time difference of arrival,
 c = the speed of light.

Therefore, R_b is:

$$R_b = R_a - D \quad (\text{B-6})$$

Substituting into equation (B-4):

$$(R_a - D)^2 = R_a^2 + R_{ab}^2 - 2R_a R_{ab} \cos(\phi - \psi) \quad (\text{B-7})$$

$$\phi = \arccos \left[\frac{R_{ab}^2 - 2R_a D + D^2}{2R_a R_{ab}} \right] + \psi \quad (\text{B-8})$$

Equation (B-8) can be used to plot the possible locations of an emitter given the locations of the sensors and the TDOA.

APPENDIX C. TDOA ORTHOGONALITY

A. BURST TDOA ORTHOGONALITY

Equation (C-1) is an approximate relationship used to calculate the loci of constant TDOA for the burst TDOA problem.

$$\text{TDOA} = \frac{\sin(\phi - \psi)}{\text{SR} \left[\frac{R_a}{R_b} - \cos(\phi - \psi) \right]} \quad (\text{C-1})$$

Where

- SR = the scan rate of the emitter in radians/second,
- R_a = the range to the emitter,
- φ = the bearing to the emitter,
- R_b = the range to receiver B,
- ψ = the bearing to receiver B, and
- θ = the angle formed by the receivers and the emitter.

A measure of the orthogonality of the TDOA observations can be found by taking the dot product of the unit vectors tangent to the loci of constant TDOA at the coordinates of the emitter. These vectors can be calculated from the slope of the line tangent to the loci at the point of interest. The dot product of the unit vectors tangent to the loci will yield the cosine of the angle formed by the two loci. The equation for the dot product is given below:

$$R_{t_1} \cdot R_{t_2} = \cos \theta \quad (\text{C-2})$$

Where

- R_{t₁} = The unit vector tangent to the loci number 1,
- R_{t₂} = the unit vector tangent to loci number 2, and
- θ = the angle formed by the two vectors.

The cosine of the angle formed by the vectors tangent to the loci is an indication of the orthogonality of the loci. If the cosine of the angle formed by the loci is close to one then

the loci are nearly parallel. If the cosine of θ is zero the loci are orthogonal and lie at right angles to each other. The slope, dyt/dxt , of the loci of constant TDOA was found by expressing equation (C-1) in Cartesian coordinates and implicitly differentiating. An assumption is made to simplify the problem. If the distance from receiver A to the emitter is much larger than the distance to receiver B, the ratio Ra/Rab will be much larger than one, and equation (C-1) can be approximated with equation (C-3).

$$TDOA = \frac{Rab \sin(\phi - \psi)}{SR(Ra)} \quad (C-3)$$

For a given loci the TDOA, Rab , and SR will be constant and are not a function of the location of the emitter. The equation can be rewritten in the following form:

$$\frac{SR(TDOA)}{Rab} = \frac{\sin \phi \cos \psi - \sin \psi \cos \phi}{Ra} \quad (C-4)$$

The following substitutions are made to solve for the equation in terms of the location of the emitter xt and yt .

$$\sin \phi = \frac{(yt - ya)}{Ra} \quad \cos \phi = \frac{(xt - xa)}{Ra} \quad Ra = [(xt - xa)^2 + (yt - ya)^2]^{1/2} \quad (C-5)$$

The resulting equation is:

$$\frac{SR(TDOA)}{Rab} = \frac{(yt - ya)\cos \psi - (xt - xa)\sin \psi}{[(xt - xa)^2 + (yt - ya)^2]} \quad (C-6)$$

The $\cos \psi$ and the $\sin \psi$ terms are retained to make the derivations more clear. Implicit differentiation was used to calculate the derivative dyt/dxt of equation (C-6). The term on

the left side of equation (C-6) is a constant and therefore its derivative is zero. The final derivative is given by equation (C-7).

$$\frac{dyt}{dxt} = \frac{[(xt - xa)^2 \sin \psi - 2(xt - xa)(yt - ya) \cos \psi - (yt - ya)^2 \sin \psi]}{[(yt - ya)^2 \cos \psi - 2(xt - xa)(yt - ya) \sin \psi - (xt - xa)^2 \cos \psi]} \quad (C-7)$$

Where xt, yt = the x and y coordinates of the emitter,
 xa, ya = the x and y coordinates of receiver A, and
 ψ = the bearing from receiver A to receiver B.

The bearing from receiver A to receiver B is calculated from the following equation:

$$\psi = \arctan \left[\frac{yb - ya}{xb - xa} \right] \quad (C-8)$$

The unit vector tangent to the loci of constant TDOA at the coordinates of the emitter is given by the following equation:

$$\bar{R}_t = \frac{1}{\sqrt{1+m^2}} \hat{x} + \frac{m}{\sqrt{1+m^2}} \hat{y} \quad (C-9)$$

Where R_t = the unit vector tangent to the loci, and
 m = the slope of the loci dyt/dxt at the emitter.

B. PULSE TDOA ORTHOGONALITY

The dot product of the unit vectors tangent to the loci of constant TDOA give the cosine of the angle between the loci of constant TDOA and a good indication of the orthogonality of TDOA observations. The unit vectors tangent to the loci are calculated from the slope of the loci. The slope of the loci of constant TDOA can be found by taking the derivative dyt/dxt of equation (C-10).

$$\text{TDOA} = \frac{\left[(x_t - x_a)^2 + (y_t - y_a)^2 \right]^{1/2} - \left[(x_t - x_b)^2 + (y_t - y_b)^2 \right]^{1/2}}{c} \quad (\text{C-10})$$

Where x_t, y_t = the x and y coordinates of the emitter,
 x_a, y_a = the x and y coordinates of sensor A,
 x_b, y_b = the x and y coordinates of sensor B, and
 c = the speed of light.

An assumption will simplify the problem and yield an approximate, but simpler solution.

If the distance from the sensors to the emitter is much larger than the distance between the sensors, the approaching pulses can be considered plane waves, and the TDOA for the pulses arriving at the sensors can be calculated from the geometry in Figure C-1.

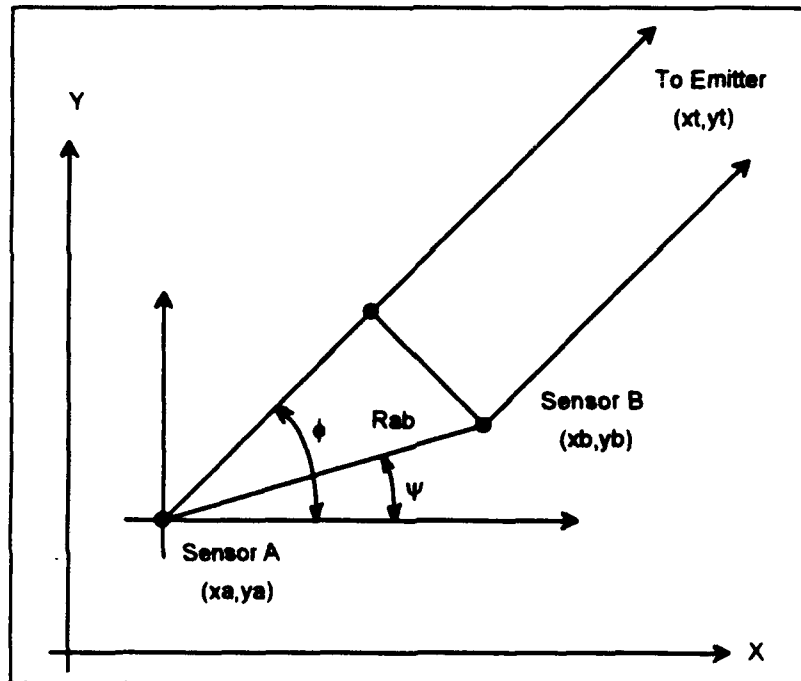


Figure C-1. Pulse TDOA geometry for emitter at a long distance

The TDOA calculated from the geometry in Figure C-1.

$$\text{TDOA} = \frac{R_{ab} \cos(\phi - \psi)}{c} \quad (\text{C-11})$$

Where R_{ab} = the distance from sensor A to sensor B,
 ϕ = the bearing to the emitter,
 ψ = the bearing from sensor A to sensor B, and
 c = the speed of light.

Using trigonometric identities and the substitutions in equations (C-12) and (C-13), equation (C-11) can be rewritten as equation (C-14).

$$\cos \phi = \frac{(xt - xa)}{[(xt - xa)^2 + (yt - ya)^2]^{1/2}} \quad (\text{C-12})$$

$$\sin \phi = \frac{(yt - ya)}{[(xt - xa)^2 + (yt - ya)^2]^{1/2}} \quad (\text{C-13})$$

$$\frac{c(\text{TDOA})}{R_{ab}} = \frac{(xt - xa)\cos \psi + (yt - ya)\sin \psi}{[(xt - xa)^2 + (yt - ya)^2]^{1/2}} \quad (\text{C-14})$$

Implicit differentiation is used to calculate the derivative of equation (C-14). The derivative of the left hand side is zero because for a given loci the terms on the left hand side of equation (C-14) are constant. The equation for the slope of the loci of constant TDOA is given in equation (C-15).

$$\frac{dyt}{dxt} = \frac{(yt - ya)^2 \cos \psi - (xt - xa)(yt - ya)\sin \psi}{(xt - xa)(yt - ya)\cos \psi - (xt - xa)^2 \sin \psi} \quad (\text{C-15})$$

Where xt, yt = the x and y coordinates of the emitter,
 xa, ya = the x and y coordinates of sensor A,
 xb, yb = the x and y coordinates of sensor B, and
 ψ = the bearing from sensor A to sensor B.

The bearing from sensor A to sensor B is calculated from the following:

$$\psi = \arctan \left[\frac{(yb - ya)}{(xb - xa)} \right] \quad (C-16)$$

The unit vector tangent to the loci of constant TDOA at the coordinates of the emitter is given by the following equation:

$$\bar{R}_t = \frac{1}{\sqrt{1+m^2}} \hat{x} + \frac{m}{\sqrt{1+m^2}} \hat{y} \quad (C-17)$$

Where R_t = the unit vector tangent to the loci, and
 m = the slope of the loci at the emitter.

APPENDIX D. BURST H_{xx} DERIVATION

The equation that calculates the TDOA observations as a function of the receiver locations, the emitter locations, and the scan rate of the emitter, is given by:

$$\text{TDOA} = \frac{1}{\text{SR}} \left[\frac{(x_t - x_a)(y_t - y_b) - (y_t - y_a)(x_t - x_b)}{[(x_t - x_a)^2 + (y_t - y_a)^2]^{1/2} [(x_t - x_b)^2 + (y_t - y_b)^2]^{1/2}} \right] \quad (\text{D-1})$$

Where x_t, y_t = the x and y coordinate of the emitter,
 x_a, y_a = the x and y coordinate of receiver A,
 x_b, y_b = the x and y coordinate of receiver B, and
SR = the scan rate of the emitter in rad/sec.

The following MATLAB function was used to evaluate the partial derivative of the observation equation (D-1). The terms and derivatives in the MATLAB function were calculated using a symbolic processor contained in the software package MATHCAD.

```
function [Hx,Hy] = hk3(xt,yt,xa,ya,xb,yb,SR);  
  
% A function to calculate the derivative of the observation equation  
% This function assumes that all of the receivers are allowed to move, and  
% Their locations are known. The scan rate is known a priori.  
%  
% Richard W. Williamson  
% Date: 18 February 1994  
% Date Revised: 18 July 1994  
%  
% This program evaluates the partial derivatives of equation (D-1)  
  
  
% Define extra variables for clarity.  
  
xa2 = xa^2;  
ya2 = ya^2;
```

```
xb2 = xb^2;  
yb2 = yb^2;
```

```
xt2 = xt^2;  
xt3 = xt^3;
```

```
yt2 = yt^2;  
yt3 = yt^3;
```

```
% Denominator of the original TDOA function; Equation (D-1)
```

```
G = ( (xt-xa)^2 + (yt-ya)^2 )*( (xt-xb)^2 + (yt-yb)^2 );
```

```
dgdx = -4*xt*yt*yb + 8*xt*xa*xb - 2*xa*xb2 - 2*xa*yt2 - 2*xa*yb2 -...  
2*xa2*xb - 2*yt2*xb - 4*yt*ya*xt - 2*ya2*xb + 4*xt3 - ...  
6*xt2*xb + 2*xt*xb2 + 4*yt2*xt + 2*xt*yb2 - 6*xt2*xa +...  
2*xa2*xt + 2*ya2*xt + 4*xa*yt*yb + 4*yt*ya*xb;
```

```
dgdy = -2*xt2*yb - 4*xt*xa*yt - 2*xa2*yb - 4*yt*xt*xb - 2*ya*xt2 - ...  
2*ya*xb2 + 8*yt*ya*yb - 2*ya*yb2 - 2*ya2*yb + 4*yt3 +...  
4*xt2*yt + 2*xa2*yt + 2*yt*xb2 - 6*yt2*yb + 2*yt*yb2 - ...  
6*yt2*ya + 2*ya2*yt + 4*xt*xa*yb + 4*ya*xt*xb;
```

```
% Numerator of the original TDOA function; Equation (D-1) expanded out
```

```
f = xt*(ya-yb) + yt*(xb-xa) + (xa*yb-xb*ya);
```

```
dfdx = (ya-yb);
```

```
dfdy = (xb-xa);
```

```
% The calculated numerators of the derivative functions
```

```
numdhdx = G*dfdx - 0.5*f*dgdx;
```

```
numdhdy = G*dfdy - 0.5*f*dgdy;
```

```
% Evaluate the partial derivatives
```

```
Hx = (1/SR)*numdhdx/(sqrt(G^3));
```

```
Hy = (1/SR)*numdhdy/(sqrt(G^3));
```

APPENDIX E. MATLAB PROGRAMS

```
% Burst.m
%
% Name: Richard W. Williamson
% Date: 18 Feburary 1994
% Date Revised: 18 July 1994
%
% This program implements an extended Kalman filter to estimate
% the location of an emitter from the TDOAs of a burst between three
% receivers. The position of the receivers are known exactly.
% The algorithm generates noise free TDOA observations and adds white
% Gaussian noise to the observations. The variance of the white Gaussian
% noise is specified in the program and can be different for each receiver.
% Twenty-five observations are processed.
%
% The sensors are initially located at the following coordinates:
%
% Receiver A (500, 100)
% Receiver B (20000, -2000)
% Receiver C (-20000, -20000)
%
% The TDOA measurements are corrupted by white Gaussian noise.
% The variance of the noise for all TDOA observations is 1.694e-15.
%
% The emitter was located at a range of 500 kilometers from the origin
% and at a bearing of 90 degrees measured from the x-axis.
% The coordinates of the emitter were:
%
% Emitter: (0, 500) kilometers.
%
% %%%%%%%%%%%
%
```



```

%
% The program outputs four figures.
%
% figure(1) The plot of the estimates of the x and y coordinates of the
% emitter
% figure(2) The Kalman gains calculated for each observation
% figure(3) An X-Y plot of the estimates of the coordinates of the emitter.
% This plot also includes the loci of constant TDOA and the
% 3σ error ellipsoids for the 1st, 8th, 15th, and 22nd estimate
% of the location.
% figure(4) A closeup of the steady state estimate of the emitter location.
% The plot is centered on the steady state estimate of the
% emitter location and the 3σ error ellipsoid corresponding
% to the steady state estimate is plotted.
%
% %%%%%%%%%%%
% The program calls four subroutines.
%
% tdoa3.m Calculates the time difference of arrival of a burst
% between two receivers. The locations of the receivers
% are arbitrary. The TDOA is calculated from the locations
% of the receivers, the location of the emitter, and the scan
% rate.
%
% hk3.m Calculates the derivative of the observation equation given
% the location of the two receivers, the scan rate, and the
% estimated location of the emitter.
%
% bloci.m Calculates the loci of constant TDOA given the TDOA
% observation and the locations of the receivers.
%
% ellip.m Calculates the error ellipsoids given the location of the point
% of interest, the error covariance matrix, and the number of
% standard deviations required.
%
% %%%%%%%%%%%
%
%

```

```

clear;

% Range and bearing to the target
Rt = 500000;
Brngt = 90;
xt = Rt*cos(Brngt*pi/180);
yt = Rt*sin(Brngt*pi/180);

% The number of observations processed.

k = 1:25;
len = length(k);

% The coordinates of receivers A, B, and C as a function of k
xa = 500*ones(1,len) + 00*k;;
ya = 100*ones(1,len) + 30*k;;
xb = 20000*ones(1,len) + 30*k;
yb = -2000*ones(1,len) - 30*k;
xc = -20000*ones(1,len) - 30*k;
yc = -20000*ones(1,len) - 30*k;

%%%%%%%%%%%%%%%%%%%%%%%%%%%%%%%%%%%%%%%%%%%%%%%%%%%%%%%%%%%%%%%%%%%%%%%%
%
% Initializing variables

Po = 1.00e+20*eye(2);      % The initial error covariance matrix
Q = 4.0e+06*eye(2);       % Variance of the state excitation noise.
RKab = 5.660e-09;         % The variance on the TDOA error Rcvr A-B
RKac = 5.660e-09;         % The variance on the TDOA error Rcvr A-C
RKbc = 5.660e-09;         % The variance on the TDOA error Rcvr A-C
Srate = 2*pi;             % The scan rate of the emitter

X = zeros(2,len);         % The state matrix
Pk = zeros(2,2);          % The error covariance matrix
HK = zeros(3,2);          % The linearized derivative of h(k)
g = zeros(2,len);         % The Kalman gains
z_tru = zeros(3,len);     % The vector of true observations
Z = zeros(3,len);         % The vector of noisy observations
Zhat = zeros(3,len);      % The vector of estimated observations

```

```

% Calculation of the observations noise free observations
for k = 1:len,
    z_tru(1,k) = tdoa3(xt,yt,xa(k),ya(k),xb(k),yb(k),Srate);
    z_tru(2,k) = tdoa3(xt,yt,xa(k),ya(k),xc(k),yc(k),Srate);
    z_tru(3,k) = tdoa3(xt,yt,xb(k),yb(k),xc(k),yc(k),Srate);
end;

% Calculate the noise on the TDOA estimates
rand('normal');
n = sqrt(RKab)*rand(3,len);

% Form the matrix of noisy observations.
Z = z_tru + n;

% A priori estimate of the location of the emitter

Xo = [0 10000]';

%%%%%%%%%%%%%%%%%%%%%%%%%%%%%%%%%%%%%%%%%%%%%%%%%%%%%%%%%%%%%%%%%%%%%%%%
% Initialize the Extended Kalman filter

Pk = Po;      % Initialize the Pk the error covariance matrix.
X(:,1) = Xo;  % Initialize the state vector

for k = 1:len,

    k

% Processes the observation for receiver A and B

% Calculates the derivative of the Rcvr A-B TDOA equation wrt x and y
[h1ab h2ab] = hk3(X(1,k),X(2,k),xa(k),ya(k),xb(k),yb(k),Srate);

% Forms the Hk matrix
HKab = [h1ab h2ab];

% Calculates the next PK based upon the previous PK

Pk = Pk + Q;

```

% Calculates the kalman gains

GKab = Pk*HKabinv(HKab*Pk*HKab' + RKab);**

**% Calculates the estimate of the observation based upon the
% estimate of the states.**

Zhat(1,k) = tdoa3(X(1,k),X(2,k),xa(k),ya(k),xb(k),yb(k),Srate);

**% Calculates an update of the state based upon the difference in
% the actual observation and the estimate of the observation.**

X(:,k) = X(:,k) + GKab*(Z(1,k)-Zhat(1,k));

**% Updates the variance matrix Pk based upon the observation
Pk = (eye(2) - GKab*HKab)*Pk;**

% Processes the observation for receiver A and C

**% Calculates the derivative of the TDOA equation wrt x and y
[h1ac h2ac] = hk3(X(1,k),X(2,k),xa(k),ya(k),xc(k),yc(k),Srate);**

% Forms the Hk matrix

HKac = [h1ac h2ac];

% Calculates the next PK based upon the previous PK

Pk = Pk + Q;

% Calculates the kalman gains

GKac = Pk*HKacinv(HKac*Pk*HKac' + RKac);**

**% Calculates the estimate of the observation based upon the
% estimate of the states.**

Zhat(2,k) = tdoa3(X(1,k),X(2,k),xa(k),ya(k),xc(k),yc(k),Srate);

**% Calculates an update of the state based upon the difference in
% the actual observation and the estimate of the observation.**

X(:,k) = X(:,k) + GKac*(Z(2,k)-Zhat(2,k));

**% Updates the variance matrix Pk based upon the observation
Pk = (eye(2) - GKac*HKac)*Pk;**

```

% Processes the observation for receiver B and C

% Calculates the derivative of the TDOA equation wrt x and y
[h1bc h2bc] = hk3(X(1,k),X(2,k),xb(k),yb(k),xc(k),yc(k),Srate);

% Forms the Hk matrix
HKbc = [h1bc h2bc];

% Calculates the next PK based upon the previous PK

Pk = Pk + Q;

% Calculates the kalman gains

GKbc = Pk*HKbc*inv( HKbc*Pk*HKbc' + RKbc );

% Calculates the estimate of the observation based upon the
% estimate of the states.
Zhat(3,k) = tdoa3(X(1,k),X(2,k),xb(k),yb(k),xc(k),yc(k),Srate);

% Calculates an update of the state based upon the difference in
% the actual observation and the estimate of the observation.
X(:,k) = X(:,k) + GKbc*( Z(3,k)-Zhat(3,k) );

% Updates the variance matrix Pk based upon the observation
Pk = (eye(2) - GKbc*HKbc)*Pk;

% Projects the next state based upon the current state

X(:,k+1) = X(:,k);

% Save the error covariance matrices
if k == 1
    P = Pk;
else,
    P = [P;Pk];
end;

% Save the Kalman gains

g(:,k) = GKbc;

end;          % End of the filtering routine

```

```
%%%%%%%%%%%%%%%%%%%%%%%%%%%%%%%%%%%%%%%%%%%%%%%%%%%%%%%%%%%%%%%%%%%%%%%%
% Output the filtered estimates of x and y
```

```
t = 1:len;
figure(1)
plot(t,X(1,t)/1000,t,X(2,t)/1000)
axis([1 25 -50 600])
pause;
```

```
% Plot of the Kalman gains
```

```
figure(2)
clg
plot(t,g(1,:),t,g(2,:))
title('Kalman Gains')
xlabel('Number of Observations')
ylabel('Magnitude')
pause
```

```
%%%%%%%%%%%%%%%%%%%%%%%%%%%%%%%%%%%%%%%%%%%%%%%%%%%%%%%%%%%%%%%%%%%%%%%%
% Calculate the steady state estimate of emitter location
```

```
xtavg = mean(X(1,k-10:k));
ytavg = mean(X(2,k-10:k));
```

```
% Calculate the coordinates of the loci of constant TDOA based
% upon noise free TDOA observations
```

```
Tab = bloci(xa(k),ya(k),xb(k),yb(k),z_tru(1,k),Srate);
```

```
Tac = bloci(xa(k),ya(k),xc(k),yc(k),z_tru(2,k),Srate);
```

```
Tbc = bloci(xb(k),yb(k),xc(k),yc(k),z_tru(3,k),Srate);
```

```
% Plot the locus of emitter locations and actual emitter locations
```

```
figure(3)
clg
% Plots coordinates of the estimates of the emitter location
% axis([-500 500 -30 1000]);
```

```

plot(X(1,+)/1000,X(2,+)/1000,'r' )
hold on

% Plots the actual emitter location
plot(xt/1000,yt/1000,'g')

% Plots the final locations of the receivers
plot(xa(k)/1000,ya(k)/1000,'*g')
plot(xb(k)/1000,yb(k)/1000,'*g')
plot(xc(k)/1000,yc(k)/1000,'*g')

% Plots the locus of possible emitter locations
plot( Tab(1,+)/1000, Tab(2,+)/1000,'b')
plot( Tac(1,+)/1000, Tac(2,+)/1000,'b')
plot( Tbc(1,+)/1000, Tbc(2,+)/1000,'b')

% Plot three sigma error ellipsoids for various points

C = 3.00; % The number of standard deviations plotted in error ellipsoids
for k = 1:7:len-1,

    P1 = [P(2*k-1,1) P(2*k-1,2); P(2*k,1) P(2*k,2)]; % The Pk Matrix

    [xg,y1,y2,Emax,Emin] = ellip(P1,C,X(1,k),X(2,k)); % Calculate ellipse

    plot((xg)/1000,(y1)/1000,'g-',(xg)/1000,(y2)/1000,'g-') % Plot the ellipse

end;

% axis;
hold off
axis([-250 250 -50 600]);
pause

% Plot the locus of emitter locations and actual emitter locations

figure(4)
clg
% Plots coordinates of the estimates of the emitter location

plot(X(1,+)/1000,X(2,+)/1000,'r' )
hold on

```

```

% Plots the actual emitter location
plot(xt/1000,yt/1000,'*g');

% Plots the locus of possible emitter locations
plot( Tab(1,+)/1000, Tab(2,+)/1000,'b');
plot( Tac(1,+)/1000, Tac(2,+)/1000,'b');
plot( Tbc(1,+)/1000, Tbc(2,+)/1000,'b');

% Plots the error ellipsoids

[xg,y1,y2,Emax,Emin] = ellip(Pk,C,xtavg,ytavg);

plot((xg)/1000,(y1)/1000,'g-',(xg)/1000,(y2)/1000,'g-')

Major = sprintf('%5.1f',Emax/1000);
Minor = sprintf('%5.1f',Emin/1000);

text((xt-0.50*Emax)/1000,(yt+0.85*Emax)/1000,['Major Axis = ' Major ' km'])
text((xt-0.50*Emax)/1000,(yt+0.75*Emax)/1000,['Minor Axis = ' Minor ' km'])

% axis;
hold off

axis([(xt-Emax)/1000 (xt+Emax)/1000 (yt-Emax)/1000 (yt+Emax)/1000]);
% axis('square')
%
%
%
```



```

% tdoa3.m
%
% Name: Richard W. Williamson
% Date: 18 February 1994
% Date Revised: 18 July 1994
%
% This program calculates the burst observation equation h(x(k)).
%
% Input:    The coordinates of receiver A (meters):      xa, ya
%           The coordinates of receiver B (meters):      xb, yb
%           The coordinates of the emitter (meters):      xt, yt
%           Scan rate of the emitter:                     SR
%
% Output    The burst time difference of arrival for
%           the specified receiver locations.              T
%
%
function T = TDOA3(xt,yt,xa,ya,xb,yb,SR)

% Numerator of the observation equation
f = xt*(ya-yb) + yt*(xb-xa) + (xa*yb-xb*ya);

% Denominator of the observation equation
G = ( (xt-xa)^2 + (yt-ya)^2 )*( (xt-xb)^2 + (yt-yb)^2 );

% Calculate the TDOA
T = f/(SR*sqrt(G));

%

```

```

% HK3.m
%
% Name: Richard W. Williamson
% Date: 18 Feburary 1994
% Date Revised: 18 July 1994
%
% This program calculates the derivative of the observation equation h(x(k)).
%
% Input:      The coordinates of receiver A (meters):      xa, ya
%             The coordinates of receiver B (meters):      xb, yb
%             The coordinates of the emitter (meters):      xt, yt
%             Scan rate of the emitter:                      SR
%
% Output      The vector of partial derivaties of h(x(k))
%             with respect to xt and yt.                    [Hx,Hy]
%
function [Hx,Hy] = hk3(xt,yt,xa,ya,xb,yb,SR);

% A function to calculate the derivative of the
% H matrix. This function does not assume that one of
% The receivers is fixed with respect to the stationary
% coordinate system. This assumes that the scan rate is known.
%
% This program is an implementation of equation ( )
%
% Define variable for easier understanding

xa2 = xa^2;
ya2 = ya^2;

xb2 = xb^2;
yb2 = yb^2;

xt2 = xt^2;
xt3 = xt^3;

yt2 = yt^2;
yt3 = yt^3;

```

```

%
% The original TDOA function;

G = ( (xt-xa)^2 + (yt-ya)^2 )*( (xt-xb)^2 + (yt-yb)^2 );

dgdx = -4*xt*yt*yb + 8*xt*xa*xb - 2*xa*xb2 - 2*xa*yt2 - 2*xa*yb2 - ...
        2*xa2*xb - 2*yt2*xb - 4*yt*ya*xt - 2*ya2*xb + 4*xt3 - ...
        6*xt2*xb + 2*xt*xb2 + 4*yt2*xt + 2*xt*yb2 - 6*xt2*xa + ...
        2*xa2*xt + 2*ya2*xt + 4*xa*yt*yb + 4*yt*ya*xb;

dgdy = -2*xt2*yb - 4*xt*xa*yt - 2*xa2*yb - 4*yt*xt*xb - 2*ya*xt2 - ...
        2*ya*xb2 + 8*yt*ya*yb - 2*ya*yb2 - 2*ya2*yb + 4*yt3 + ...
        4*xt2*yt + 2*xa2*yt + 2*yt*xb2 - 6*yt2*yb + 2*yt*yb2 - ...
        6*yt2*ya + 2*ya2*yt + 4*xt*xa*yb + 4*ya*xt*xb;

f = xt*(ya-yb) + yt*(xb-xa) + (xa*yb-xb*ya);

dfdx = (ya-yb);
dfdy = (xb-xa);

% The calculated numerators of the derivative functions

numdhdx = G*dfdx - 0.5*f*dgdx;
numdhdy = G*dfdy - 0.5*f*dgdy;

% The actual derivative functions

Hx = (1/SR)*numdhdx/(sqrt(G^3));
Hy = (1/SR)*numdhdy/(sqrt(G^3));

```

```

% Bloci.m
%
% Name: Richard W. Williamson
% Date: 18 Feburary 1994
% Date Revised: 18 July 1994
%
% This program calculates the coordinates of the loci of constant TDOA for
% a pair of receivers.
%
% Input:   The coordinates of receiver A (meters):      xa, ya
%          The coordinates of receiver B (meters):      xb, yb
%          The Time Difference of Arrival (sec):         TD
%          Scan rate of the emitter:                   SR
%
% Output  The vector of x and y coordinates of the loci
%          of constant TDOA.                            T
%
function T = bloci(xa,va,xb,yb,TD,Srate)

% Polar plot of the receivers, the emitter,and the locus of possible
% emitter location.

% The angles of phi to be plotted.
phi = 0:pi/100:pi;

% Calculates the range and bearing to the receivers.
Rab = sqrt( (xb-xa)^2 + (yb-ya)^2 );

psi = atan2(yb-ya,xb-xa)*ones(1,1:length(phi));

% Initialize the range variables
Ra = zeros(1,length(phi));

Ra = Rab*( sin(phi-psi)/tan(TD*Srate) + cos(phi-psi) );

dxa = xa*ones(1,1:length(phi));
dya = ya*ones(1,1:length(phi));

% Plots the locus of possible emitter location.
T = [Ra.*cos(phi)+dxa ; Ra.*sin(phi)+dya ]
;

```

```

% pulse.m
%
% This program implements an extended Kalman filter to estimate
% the location of an emitter from the TDOA of a pulse between two
% sensors. Two receiver platforms are used and their location is
% known exactly. Each receiver platform consists of two sensors. The
% algorithm generates noise free TDOA observations for the known receiver
% and emitter locations and adds white Gaussian noise to the observations.
% The variance of the white Gaussian noise is specified in the program
% and can be different for each receiver platform. Sixty observations
% are processed.
%
%
% The sensors are located at the following coordinates:
%
% Receiver 1  Sensor A (0,0)
% Receiver 1  Sensor B (500,0)
% Receiver 2  Sensor A (20000,0)
% Receiver 2  Sensor B (20500,0)
%
% The TDOA measurements are corrupted by white Gaussian noise.
% The variance of the noise for both receivers is 1.694e-15.
%
% The emitter was located at a range of 30 kilometers from the origin
% and at a bearing of 60 degrees measured from the x-axis.
% The coordinates of the emitter were:
%
% Emitter: (15, 26) kilometers.
%
% %%%%%%%%%%%
%

```

```

% The program outputs four figures.
%
%   figure(1)   The plot of the estimates of the x and y coordinates of
%               the emitter
%   figure(2)   The Kalman gains calculated for each observation
%   figure(3)   An X-Y plot of the estimates of the coordinates of
%               the emitter.
%               This plot also includes the loci of constant TDOA and the
%               3σ error ellipsoids for the first, 20th, 39th, and 58th
%               estimate of the emitter.
%   figure(4)   A closeup of the steady state estimate of the emitter
%               location. The plot is centered on the steady state
%               estimate of the emitter location and the 3σ error
%               ellipsoid corresponding to the steady state estimate
%               is plotted.
%
% %%%%%%%%%%%
%
% The program calls two subroutines.
%
%   ploci.m     Calculates the loci of constant TDOA given the TDOA
%               observation and the locations of the receivers.
%   ellip.m     Calculates the error ellipsoids given the location of the point
%               of interest, the error covariance matrix, and the number of
%               standard deviations required.
%
% %%%%%%%%%%%
%
% Initialize the variables
%
c = 3.00e+08;           % The speed of light
R1 = 1.694e-15;        % The covariance of measurement error receiver 1
R2 = 1.694e-15;        % The covariance of measurement error receiver 2
Q = 5.0e+02*eye(2);    % Variance of Plant excitation noise
P0 = 5.0e+20*eye(2);   % Initial error covariance

% Choose to calculate the error covariance of 3 sigma
C = 3.0;

t = (0:60);           % Time vector total of 61 observations
l = ones(1,len);      % occurring 50 micro seconds apart

```

```

% Initialize storage for Kalman gains and the states.
g = zeros(2,length(t));
X = zeros(2,len);

% Emitter location
Rt = 30000;           % Range to the emitter
Bt = 60.00;          % Bearing to the emitter from the origin

xt = Rt*cos(Bt*pi/180); % X coordinate of the emitter
yt = Rt*sin(Bt*pi/180); % Y coordinte of the emitter

% A priori estimate of the location of the target;
X0 = [10000;5000];
%
% The location of the emitter specified for all point in time

xa1 = 0*t + 0*t;      % Receiver 1 Sensor A moves in a straight line
ya1 = 0*t + 0*t;      % at a constant speed

xb1 = 500*t + 0*t;    % Receiver 1 Sensor B moves in a straight line
yb1 = 0*t + 0*t;      % at a constant speed

xa2 = 20000*t + 0*t;  % Receiver 2 Sensor A moves in a straight line
ya2 = 000.00*t + 0*t; % at a constant speed

xb2 = 20500*t + 0*t;  % Receiver 2 Sensor B moves in a straight line
yb2 = 000*t + 0*t;    % at a constant speed

% Calculate the TDOA observations for the two receivers

% Equation
% 
$$\hat{z}(k+1|k) = \frac{[(\hat{x}t(k) - xa(k))^2 + (\hat{y}t(k) - ya(k))^2]^{1/2} - [(\hat{x}t(k) - xb(k))^2 + (\hat{y}t(k) - yb(k))^2]^{1/2}}{c}$$


% Calculate the observations for receiver 1

Z1 = (1/c)*( sqrt( (xt-xa1).^2 + (yt-ya1).^2 ) - ...
        sqrt( (xt-xb1).^2 + (yt-yb1).^2 ) );

% Calculate the observations for receiver 2
Z2 = (1/c)*( sqrt( (xt-xa2).^2 + (yt-ya2).^2 ) - ...

```

```

    sqrt( (xt-xb2).^2 + (yt-yb2).^2 ) );

% Inject zero mean, noise into the observations
rand('normal');
n1 = sqrt(R1)*rand(1,len);
n2 = sqrt(R2)*rand(1,len);

Z1n = Z1 + n1;
Z2n = Z2 + n2;

% Initialize the Kalman filter

X(:, 1) = X0;           % A priori estimate of the emitter location
PK = P0;               % Initial error covariance matrix

% Calculate the filtered estimates of the emitter location

for k = 1:len-1,

% Process TDOA observation Receiver #1
%%%%%%%%%%%%%%%%%%%%%%%%%%%%%%%%%%%%%%%%%%%%%%%%%%%%%%%%%%%%%%%%%%%%%%%%

% Calculate the HK matrix for receiver platform 1

% Equation

$$H(k) = \left[ \frac{1}{c} \left( \frac{\hat{x}t(k) - xa}{Ra(k)} - \frac{\hat{x}t(k) - xb}{Rb(k)} \right) \quad \frac{1}{c} \left( \frac{\hat{y}t(k) - ya}{Ra(k)} - \frac{\hat{y}t(k) - yb}{Rb(k)} \right) \right]$$


% Equation

$$Ra(k) = \left[ (\hat{x}t(k) - xa)^2 + (\hat{y}t(k) - ya)^2 \right]^{1/2}$$


% Equation

$$Rb(k) = \left[ (\hat{x}t(k) - xb)^2 + (\hat{y}t(k) - yb)^2 \right]^{1/2}$$


Ra1 = sqrt( (X(1,k)-xa1(k)).^2 + (X(2,k)-ya1(k)).^2 );
Rb1 = sqrt( (X(1,k)-xb1(k)).^2 + (X(2,k)-yb1(k)).^2 );

h1x = (1/c)*( (X(1,k)-xa1(k))./Ra1 - (X(1,k)-xb1(k))./Rb1 );
h1y = (1/c)*( (X(2,k)-ya1(k))./Ra1 - (X(2,k)-yb1(k))./Rb1 );

HK = [h1x h1y];

% Calculate the estimates of the TDOA based upon the estimate
% of emitter location and location of receiver platform 1

```


% Equation

$$\hat{z}(k+1|k) = \frac{\left[(\hat{x}_t(k) - x_a(k))^2 + (\hat{y}_t(k) - y_a(k))^2 \right]^{1/2} - \left[(\hat{x}_t(k) - x_b(k))^2 + (\hat{y}_t(k) - y_b(k))^2 \right]^{1/2}}{c}$$

$$\text{Zhat1} = (1/c) * (\text{sqrt}((X(1,k)-x_{a1}(k))^2 + (X(2,k)-y_{a1}(k))^2) - \dots \\ \text{sqrt}((X(1,k)-x_{b1}(k))^2 + (X(2,k)-y_{b1}(k))^2));$$

% The new error covariance is the same as the old plus Q.

$$\text{PK} = \text{PK} + \text{Q};$$

% Calculate the Kalman gains

$$\text{GK} = \text{PK} * \text{HK}' * \text{inv}(\text{HK} * \text{PK} * \text{HK}' + \text{R1});$$

% Calculate the updated error covariance matrix

$$\text{PK} = (\text{eye}(2) - \text{GK} * \text{HK}) * \text{PK};$$

% Calculate a smoothed estimate of the bearing to the emitter

$$X(:,k) = X(:,k) + \text{GK} * (\text{Z1n}(k) - \text{Zhat1});$$

% estimate of the emitter location for receiver #2 is same as previous

$$X(:,k) = X(:,k);$$

% Process TDOA observation receiver #2

%%%%%%%%%

% Calculate the HK matrix for receiver platform 2

$$\text{Equation} \quad H(k) = \left[\frac{1}{c} \left(\frac{\hat{x}_t(k) - x_a}{R_a(k)} - \frac{\hat{x}_t(k) - x_b}{R_b(k)} \right) \quad \frac{1}{c} \left(\frac{\hat{y}_t(k) - y_a}{R_a(k)} - \frac{\hat{y}_t(k) - y_b}{R_b(k)} \right) \right]$$

$$\text{Equation} \quad R_a(k) = \left[(\hat{x}_t(k) - x_a)^2 + (\hat{y}_t(k) - y_a)^2 \right]^{1/2}$$

$$\text{Equation} \quad R_b(k) = \left[(\hat{x}_t(k) - x_b)^2 + (\hat{y}_t(k) - y_b)^2 \right]^{1/2}$$

$$R_{a2} = \text{sqrt}((X(1,k)-x_{a2}(k)).^2 + (X(2,k)-y_{a2}(k)).^2);$$

$$R_{b2} = \text{sqrt}((X(1,k)-x_{b2}(k)).^2 + (X(2,k)-y_{b2}(k)).^2);$$

$$h_{2x} = (1/c) * ((X(1,k)-x_{a2}(k))./R_{a2} - (X(1,k)-x_{b2}(k))./R_{b2});$$

$$h_{2y} = (1/c) * ((X(2,k)-y_{a2}(k))./R_{a2} - (X(2,k)-y_{b2}(k))./R_{b2});$$

```
HK = [h2x h2y];
```

```
% Calculate the estimates of the TDOA based upon the estimate  
% of the emitter location and location of receiver Platform 2
```

```
% Equation
```

```
%  $\hat{z}(k+1|k) = \frac{[\hat{x}_t(k) - x_a(k)]^2 + [\hat{y}_t(k) - y_a(k)]^2}{c} - \frac{[\hat{x}_t(k) - x_b(k)]^2 + [\hat{y}_t(k) - y_b(k)]^2}{c}$ 
```

```
Zhat2 = (1/c)*(sqrt( (X(1,k)-xa2(k))^2 + (X(2,k)-ya2(k))^2 ) - ...  
sqrt( (X(1,k)-xb2(k))^2 + (X(2,k)-yb2(k))^2 ));
```

```
% The new error covariance is the same as the old plus Q.
```

```
PK = PK + Q;
```

```
% Calculate the Kalman gains
```

```
GK = PK*HK'*inv(HK*PK*HK' + R2);
```

```
% Calculate the updated error covariance matrix
```

```
PK = (eye(2) - GK*HK)*PK;
```

```
% Calculate a smoothed estimate of the bearing to the emitter
```

```
X(:,k) = X(:,k) + GK*(Z2n(k)-Zhat2);
```

```
% Estimate of the location for next observations is same as previous
```

```
X(:,k+1) = X(:,k);
```

```
% Save the error covariance matrices
```

```
if k == 1
```

```
    P = PK;
```

```
else,
```

```
    P = [P;PK];
```

```
end;
```

```
% Save the Kalman gains
```

```
g(:,k) = GK;
```

```
end;
```

```
% end of the Kalman filtering routine
```

```

% %%%%%%%%%%
%
%
% Plot the output
%
%

% Plot of the estimate of the x and y coordinates
figure(1)
clg;
plot(t,X(1,+)/1000,t,X(2,+)/1000)
title(' Estimate of x and y coordinates');
xlabel('Number of Observations')
ylabel('X location in kilometers')
pause

% Plot of the Kalman gains
figure(2)
clg
plot(t,g(1,+)/t,g(2,+/))
title('Kalman Gains')
xlabel('Number of Observations')
ylabel('Magnitude')
pause

% Calculate the steady state estimate of emitter location
xtavg = mean(X(1,k-10:k));
ytavg = mean(X(2,k-10:k));

% Calculate the loci of constant TDOA based upon noise free TDOA
% observations

R1a = 5000:5000:40000;

% T1 is a vector of the X and Y coordinates of the loci.
T1 = ploci(xa1(k),ya1(k),xb1(k),yb1(k),Z1(k),R1a);

R2a = 5000:5000:40000;
% T2 is a vector of the X and Y coordinates of the loci.
T2 = ploci(xa2(k),ya2(k),xb2(k),yb2(k),Z2(k),R2a);

```

```

% X-Y Plot of the estimate of the coordinates of the emitter
figure(3)

% True emitter location
subplot(111), plot(xt/1000,yt/1000,'*')

hold on
% Plots the final locations of the sensors
plot(xa1(k)/1000,ya1(k)/1000,'r*',xb1(k)/1000,yb1(k)/1000,'r*')
plot(xa2(k)/1000,ya2(k)/1000,'r*',xb2(k)/1000,yb2(k)/1000,'r*')

% A priori estimate of emitter location
plot(X0(1)/1000,X0(2)/1000,'+')

% Estimates of emitter location
plot(X(1,:)/1000,X(2,:)/1000)

% Plot three sigma error ellipsoids for various points
for k = 1:19:len-1,

% Selects the error covariance from those saved in vector P.
P1 = [P(2*k-1,1) P(2*k-1,2); P(2*k,1) P(2*k,2)];

% Calculates the coord. of ellipse.
[xg,y1,y2,Emax,Emin] = ellip(P1,C,X(1,k),X(2,k));

% Plots on graph
plot((xg)/1000,(y1)/1000,'g-',(xg)/1000,(y2)/1000,'g-')           end;

% Plots the loci of constant TDOA
plot(T1(1,:)/1000,T1(2,:)/1000,':')
plot(T2(1,:)/1000,T2(2,:)/1000,':')

hold off
title('Estimate of Position of the Emitter: tgt')
% axis;
axis([0 30 0 30]);
pause;

```

```

% Plot the closeup of the estimate of the emitter location
figure(4)

% True Emitter location
subplot(111), plot(xt/1000,yt/1000,'*')

hold on
% Estimate of emitter location
plot(X(1:1000),X(2,:)/1000);

% Calculate and plot error ellipsoids for steady state estimate

[xg,y1,y2,Emax,Emin] = ellip(PK,C,xtavg,ytavg);
plot((xg)/1000,(y1)/1000,'g-',(xg)/1000,(y2)/1000,'g-')

% Plot on the graph the major and minor axis.
Major = sprintf('%5.1f',Emax/1000);
Minor = sprintf('%5.1f',Emin/1000);

text((xt-0.50*Emax)/1000,(yt+0.85*Emax)/1000,['Major Axis = ' Major ' km'])
text((xt-0.50*Emax)/1000,(yt+0.75*Emax)/1000,['Minor Axis = ' Minor ' km'])

% Plot the loci of constant TDOA
plot(T1(1,:)/1000,T1(2,:)/1000,':')
plot(T2(1,:)/1000,T2(2,:)/1000,':')

hold off
title('Closeup of Position of the Emitter;')
% axis;
axis([(xt-Emax)/1000 (xt+Emax)/1000 (yt-Emax)/1000 (yt+Emax)/1000]);

```

```

% Ploci.m
%
% This program calculates the coordinates of the loci of constant TDOA for
% a pair of sensors.
%
% Input:   The coordinates of sensor A (meters):      xa, ya
%          The coordinates of sensor B (meters):      xb, yb
%          The Time Difference of Arrival (sec):        TDOA
%          The range from sensor A over which
%          the loci of constant TDOA will be plotted:  R
%
% Output  The vector of x and y coordinates of the loci
%          of constant TDOA.                          T
%
%

```

```
function T = ploci(xa,ya,xb,yb,TDOA,R);
```

```
% Calculate the distance from sensor A to Sensor B
Rab = ones(1,length(R))*sqrt((xb-xa)^2 + (yb-ya)^2);
```

```
% Calculate the bearing of sensor B from sensor A
psi = ones(1,length(R))*atan2(yb-ya,xb-xa);
```

```
% Calculate the difference in path length for the pulse
D = 3.0e+08*TDOA*ones(1,length(R));
```

Equation
$$\phi = \arccos \frac{[(R-D)^2 - R^2 - R_{ab}^2]}{-2R_{ab}R} + \psi$$

```
% Calculate the bearing required for each range
phi = acos( ( (R-D).^2 - (R).^2 - Rab.^2 )./(-2*R.*Rab) ) + psi;
```

```
J = ones(1,length(R));
```

```
% Calculate the x and y coordinates
T = [R.*cos(phi)+xa*J; R.*sin(phi)+ya*J];
```

```

% ellip.m
%
% This program calculates the coordinates of the 2D error ellipsoids given the
% error covariance matrix and the location of the estimate.
%
% Input:      The 2D Error Covariance Matrix           PK
%            The number of standard deviations        C
%            The x and y coordinates of the estimate   xt, yt
%
% Output     The x vector along which the ellipsoid is
%            plotted.                                  xgout
%            The y vectors corresponding to the upper
%            and lower parts of the ellipsoid          y1out, y2out
%            The length of the major axis of the ellipse Axmax
%            The length of the minor axis of the ellipse Axmin
%
function [xgout,y1out,y2out,Axmax,Axmin] = ellip(PK,C,xt,yt)

% Inputs the error covariance matrix, the number of
% standard deviations, and the location where plotted

% Calculate the inverse of the error covariance matrix
P = inv(PK);
P11 = P(1,1);
P12 = P(1,2);
P21 = P(2,1);
P22 = P(2,2);

% Calculate the upper and lower limits on the x axis

% Equation  $xt = \pm \sqrt{P_{11}c^2}$ 
f = sqrt(P11*C^2);

% Define the vector along the x axis over which the ellipsoid lies
xg = -f:(2*f)/1000:f;

```

% Calculate the upper and lower curves of the ellipse.

% Equation
$$y_t = \frac{P_{12}\tilde{x}_t}{P_{11}} \pm \sqrt{\frac{(P_{11}P_{22} - P_{12}^2)}{P_{11}^2}(P_{11}c^2 - \tilde{x}_t^2)}$$

$$y1 = -(P12/P11)*xg + \text{sqrt}(((P11*P22 - P12^2)/P11^2)*... \\ (P11*C^2*\text{ones}(1,\text{length}(xg)) - xg.^2));$$

$$y2 = -(P12/P11)*xg - \text{sqrt}(((P11*P22 - P12^2)/P11^2)*... \\ (P11*C^2*\text{ones}(1,\text{length}(xg)) - xg.^2));$$

% Calculate the distance of the ellipse from the center

$$R_{\text{ellip}} = \text{sqrt}(xg.^2 + y1.^2);$$

% Calculate the major and minor axis of the ellipse

$$Ax_{\text{max}} = \text{abs}(2*\text{max}(R_{\text{ellip}}));$$

$$Ax_{\text{min}} = \text{abs}(2*\text{min}(R_{\text{ellip}}));$$

% Calculate the coordinates of the ellipse over the estimate

$$y1_{\text{out}} = y1 + y_t * \text{ones}(1, \text{length}(xg));$$

$$y2_{\text{out}} = y2 + y_t * \text{ones}(1, \text{length}(xg));$$

$$xg_{\text{out}} = xg + x_t * \text{ones}(1, \text{length}(xg));$$

%


```

% Burdist.m
%
% Name: Richard W. Williamson
% Date: 18 February 1994
% Date Revised: 18 February 1994
%
% This program generates a simulated burst of pulses generated by a
% circularly scanning emitter. The length of the burst is 2.0 milliseconds the
% maximum amplitude is 1.0, and the PRF varies from 3 kHz to 12 kHz.
% The program calculates the probability density function for the centroid of
% the burst for a peak signal to noise ratio of 20 dB.
%
% %%%%%%%%%%
%
% The program outputs one figure.
%
% figure(1) A plot of the probability density function for the burst centroid.
%
% %%%%%%%%%%
%
% Input Variables:
%
%     BW = Beam width in degrees
%     SR = Scan rate of emitter in degrees/sec.
%     PRF = Pulse Repetition Frequency in Pulses/sec
%     PW = Pulse width in seconds.
%     FS = Sampling Frequency in samples/sec
%
%
% Output Variables:
%
%     Bur = The noise free Burst vector
%
% %%%%%%%%%%
clear;

% Initialize the variables

BW = 1.00;
SR = 500.0;
PRFk = [3000 6000 9000 12000]
PW = 1.0e-06;
FS = 8.0e+06;

```

```

muz = [0 0 0 0];
sigz = [0 0 0 0];

zk = (0.90:(1.10-0.900)/200:1.10)/1000;
dtz = zk(2)-zk(1);

for m = 1:length(PRFk)

PRF = PRFk(m);

% Calculated Variables

Bur_Len = BW/SR; % Burst length in seconds;
N_Bur = Bur_Len*FS; % Number of samples per burst

N_PW = PW*FS; % Number of samples per pulse width
N_PRF = (1/PRF)*FS; % Number of samples per PRF

Bur = zeros(1,N_Bur); % Initialize the Burst vector
t = 0:N_Bur-1; % Initialize the time vector

% Load the individual pulses in the burst vector.

for l = 1:N_PRF:N_Bur,
    Bur(l:l+N_PW-1) = ones(1,N_PW);
end;

% Define burst envelope and form noise free burst vector

Bur_env = 1.0*sin(pi*t/N_Bur);
Bur = Bur.*Bur_env;

dt = 1/FS;
% The variance of the noise power added to the pulse
V = 0.010;

ns = Bur;

N = length(ns); % Length of the burst.

```

```

% Numerator = x Denominator = y;
% Initialization of the mean and sigma variables
mux = 0;
muy = 0;
sigx = 0;
sigy = 0;
cov = 0;

% Calculate the statistics of the numerator and
% the denominator of the centroid equation.

Np = 0;

for k = 1:N,

Np = Np + 1;

    if ns(k) > 0;

        mux = mux + k*dt*ns(k);
        sigx = sigx + ((k*dt)^2)*V;
        muy = muy + ns(k);
        sigy = sigy + V;
        cov = cov + k*dt*V;

    end;

end;

sigx = sqrt(sigx);
sigy = sqrt(sigy);

rho = cov/(sigx*sigy)           % The correlation coefficient

c_bar = mux/muy

dty = (10*sigy)/60;
yk = (muy-5*sigy):dty:(muy+5*sigy);

p = zeros(length(yk),length(zk));

```

```

% Calculate the probability distribution for f(zy,y)
for l = 1:length(zk),

    for k = 1:length(yk),

        y = yk(k);
        z = zk(l);
        g1 = (y*z-mux)/sigx;
        h1 = (y-muy)/sigy;

        fxy = (1/(2*pi*sigx*sigy*sqrt(1-rho^2))) * ...
            exp( (-1/(2*(1-rho^2)))*(g1^2 -2*rho*g1*h1 + h1^2));

        p(k,l) = fxy;

    end;
end;

% Initialize the variables.
z = zeros(1,length(zk));

% Integrate the probability distribution across y to
% calculate the marginal density for z the centroid variable.

for l = 1:length(zk),
H = 0;
    for k = 1:length(yk)-1,

        H = H + dty*( yk(k)*p(k,l) + yk(k+1)*p(k+1,l) )/2;

    end;
    z(l) = H;
end;

```

```

% Check the summation of the f(z) density

F = 0;

% Change the scale on the z axis scaled in terms of millisecond
t = zk*1000;

for k = 1:length(zk)-1,

    F = F + dtz*( z(k) + z(k+1) )/2;
    muz(m) = muz(m) + (t(k)+t(k+1))*dtz*( z(k) + z(k+1) )/4;

end;

F
muz

for k = 1:length(t)-1,

    sigz(m) = sigz(m) + ((t(k)-muz(m))^2)*dtz*( z(k) + z(k+1) )/2;

end;

sigz(m) = sqrt(sigz(m))

w = -0.5*( ( t-muz(m)*ones(1,length(zk)) )/sigz(m) ).^2;

d_app = (1/(sqrt(2*pi)*sigz(m)))*exp(w);

dtt = t(2)-t(1);

tgz(m,:) = z*dtz;
tgapp(m,:) = d_app*dtt;

end

% Output the probability density functions

figure(1)
plot(t,tgz/dtt)
xlabel('Centroid Time of Arrival (milliseconds)')
ylabel('Probability Density (1/milliseconds)')
title('Sampling Frequency 8 MHz')
text(1.025,20,'3000 Hz')

```

```
text(1.015,32,'6000 Hz')
text(1.010,44,'9000 Hz')
text(1.005,60,'12000 Hz')
text(0.96,60,'Peak S/N = 20 dB')
axis([0.95 1.05 0 200.0])

% sigzout = sprintf('%5.4f',sigz(1));
% muzout = sprintf('%5.4f',muz(1));

% text(1.25,3,'S/N 15 dB')
% text(1.25,2.5,['Mean = ' muzout])
% text(1.25,2.0,['Std = ' sigzout])
% text(-0.25,5.0,'Calculated Density')
% % text(-0.25,3.0,'Gaussian Approximation')
%
```

```

% Puldist.m
%
% Name: Richard W. Williamson
% Date: 18 February 1994
% Date Revised: 18 February 1994
%
% This program generates a simulated pulse. The length of the pulse is
% 1.0 microseconds the maximum amplitude is 1.0, and the sampling rate is
% 8.0 MHz. The probability density function is calculated for peak signal to
% noise ratios of 15, 20, 25 and 30 dB.
%
% %%%%%%%%%%
%
% The program outputs one figure.
%
% figure(1) A plot of the probability density function for the pulse centroid.
%
% %%%%%%%%%%
%
clear;

% Initialize the variables
%

muz = [0 0 0 0];
sigz = [0 0 0 0];

Vk = [0.03162 0.0100 0.003162 0.00100]

% Initialize the variables.

Dyk = [3:(9-3)/60:9; 3:(9-3)/60:9; 4:(8-4)/60:8; 5:(7-5)/60:7];

zk = 3:(7-3)/200:7;
z = zeros(length(Vk),length(zk));

for m = 1:length(Vk),

yk = Dyk(m,:);
dtz = zk(2)-zk(1);
dty = yk(2)-yk(1);

dt = 1.00;
%

```

```

% The variance of the noise power added to the pulse
V = Vk(m);

% The pulse without noise.
s = [0 0.5 1 1 1 1 1 0.5 0];
N = length(s);           % Length of the pulse.

% Generation of the noise

ns = s;

% Numerator = x Denominator = y;
% Initialization of the mean and sigma variables
mux = 0;
muy = 0;
sigx = 0;
sigy = 0;
cov = 0;

% Calculate the statistics of the numerator and
% the denominator of the centroid equation.

for k = 1:N,

mux = mux + k*dt*ns(k);
sigx = sigx + ((k*dt)^2)*V;
muy = muy + ns(k);
sigy = sigy + V;
cov = cov + k*dt*V;

end;

sigx = sqrt(sigx);
sigy = sqrt(sigy);

rho = cov/(sigx*sigy);   % The correlation coefficient

c_bar = mux/muy;

```



```

% Calculate the probability distribution for f(zy,y)
for l = 1:length(zk),

    for k = 1:length(yk),

        y = yk(k);
        z = zk(l);
        g1 = (y*z-mux)/sigx;
        h1 = (y-muy)/sigy;

        fxy = (1/(2*pi*sigx*sigy*sqrt(1-rho^2))) * ...
            exp( (-1/(2*(1-rho^2)) )*(g1^2 -2*rho*g1*h1 + h1^2));
        p(k,l) = fxy;

    end;

end;

% Integrate the probability distribution across y to
% calculate the marginal density for z the centroid variable.

for l = 1:length(zk),

    H = 0;
    for k = 1:length(yk)-1,
        H = H + dtz*(yk(k)+yk(k+1))*( p(k,l) + p(k+1,l))/4;
    end;
    z(m,l) = H;

end;

% Check the summation of the f(z) density
% and compute the mean of the distribution
F = 0;

% Change the scale on the z axis
t = (zk-ones(1,length(zk)))/(N-1);

for k = 1:length(zk)-1,

    F = F + dtz*( z(m,k) + z(m,k+1) )/2;
    muz(m) = muz(m) + (t(k)+t(k+1))*dtz*( z(m,k) + z(m,k+1) )/4;

end;

```

```

for k = 1:length(t)-1,

    sigz(m) = sigz(m) + ((t(k)-muz(m))^2)*dtz*( z(m,k) + z(m,k+1) )/2;

end;

sigz(m) = sqrt(sigz(m))
tg(m,:) = z(m,:);

end;

figure(1)
t = (zk-ones(1,length(zk)))/(N-1);
dt = t(2)-t(1);
plot(t, dtz*tg/dt)
title('Sampling Frequency 8 MHz')
xlabel('Centroid Time of Arrival (microseconds)')
ylabel('Probability Density (1/microseconds)')

% The statistics for 15 dB
sigzout = sprintf('%5.5f',sigz(1));
muzout = sprintf('%5.4f',muz(1));

text(0.545,25,'S/N = 15 dB')
text(0.545,20,['Mean = ' muzout])
text(0.545,15,['Std = ' sigzout])

% The statistics for 20 dB
sigzout = sprintf('%5.5f',sigz(2));
muzout = sprintf('%5.4f',muz(2));

text(0.545,45,'S/N = 20 dB')
text(0.545,40,['Mean = ' muzout])
text(0.545,35,['Std = ' sigzout])

% The statistics for 25 dB
sigzout = sprintf('%5.5f',sigz(3));
muzout = sprintf('%5.4f',muz(3));

text(0.545,65,'S/N = 25 dB')
text(0.545,60,['Mean = ' muzout])
text(0.545,55,['Std = ' sigzout])

```

```
% The statistics for 30 dB
sigzout = sprintf('%5.5f',sigz(4));
muzout = sprintf('%5.4f',muz(4));
```

```
text(0.545,85,'S/N = 30 dB')
text(0.545,80,['Mean = ' muzout])
text(0.545,75,['Std = ' sigzout])
```

```
% axis([0.4 0.6 0 90])
```

LIST OF REFERENCES

1. Dougherty, Edward, *Probability and Statistics for the Engineering, Computing, and Physical Sciences*, Prentice Hall, Englewood Cliffs, NJ, 1990.
2. Papoulis, Athanasios, *Probability, Random Variables, and Stochastic Processes*, McGraw-Hill Inc., New York, NY, 1991.
3. Skolnik, Merrill L., *Introduction to Radar Systems*, McGraw-Hill Inc., New York, NY, 1980
4. Catlin, Donald E., *Estimation, Control, and the Discrete Kalman Filter*, Springer-Verlag, New York, NY, 1989.
5. Couch II, Leon W., *Digital and Analog Communications Systems*, Macmillan Publishing Company, New York, NY, 1993.
6. Olcovich, George E., "Passive Acoustic Target Motion Analysis," Masters Thesis, Naval Postgraduate School, Monterey, CA, June 1986.
7. Burl, Jeffery, "The Extended Kalman Filter Equations," Unpublished notes.

INITIAL DISTRIBUTION LIST

1. Defense Technical Information Center 2
Cameron Station
Alexandria, VA 22304-6145
2. Library, Code 52 2
Naval Postgraduate School
Monterey, CA 93943-5101
3. Chairman, Code EC 1
Department of Electrical and Computer Engineering
Naval Postgraduate School
Monterey, CA 93943-5121
4. Professor Harold Titus, Code EC/Ts 2
Department of Electrical and Computer Engineering
Naval Postgraduate School
Monterey, CA 93943-5121
5. Professor Phillip E. Pace, Code EC/Pc 1
Department of Electrical and Computer Engineering
Naval Postgraduate School
Monterey, CA 93943-5121
6. Director, Training and Education 1
MCCDC, Code C46
1019 Elliot Road
Quantico, VA 22134-5027
7. Naval Research Laboratory 2
Code 9100
4555 Overlook Ave.
Washington, DC 20375-5320

8. Dr. Jill P. Burt
Defense Intelligence Agency
Missile and Space Intelligence Center
ATTN: MSC-6
Redstone Arsenal, AL 35898-5500 2

9. Capt. Richard W. Williamson 2
185 Indian Corner Road
Saunderstown, RI 02874